

Ammonia volatilization from broadcast urea: measurements using a micrometeorological approach and modeling with the Denitrification-Decomposition (DNDC) model.

by

Vinicius Perin

B.S., University of Sao Paulo, 2016

A THESIS

submitted in partial fulfillment of the requirements for the degree

MASTER OF SCIENCE

Department of Agronomy  
College of Agriculture

KANSAS STATE UNIVERSITY  
Manhattan, Kansas

2019

Approved by:

Major Professor  
Eduardo Alvarez Santos

# Copyright

© Vinicius Perin 2019.

## Abstract

Synthetic N fertilizers, such as urea, are one of the main anthropogenic sources of atmospheric ammonia ( $\text{NH}_3$ ).  $\text{NH}_3$  volatilization from N fertilizer application can significantly reduce agronomic efficiency (AE), contribute to air pollution, soil acidification and eutrophication of water bodies. Therefore, understanding the processes and factors influencing  $\text{NH}_3$  volatilization from broadcast urea is pivotal to improve agricultural sustainability. In Chapter 2 of this thesis, the integrated horizontal flux (IHF) approach was used to measure  $\text{NH}_3$  volatilization from eight field experiments under cold weather conditions in Kansas.  $\text{NH}_3$  volatilization was measured from circular plots (20-m radius) fertilized with urea and urea amended with urease inhibitor (NBPT) both at rate of  $60 \text{ kg of N ha}^{-1}$ . The impact of  $\text{NH}_3$  volatilization losses on winter wheat was evaluated through experimental plots arranged in a complete randomized block design with treatments consisting of four different rates of application ( $30, 60, 90$  and  $120 \text{ kg N ha}^{-1}$ ) of urea and urea + NBPT and control ( $0 \text{ kg N ha}^{-1}$ ).  $\text{NH}_3$  cumulative losses varied from  $<1\%$  to  $29\%$  of applied N. Largest losses occurred when urea was broadcast to soils with high water content followed by a dry period. The use of urease inhibitor NBPT reduced  $\text{NH}_3$  volatilization losses in more than  $20\%$  at locations where the largest losses ( $> 25\%$ ) occurred. No statistical difference was found in terms of grain yield, N recovery and AE, when comparing urea and urea + NBPT treatments. In Chapter 3, simulations provided by two versions of the Denitrification-Decomposition (DNDC) process-based model (DNDC 9.5 and DNDC v.CAN) were compared with flux data obtained in 29  $\text{NH}_3$  volatilization sampling campaigns. These sampling campaigns were conducted in Kansas and Montana using the IHF method over circular plots. Overall, the DNDC v.CAN simulated  $\text{NH}_3$  emissions with smaller average root mean square error ( $\overline{\text{RMSE}} = 10.9 \text{ kg of N ha}^{-1}$ ) compared to the DNDC 9.5 ( $\overline{\text{RMSE}} = 32.8 \text{ kg of N ha}^{-1}$ ). Our sensitivity analysis

showed that soil pH and soil temperature were the main input variables affecting NH<sub>3</sub> volatilization in both models. In addition, our analysis demonstrated several drawbacks that could be improved in future versions of the model to better simulate NH<sub>3</sub> volatilization. These potential areas for improvements the DNDC model versions include: *i*) limitations in the soil-hydrology water sub-model affected the accuracy of the simulations of the effects of soil water content on urea hydrolysis, which has direct effect on NH<sub>3</sub> volatilization; *ii*) both models failed to simulate the effects of accumulated precipitation ( $\geq 20$  mm) on NH<sub>3</sub> volatilization during the first 5-15 d post fertilization; *iii*) future developments of the DNDC should consider adding a more robust routine to simulate the effects of urease inhibitor on NH<sub>3</sub> volatilization and *iv*) the timing of the NH<sub>3</sub> volatilization peak after fertilization was underestimated by the DNDC v.CAN and largely overestimated by the DNDC 9.

## Table of Contents

|   |     |
|---|-----|
| List of Figures .....   | vii |
| List of Tables .....  | x   |
| Acknowledgments.....  | xi  |
| Chapter 1 - Overview on ammonia volatilization from broadcast urea.....   | 1   |
| 1.1 Ammonia volatilization process .....  | 1   |
| 1.2 Field scale measurements of NH <sub>3</sub> volatilization.....   | 4   |
| 1.3 Denitrification-Decomposition (DNDC) process-based model to simulate NH <sub>3</sub><br>volatilization .....                            | 5   |
| Chapter 2 - Ammonia volatilization from broadcast urea: mitigation by urease inhibitor and<br>impact on winter wheat production .....       | 8   |
| 2.1 Introduction.....   | 9   |
| 2.2 Material and Methods .....  | 11  |
| 2.2.1 Site description.....   | 11  |
| 2.2.2 The IHF approach .....  | 12  |
| 2.2.3 NH <sub>3</sub> volatilization sampling campaigns.....  | 12  |
| 2.2.4 Experimental plots to assess the influence of NH <sub>3</sub> volatilization on winter wheat .....                                    | 14  |
| 2.2.5 Environmental data for gas sampling campaigns and winter wheat experimental plots<br>.....  | 15  |
| 2.2.6 Analytical methods and interpretation .....   | 16  |
| 2.3 Results and Discussion .....  | 16  |
| 2.3.1 Environmental conditions .....  | 16  |
| 2.3.2 NH <sub>3</sub> fluxes measurements from sampling campaigns .....   | 17  |
| 2.3.3 Cumulative N losses from sampling campaigns .....   | 18  |
| 2.3.4 Effect of N rate application on winter wheat grain yield, N recovery and AE.....  | 20  |
| 2.4 Conclusions.....  | 23  |
| 2.5 Acknowledgments .....   | 24  |
| Chapter 2 – Tables and Figures .....  | 25  |
| Chapter 3 - Assessment of the Denitrification-Decomposition (DNDC) model simulations of<br>ammonia volatilization from broadcast urea ..... | 33  |

|   |    |
|---|----|
| 3.2 Material and Methods .....  | 36 |
| 3.2.1 NH <sub>3</sub> emission sampling campaigns.....  | 36 |
| 3.2.2 Meteorological data.....  | 38 |
| 3.2.3 DNDC model description and NH <sub>3</sub> volatilization sub-model.....                      | 38 |
| 3.2.5 Model evaluation and statistical analysis.....  | 42 |
| 3.2.6 Sensitivity analysis.....   | 43 |
| 3.3 Results.....  | 44 |
| 3.3.1 NH <sub>3</sub> volatilization simulations from broadcast urea and urea amended with NBPT...  | 44 |
| 3.3.2 Daily soil temperature and $\theta_v$ simulations .....                                       | 46 |
| 3.3.3 Sensitivity analysis and factors influencing NH <sub>3</sub> volatilization simulations ..... | 46 |
| 3.4 Discussion.....   | 47 |
| 3.5 Conclusions.....  | 53 |
| Chapter 3 – Tables and Figures .....  | 54 |
| References.....   | 63 |
| Appendix A - Figures and Tables Chapter 3 .....   | 75 |

## List of Figures

Figure 1.1 - DNDC processes involved on the calculation of soil ammonium ( $\text{NH}_4^+$ ) and ammonia ( $\text{NH}_3$ ) concentration and volatilization from the soil-plant system.  $\text{NH}_4^+_{\text{clay}}$  represents the  $\text{NH}_4^+$  adsorbed by the soil clay minerals and  $\text{NH}_4^+_{(l)}$  and  $\text{NH}_3_{(l)}$  are referred to the dissolved  $\text{NH}_4^+$  and  $\text{NH}_3$  in the soil solution. This scheme was adapted from Dubache et al. (2019) and it represents the processes regarded  $\text{NH}_3^+$  volatilization from the source code of the DNDC base model (DNDC 9.5) available at <http://www.dnnc.sr.unh.edu/>. ..... 7

Figure 2.1 - Frequency distribution of wind speed and direction during the  $\text{NH}_3$  volatilization measurements period (Table 2.1) for all five locations. .... 26

Figure 2.2 Average daily soil temperature ( $^{\circ}\text{C}$ ) and volumetric soil water content ( $\theta_v$ )( $\text{cm}^3\text{cm}^{-3}$ ) (upper panels – a, c, e, g and i).  $\text{NH}_3$  flux for soil plots treated with urea and urea + NBPT (lower panels – b, d, f, h and j). Soil temperature was measured at 5 cm depth and obtained from the closest Kansas Mesonet weather station for Ash1 and Sol. For Ash2, Ash3 and Kon soil temperature was measured at 2 cm depth using dual-probe heat-pulse sensors (Campbell et al., 1991; Bristow et al., 1994). For Ash1 and Sol,  $\theta_v$  was measured from seven soil samples (depth 5 cm) using a metal cylinder (height = 5 cm and radius = 2.5 cm). For Ash1, Ash3 and Kon  $\theta_v$  was measured at 2 cm depth using dual-probe heat-pulse sensors (Campbell et al., 1991; Bristow et al., 1994). ..... 28

Figure 2.3 Cumulative N losses (% of N applied) for all five sampling campaigns, for urea and urea + NBPT. .... 29

Figure 2.4 Grain yield response to soil available N (0-60 cm) + N application rates (kg of N  $\text{ha}^{-1}$ ) for the three experimental locations (Ash1, Sol and Ash2) and for all locations combined. Bars represent standard errors. .... 30

Figure 2.5 N recovery as a function of soil available N (0-60 cm) + N application rates (kg of N  $\text{ha}^{-1}$ ) for the three experimental locations (Ash1, Sol and Ash2) and for all locations combined. Bars represent standard errors. .... 31

Figure 2.6 Agronomic efficiency (AE) as a function of soil available N (0-60 cm) + N application rates (kg of N  $\text{ha}^{-1}$ ) for the three experimental locations (Ash1, Sol and Ash2) and for all locations combined. Bars represent standard errors. .... 32

Figure 3.1 Simulated and observed cumulative N losses for all sampling campaigns, for urea (A) and urea + NBPT (B) ..... 60

Figure 3.2 Results of the sensitivity tests performed by varying each environmental or management input parameter in + 20% with steps of 5%. Horizontal bars represent the variation from the sampling campaign 29 baseline scenario (Table 3). Soil pH, ‘Rate’ (urea rate of application in kg of N ha<sup>-1</sup>), ‘SOC’ (soil organic carbon in kg of C kg<sup>-1</sup> soil), ‘Efficiency’ (urease inhibitor efficiency in %), ‘Duration’ (urease inhibitor duration in d) and ‘Clay’ (soil clay content in %) ..... 61

Figure 3.3 Relative variable importance (0 – 1; from least to most important) in Random forest models of input variables for the NH<sub>3</sub> volatilization simulations using DNDC v.CAN and DNDC 9.5. Variable importance was based on model output values of soil pH, soil temperature, SOC, soil moisture, air humidity, precipitation, snowpack and wind speed. .. 62

Figure A.1- Cumulative N losses (kg of N ha<sup>-1</sup>) from broadcast urea for campaigns 1-12. Field sampling campaigns were obtained from Engel et al. (2011). Wilmot index of agreement (Willmott et al., 2018) is represented as ‘d’ and root mean square error by ‘rmse’ .....84

Figure A.2 - Cumulative N loss (kg of N ha<sup>-1</sup>) from broadcast urea for campaigns 13-21. Field sampling campaigns were obtained from Engel et al. (2017) and Romero et al. (2017). Wilmot index of agreement (Willmott et al., 2018) is represented as ‘d’ and root mean square error by ‘rmse’ .....85

Figure A.3 - Cumulative N loss (kg of N ha<sup>-1</sup>) from broadcast urea for campaigns 22-29. Field sampling campaigns are described on Chapter 2. Wilmot index of agreement (Willmott et al., 2018) is represented as ‘d’ and root mean square error by ‘rmse’. .....86

Figure A.4 - Cumulative N loss (kg of N ha<sup>-1</sup>) from broadcast urea amended with urease inhibitor NBPT for campaigns 1-12. Field sampling campaigns were obtained from Engel et al. (2011). Wilmot index of agreement (Willmott et al., 2018) is represented as ‘d’ and root mean square error by ‘rmse’. .....87

Figure A.5 - Cumulative N loss (kg of N ha<sup>-1</sup>) from broadcast urea amended with urease inhibitor NBPT for campaigns 13-21. Field sampling campaigns were obtained from Engel et al. (2017) and Romero et al. (2017). Wilmot index of agreement (Willmott et al., 2018) is represented as ‘d’ and root mean square error by ‘rmse’. .....88



Figure A.6 - Cumulative N loss (kg of N ha<sup>-1</sup>) from broadcast urea amended with urease inhibitor NBPT for campaigns 22-29. Field sampling campaigns are described on Chapter 2. Wilmot index of agreement (Willmott et al., 2018) is represented as ‘d’ and root mean square error by ‘rmse’ .....89

Figure A.7 - Soil temperature (1-cm depth) for campaigns 1-12. Field observations were obtained from Engel et al., (2011). Wilmot index of agreement (Willmott et al., 2018) is represented as ‘d’ and root mean square error by ‘rmse’. .....90

Figure A.8 - Soil temperature (1-cm depth) for campaigns 13-21. Field observations were obtained from Engel et al., (2017) and Romero et al., (2017). Wilmot index of agreement (Willmott et al., 2018) is represented as ‘d’ and root mean square error by ‘rmse’ .....91

Figure A.9 - Soil temperature (5-cm depth) for campaigns 22-29. Field observations collection are described on Chapter 2. Wilmot index of agreement (Willmott et al., 2018) is represented as ‘d’ and root mean square error by ‘rmse’ .....92

Figure A.10 – Volumetric soil water content (cm<sup>3</sup> cm<sup>-3</sup>) (5-cm depth) for campaigns 22-29. Field observations collection are described on Chapter 2. Wilmot index of agreement (Willmott et al., 2018) is represented as ‘d’ and root mean square error by ‘rmse’ .....93

## List of Tables

|  |    |
|--|----|
| Table 2.1- Field experiments locations, fertilization date, sampler exchange dates and winter wheat plots planting and harvest date and seeding rate. ....   | 25 |
| Table 2.2 - Soil characteristics (particle size distribution,, cation exchange capacity (CEC), pH and organic matter) for all five locations and tillage practice. Except for NO <sub>3</sub> -N, all other soils characteristics were measured at depth: 0 to 15 cm. ....   | 25 |
| Table 2.3 - Pairwise comparisons (p = 0.05) between urea and urea + NBPT for different nitrogen application rates (30, 60, 90 and 120 kg N ha <sup>-1</sup> ), considering yield, N recovery and AE. ....  | 25 |
| Table 3.1 - Location, NH <sub>3</sub> sampling campaign year, soil series, soil particles distribution, cation exchange capacity (CEC), pH and SOC for all campaigns.....  | 55 |
| Table 3.2 - Sampling campaigns agricultural management system and state county in which the field experiment was conducted.....  | 56 |
| Table 3.3 - Model input parameters for simulations for both DNDC model versions (DNDC 9.5 and DNDC v.CAN).....   | 57 |
| Table 3.4 - Baseline (Sampling campaign 29) and alternative scenarios for sensitivity tests.....   | 58 |
| Table 3.5 - Statistical indices of the DNDC v.CAN and DNDC 9.5 simulations of cumulative NH <sub>3</sub> volatilization (kg of N ha <sup>-1</sup> ) after urea and urea +NBPT broadcast for all sampling campaigns. ....   | 59 |
| Table A.1 - Meteorological stations used to extract climatic information for DNDC model simulations. ....  | 95 |
| Table A.2 - Performance parameters of DNDC v.CAN and DNDC 9.5 of simulations of mean daily soil temperature (°C, campaigns 1-21: 2-cm depth and campaigns 22-29: 5-cm depth) after urea application during NH <sub>3</sub> volatilization measurement periods for all sampling campaigns. MAE (Mean Absolute Error) and RMSE (Root Mean Square Error)..... | 95 |

## **Acknowledgments**

First and foremost, thanks and praise to God for his blessings throughout my research at Kansas State University.

I would also like to express my deep and sincere gratitude to my major professor Dr. Eduardo Alvarez Santos and committee members Dr. Romulo Lollato and Dr. Dorivar Ruiz-Diaz. I am also grateful to Dr. Gerald J. Kluitenberg for the guidance and patience during the past two years.

My sincere and deep thanks to Lab mates, family, friends and my gorgeous girlfriend Isabella Possignolo.

# **Chapter 1 - Overview on ammonia volatilization from broadcast urea**

## 1.1 Ammonia volatilization process

During the last century the world's consumption of synthetic fertilizers increased remarkably contributing to changes in the nitrogen global cycle (Mosier et al., 2013). Urea is one of the most used ammonium-based nitrogen fertilizers (Galloway et al., 2004; Glibert et al., 2006; Mosier et al., 2013). However, previous studies show that once urea is applied to the soil surface most of the N (up to 60%) originated from the urea granules can be lost to the atmosphere through the process of ammonia ( $\text{NH}_3$ ) volatilization (Sommer et al., 2004; Rochette et al., 2009; Silva et al., 2017).

Once urea is broadcast or incorporated into the soil the urea granules start to breakdown through a hydrolysis reaction, which is boosted by the activity of the urease enzyme. Urea is transformed in ammonium carbonate, an unstable compound that can be quickly transformed into  $\text{NH}_3$ . The balance between  $\text{NH}_4^+$  and  $\text{NH}_3$ , and the retention of these forms in the soil depends on the local environmental conditions, for example soil temperature, soil pH, soil water content, etc. (Ernst and Massey, 1960; Kissel et al., 2008; Behera et al., 2013). Additionally, the rate of urea hydrolysis is driven by urease concentration in the soil and by the factors influencing urease activity (e.g. soil temperature, pH, etc.) and the  $\text{NH}_4^+/\text{NH}_3$  balance (Kissel et al., 2008).

Soil temperature has a critical role on  $\text{NH}_3$  volatilization from the soil to the atmosphere. Studies have shown that warmer soil temperatures results on a greater potential of  $\text{NH}_3$  volatilization (Ernst and Massey, 1960; Kissel et al., 2008; Behera et al., 2013). In addition,  $\text{NH}_3$  volatilization will vary based on the soil type and there is an optimum temperature range (between 20 °C and 30 °C) enhancing  $\text{NH}_3$  volatilization rate (Ernst and Massey, 1960). Moreover, high soil temperature favors greater concentration of  $\text{NH}_3$  over  $\text{NH}_4^+$  and, as consequence, higher  $\text{NH}_3$

volatilization rates occur during warmer months of the year and warmer periods of the day (Mikkelsen, 2009). Additionally, higher temperatures results in higher hydrolysis reaction rate, following an increase in soil pH and greater  $\text{NH}_3$  concentration, and contributing to increase the potential for  $\text{NH}_3$  losses (Ernst and Massey, 1960; Mikkelsen, 2009). Yan et al. (2016) showed that the rate of volatilization under an ambient temperature of 25 °C was increased by twofold when compared to ambient conditions under 15 °C. The authors also reported a change on the peak of  $\text{NH}_3$  volatilization. Under warmer conditions (temperature > 25 °C)  $\text{NH}_3$  volatilization peaked at 5 d post fertilization, and under a cooler environment (temperature < 15 °C),  $\text{NH}_3$  volatilization peaked after 20 d post fertilization.

Jones et al. (2013) reported that soils with high clay content, organic matter and/or bicarbonate content are more likely to have a lower potential of  $\text{NH}_3$  volatilization from broadcast urea due to a greater soil pH buffer capacity and higher CEC. The reaction of hydrolysis increases the pH on the surroundings of the urea granules (Kissel et al., 2008). Nevertheless, soils with high CEC often present higher amount of exchangeable calcium, which contribute to offset the increase of the soil pH and to decrease the potential for  $\text{NH}_3$  volatilization (Jones et al., 2013). In addition, the reaction of  $\text{NH}_4^+$  with soil organic matter and clay particles present in the soil, reduces the  $\text{NH}_4^+$  concentration in the soil solution, decreasing the  $\text{NH}_3$  available to volatilize (Kissel et al., 2008; Mikkelsen, 2009).

The soil pH has a major effect on the equilibrium between the relative concentration of  $\text{NH}_4^+$  and  $\text{NH}_3$  (Freney, 1988; Kissel et al., 2008). Freney (1988) compiled an extensive list of studies showing that  $\text{NH}_3$  losses increase when increasing the soil pH. Soils with higher pH tend to have a higher rate of  $\text{NH}_3$  volatilization, resulting from an increase on the concentration of  $\text{NH}_3$

in the soil solution. This phenomenon is evident when urea is surface applied on an alkaline soils (Freney et al., 1983; Kissel et al., 2008).

Al-Kanani et al. (1991) found a positive linear relationship between  $\text{NH}_3$  volatilization losses and soil moisture, up to soil water saturation. Moreover, soil water content plays a major role in the urea transport from the soil surface to the plant roots (Ernst and Massey, 1960; Freney et al., 1983; Otto et al., 2017). On the other hand, lower  $\text{NH}_3$  volatilization rates are associated with the occurrence of a single rainfall or irrigation event  $\geq 15$  mm, as the broadcast N fertilizer is transported to deeper layers in the soil (Jones et al., 2007, 2013). Higher chances in  $\text{NH}_3$  volatilization occur when the soil is warm and moist, and the relative humidity of the air is higher than the critical relative humidity (i.e. relative humidity above which the fertilizer starts to absorb moisture from the atmosphere) of urea granules (IPNI, 2008; Mikkelsen, 2009). Significant N losses (33 to 44% of applied N) were reported by Jones et al. (2013) when urea was surface-applied on a moist soil following a dry period while lower 10 to 20% of N losses were found when urea was surface-applied on dry soil, followed by a light rainfall event  $\leq 8$  mm. Minimal N losses ( $\leq 10\%$  of applied N) were reported by Engel et al. (2011) when urea was surface-applied and following rainfall events that added up to 19 mm.

The presence of crop residue and thatch on the soil surface has been shown to increase the urease activity, and as consequence, the potential of  $\text{NH}_3$  volatilization from broadcast urea (Van Doren Jr et al., 1977; Torello and Wehner, 1983; McInnes et al., 1986; Rochette et al., 2009). Rochette et al. (2009) carried out a laboratory experiment to compare the urease activity and  $\text{NH}_3$  volatilization between a no-till and moldboard soils after urea was broadcast. These authors found higher rates of urease activity and  $\text{NH}_3$  volatilization in the no-till soil. They concluded that the possible cause for that was a higher urease enzyme activity inherent in no-till soils, and a decreased

of urea granules contact with the soil surface, reducing  $\text{NH}_4^+$  adsorption by soil particles. When comparing long-term no-till practices with conventional tillage, Van Doren Jr et al. (1977) reported that the urea presence and its activity were significantly greater in a no-till system at a 0-7.5 cm depth than in soil under conventional tillage. Torello and Wehner (1983) evaluated  $\text{NH}_3$  volatilization from urea surface-applied on turf-grass under different environmental conditions. Their results suggested that the high content of urease on the thatch increased the  $\text{NH}_3$  volatilization from broadcast urea.

## 1.2 Field scale measurements of $\text{NH}_3$ volatilization

The measurement of  $\text{NH}_3$  volatilization from agricultural fields can be done by employing several different methods (e.g. chambers, wind tunnels, mass balance methods, eddy covariance, etc.). The importance of understanding and measuring  $\text{NH}_3$  emissions from fertilized fields led several authors to review the concepts, advantages and disadvantages of various available methodologies (Freney, 1988; Harper, 2005; Shah et al., 2006; Liu, 2018). Within the different available methods, the micrometeorological integrated horizontal flux (IHF) approach has been commonly employed and is one of the most reliable methods to measure  $\text{NH}_3$  volatilization (Denmead, 1983; Shah et al. 2006; Liu, 2018). The IHF method relies on measurements of vertical concentration gradients of  $\text{NH}_3$ , wind speed and direction to quantify  $\text{NH}_3$  from a well-defined source area (Denmead et al., 1983).

Sanz-Cobena et al. (2008) used the IHF approach to estimate  $\text{NH}_3$  emissions from sunflower fields fertilized with urea and urea amended with urease inhibitor (N-(n-butyl) thiophosphoric triamide, NBPT). The authors also investigated the effects of incorporating urea into soil by irrigation on  $\text{NH}_3$  emissions. These researchers concluded that both irrigation and the use of urease inhibitor were effective in reducing cumulative  $\text{NH}_3$  losses. Engel et al. (2011) used

the IHF approach with passive samplers to measure NH<sub>3</sub> volatilization from winter wheat fields fertilized with urea during cold months in Montana, US. The authors found significant NH<sub>3</sub> losses (up to 44% of applied N) contradicting the assumption that NH<sub>3</sub> losses during cold temperatures (below <10 °C) are minimal. The authors also mentioned that cold temperatures contributed to a prolonged period of NH<sub>3</sub> volatilization.

The IHF method has been used in a large range of studies. Including studies aiming to improve new techniques to measure NH<sub>3</sub> volatilization (Pacholski et al., 2006), to evaluate the effectiveness of the urease inhibitor (Sanz-Cobena et al., 2008; Engel et al., 2011; Abalos et al., 2012) and to assess the impact of NH<sub>3</sub> volatilization on crop production (Engel et al., 2017; Romero et al., 2017).

### 1.3 Denitrification-Decomposition (DNDC) process-based model to simulate NH<sub>3</sub> volatilization

The use of a process-based biogeochemical models (e.g. DNDC, Volt'Air, HERMES, DAYCENT, etc.) to simulate nitrogen cycling in agroecosystems is an alternative to evaluate different strategies to increase N use efficiency (Cui et al. 2014; Dutta et al. 2016; Pacholski et al. 2017). These process-based models can also be used to investigate how different drivers influence NH<sub>3</sub> volatilization measurements, since they can provide a better understanding of the processes governing nitrogen cycling at the field scale. Among these models, the DNDC has been widely used to simulate greenhouse gas emissions from agroecosystemns (Cui et al. 2014; Dutta et al. 2016; Congreaves et al. 2016; Dubache et al. 2019; Siqu Li et al. 2019). Futhermore, the DNDC has been often employed around the world to simulate NH<sub>3</sub> emissions from broadcast urea (Cui et al. 2014; Dutta el al. 2016; Giltrap et al. 2017; Dubache et al. 2019, Siqu Li et al. 2019). However, there is no recent study that used the DNDC to simulate N losses through NH<sub>3</sub> volatilization from broadcast urea in the US.



The original version of the DNDC consists of six interconnected modules. These modules are: soil climate, crop growth, organic matter decomposition, nitrification, denitrification and fermentation (Li et al. 1992a; Li et al. 1992b). Dubache et al. (2019) created a diagram to illustrate the main biogeochemical processes influencing  $\text{NH}_3$  volatilization in the soil-plant system (Fig. 1.1).

Recently, several improvements were made on model representations of processes governing  $\text{NH}_3$  volatilization (Giltrap et al., 2015; Dutta et al., 2016; Congreaves et al., 2017; Dubache et al., 2019). Giltrap et al. (2015) recommended the addition of a different algorithm to better represent soil pH changes during the process of urea hydrolysis. Dutta et al. (2016) included a soil pH buffer factor in the Canadian version of the DNDC. The authors concluded that  $\text{NH}_3$  estimation was further improved when compared to the original model version (DNDC 9.5, Li et al. (1992)). More recently, Dubache et al. (2019) compared simulated  $\text{NH}_3$  emissions with field measurements in the UK, and reported that the original version of the model was not able to capture the influence of precipitation on  $\text{NH}_3$  emissions from broadcast urea. In addition, the authors pointed that possible model biases for simulating  $\text{NH}_3$  emissions are originated from the model limitations to account for the effect of soil clay fraction, soil organic matter and/or straw retention fraction on the  $\text{NH}_3$  volatilization process.

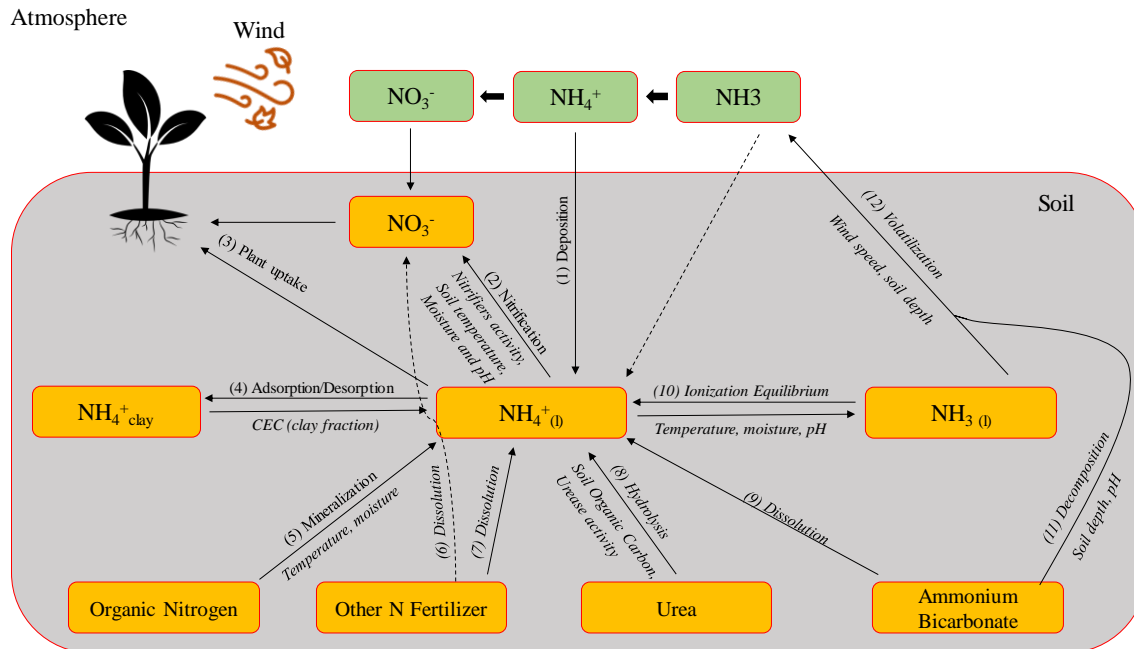


**Figure 1.1** - DNDC processes involved on the calculation of soil ammonium ( $\text{NH}_4^+$ ) and ammonia ( $\text{NH}_3$ ) concentration and volatilization from the soil-plant system.  $\text{NH}_4^+$ <sub>clay</sub> represents the  $\text{NH}_4^+$  adsorbed by the soil clay minerals and  $\text{NH}_4^+$ <sub>(l)</sub> and  $\text{NH}_3$ <sub>(l)</sub> are referred to the dissolved  $\text{NH}_4^+$  and  $\text{NH}_3$  in the soil solution. This scheme was adapted from Dubache et al. (2019) and it represents the processes regarded  $\text{NH}_3^+$  volatilization from the source code of the DNDC base model (DNDC 9.5) available at <http://www.dndc.sr.unh.edu/>.

## **Chapter 2 - Ammonia volatilization from broadcast urea: mitigation by urease inhibitor and impact on winter wheat production**

### **ABSTRACT**

A large proportion of urea broadcast to winter wheat (*Triticum aestivum* L.) during cold weather months can be lost through the process of ammonia (NH<sub>3</sub>) volatilization. The objectives of this study were: 1) to quantify nitrogen (N) losses through NH<sub>3</sub> volatilization from fallow plots fertilized with urea and urea amended with a urease inhibitor (NBPT) and 2) to investigate the impact of possible N losses through NH<sub>3</sub> volatilization on winter wheat under cold weather conditions. NH<sub>3</sub> volatilization quantification sampling campaigns were conducted at five locations in Kansas. In addition, at three of these locations, companion experiments were carried out to investigate the effect of NH<sub>3</sub> volatilization losses on winter wheat production. NH<sub>3</sub> emissions were quantified using the integrated horizontal flux micrometeorological method with passive NH<sub>3</sub> samplers over circular plots (20-m radius), which were fertilized with broadcast urea and urea + NBPT both at rate of 60 kg of N ha<sup>-1</sup>. The impact of NH<sub>3</sub> volatilization losses on winter wheat production was evaluated through experimental plots arranged in a randomized complete block statistical design with treatments consisting of four different application rates (30, 60, 90 and 120 kg N/ha) of urea and urea + NBPT. NH<sub>3</sub> total losses varied from <1% to 29%. Largest N losses happened when urea was broadcasted to soils with high water content followed by a dry period. NBPT amendment did not show consistent NH<sub>3</sub> volatilization mitigation effects at the locations where N losses were low to moderate (<1% to 17%). Nevertheless, NBPT reduced NH<sub>3</sub> volatilization losses by more than 20% at locations where the largest N losses occurred. Minimal agronomic benefits on winter wheat grain yield, N recovery and agronomic efficiency (AE) was found when amending urea with NBPT. Our results suggest that winter wheat growers should

carefully evaluate the soil moisture conditions before broadcasting urea to avoid potential  $\text{NH}_3$  volatilization losses.

## 2.1 Introduction

Urea accounts for more than 50% of the total world consumption of synthetic N fertilizers (IFA, 2018). Although urea is widely applied to croplands, it is susceptible to substantial N losses through  $\text{NH}_3$  volatilization (Freney et al., 1983; Sommer et al., 2004; Mosier et al., 2013). In the US Southern Great Plains (Kansas, Oklahoma and Texas), 94% of the total wheat acreage has been fertilized with some form of N fertilizer, and urea is the primary N source applied by farmers (USDA-ERS, 2018). Nitrogen fertilization of winter wheat is typically done before sowing and/or during tillering to anthesis (early spring application). Usually, pre-plant application is done by incorporating fertilizer into the soil, and the spring application by broadcasting urea to the soil surface (Shroyer et al., 1997). The latter is commonly done during cold weather months, usually from February to March.

Once the broadcast urea granules come into contact with the soil surface, the process of urea hydrolysis is triggered leading to N losses through  $\text{NH}_3$  production. The urea hydrolysis rate is governed by the activity of the urease enzyme in the soil as well as the soil temperature and water content (Ernst and Massey, 1960; Kissel et al., 2008; Behera et al., 2013). According to Engel et al. (2011), there is a widespread belief among growers and fertilizer specialists that  $\text{NH}_3$  volatilization risks are reduced when urea is broadcast to soils under cold weather conditions. Nonetheless, Engel et al. (2011) found significant losses (up to 44% of applied N) when urea was broadcast to cold soils with high water content followed by a dry period. Despite the potential for substantial N losses, only a few studies have been conducted to evaluate N losses through  $\text{NH}_3$

volatilization from broadcast urea under cold weather conditions (Engel et al., 2011, 2017; Romero et al., 2017).

A common approach to mitigate  $\text{NH}_3$  volatilization losses is to amend urea with an urease inhibitor, such as *N-(n-butyl) thiophosphoric triamide* (NBPT) (Jones et al., 2013; Cantarella et al., 2018). Silva et al. (2017) carried out a comprehensive meta-analysis across several locations around the world to evaluate  $\text{NH}_3$  volatilization from broadcast urea and urea + NBPT. They found an average  $\text{NH}_3$  volatilization loss of 31% of total applied N when urea was broadcast to the soil surface. They also reported an average reduction of 52% on  $\text{NH}_3$  volatilization losses when the urea was amended with NBPT. Finally, the authors concluded that NBPT has the potential to increase the yield of major crops by 5.3%.

Micrometeorological methods provide near-continuous flux measurements and integrate gas emissions over larger areas, when compared to enclosure techniques (e.g., chambers and wind tunnels). In addition, micrometeorological methods cause minimal disturbance to the source area over which fluxes are being measured (Denmead, 1983; Harper, 2005). Among micrometeorological techniques, the integrated horizontal flux (IHF) approach has been widely used to measure  $\text{NH}_3$  fluxes (Denmead, 1983; Leuning et al., 1985; Wilson and Shum, 1992; Liu, 2018). The IHF approach is based on mass balance principles, and is suitable for estimating gas emissions from well-defined source areas (Beauchamp et al., 1978; Denmead, 1983). The IHF method relies on the assumption that the gas flux from a known source area of limited upwind extent can be equated to the rate at which the gas is transported by the wind through a vertical plane downwind from the source area (Denmead, 1983). Typically, the IHF method requires wind and concentration vertical profile measurements over the source area. Leuning et al. (1985) developed a passive  $\text{NH}_3$  “shuttle” sampler that eliminates the need for wind measurements when

applying the IHF method to quantify  $\text{NH}_3$  fluxes. The use of this sampler reduces the IHF instrumentation costs and the uncertainties introduced by errors in wind velocity measurements. This sampler has been successfully used in previous studies to measure  $\text{NH}_3$  emissions from a fertilized plots (Sanz-Cobena et al., 2008; Turner et al., 2010; Engel et al., 2011, 2017; Romero et al., 2017).

In this study, we applied the IHF method with passive samplers (Leuning et al., 1985) to estimate  $\text{NH}_3$  emissions from circular plots in fallow field fertilized with urea and urea + NBPT. In addition, we established winter wheat experimental plots in areas adjacent to the circular plots where  $\text{NH}_3$  volatilization was measured in three out of the five experimental sites. The winter wheat plots were fertilized with different rates of urea and urea + NBPT. The goals of this study were to: 1) quantify  $\text{NH}_3$  emissions from broadcast urea and urea + NBPT and 2) assess the impact of possible N losses on winter wheat during cold months in Kansas.

## 2.2 Material and Methods

### 2.2.1 Site description

Five sampling campaigns, lasting from 29 to 42 days, were carried out to measure  $\text{NH}_3$  emissions from fertilized plots in Kansas during the winter wheat growing seasons of 2016-17 and 2017-18. Three sampling campaigns were conducted under conventional tillage system at Ash1, Ash2 and Ash3 (Tables 2.1 and 2.2). The other two campaigns were carried out under no-tillage system: Sol (following winter wheat) and Kon (following maize, *Zea mays* L.). At Sol, the stubble originated from winter wheat grown during the previous growing season. At Kon, the stubble originated from maize grown during the 2018 season. Soil and management practices are shown in Table 2.2. Soil pH, particle size distribution, cation exchange capacity (CEC) and soil organic carbon (SOC) content were determined from composite soil samples consisting of six individual

soil cores. These soil samples were collected at each location prior to the fertilization date. Samples were collected from two depths: 0-15 cm and 15-60 cm.

### 2.2.2 The IHF approach

The IHF method was used with passive samplers to measure NH<sub>3</sub> volatilization. Leuning et al. (1985) demonstrated that the mass of NH<sub>3</sub> collected by this NH<sub>3</sub> sampler is proportional to the mean horizontal NH<sub>3</sub> flux density. Following the procedure described by these authors, we calculated the NH<sub>3</sub> vertical flux ( $F$ ,  $\mu\text{g m}^{-2} \text{day}^{-1}$ ) using the following expression:

$$F = \frac{1}{x} \int_0^z \frac{M(z)}{At} - \frac{M_b(z)}{At} dz \quad (2.1)$$

where  $x$  is the fetch distance corresponding to the radius of the circular plot (20 m in this study),  $M$  and  $M_b$  are the mass of NH<sub>3</sub> ( $\mu\text{g}$ ) collected by samplers deployed at different heights ( $z$ ) above fertilized and unfertilized (background) areas, respectively,  $t$  is time (d) and  $A$  is the effective cross-sectional sampling area of the sampler, which is  $2.42 \times 10^{-5} \text{ m}^2$  as determined by Leuning et al. (1985).

### 2.2.3 NH<sub>3</sub> volatilization sampling campaigns

NH<sub>3</sub> emissions were measured above three circular plots with 20-m radius at each location. Custom build NH<sub>3</sub> samplers (Advanced Manufacturing Institute, Manhattan, KS), manufactured following the exact technical specifications described by Leuning et al. (1985), were used in the NH<sub>3</sub> volatilization measurements. A mast with five NH<sub>3</sub> samplers was set up in the center of each circular plot. The samplers were deployed at the following heights: 0.30, 0.50, 0.95, 1.55 and 2.60 m for locations Ash1, Ash3 and Sol, and 0.34, 0.55, 1.05, 1.60 and 2.60 m for locations Ash2 and Kon. The difference of sampler height among some locations was necessary due to the presence of plant residue on the soil surface at certain locations requiring an increase of the lowest sampler

height. The circular plots were positioned so that the masts were located at least 100 m from each other to avoid contamination among plots (Leuning et al., 1985).

$\text{NH}_3$  volatilization sampling campaigns for each location consisted of two treatments, urea and urea + NBPT applied at a rate of 60 kg of N  $\text{ha}^{-1}$ , which corresponds to the average N fertilizer rate for wheat in Kansas (USDA-ERS, 2017). The third circular plot was not fertilized to provide measurements of the  $\text{NH}_3$  background concentrations required for the flux calculations (Eq. 1). The urea + NBPT treatment consisted of urea amended with a liquid formulation (1 g  $\text{kg}^{-1}$ ) of NBPT (Agrotain Ultra, Koch Agronomic Services, Wichita, KS) at the recommended manufacturer rate of 2.1  $\text{cm}^3 \text{kg}^{-1}$ .

Before field deployment, the samplers were activated following the procedure described by Leuning et al. (1985). Initially, the sampler interiors, containing a stainless steel coil, were coated with a solution of 30 g  $\text{L}^{-1}$  of oxalic acid in acetone (Leuning et al., 1985). Prior to the acid activation, the samplers were sealed using custom-made PVC (Polyvinyl Chloride) caps with O-rings that created a water-tight seal. Then, a 40-mL aliquot of the oxalic acid solution was poured into the sampler through an orifice in one of the PVC caps. The orifice was closed with a plastic threaded plug and the sampler was rolled over a laboratory bench for at least 15 s to ensure uniform distribution of the acid solution inside the sampler. The cap orifice was opened to drain the excess solution under a fume hood. After the sampler was dry, the orifice was closed again with the threaded plastic plug for transportation to the field.

The  $\text{NH}_3$  samplers from all plots were replaced on a weekly basis by new samplers. Fertilization date and samplers exchange dates are shown on Table 2.1. The previously-deployed samplers were brought back to the laboratory and rinsed with 200 mL of distilled water, added through the sampler cap orifice. This orifice was closed, and the sampler was shaken at a constant



speed for 45 s with a reciprocal shaker (Eberbach analytical shaker, Corporation Ann Arbor, MI). A 40-mL aliquot of the water solution was then taken from each sampler and transferred to a polypropylene container. An aliquot of  $\text{NH}_4^+$  concentration was determined using the indophenol colorimetric reaction method (Alpkem Corporation. 1986. RFA Methodology No. A303-S021) and a rapid flow analyzer (Model RFA-300, Alpkem Corporation, Clackamas, OR).

#### 2.2.4 Experimental plots to assess the influence of $\text{NH}_3$ volatilization on winter wheat

The effect of  $\text{NH}_3$  volatilization and different N application rates on winter wheat grain yield, N recovery and AE was evaluated at experimental plots established adjacent to the  $\text{NH}_3$  volatilization plots at Ash1, Sol, and Ash2. A two-way complete factorial treatment structure was arranged in a randomized complete block design with four replications for a total of eight treatments plus a control. The treatments consisted of four N application rates (30, 60, 90 and 120 kg of N  $\text{ha}^{-1}$ ) and two N sources (urea and urea + NBPT). Winter wheat plots were sown at 2.1 million seeds per hectare. Each plot measured 1.5 x 12 m. The hard red winter wheat variety WB 4458 was sown at the three locations, and the fertilizer was broadcast uniformly in all plots on the same day that the circular plots were fertilized (Table 2.2).

The wheat plots were harvested using a plot combine (Hege 140, Hege Equipment, Colwich, KS). Grain yield was determined by harvesting the entire experimental unit. The total N concentration was determined from wheat grain samples, which were cleaned using an air-blast seed cleaner (Alma, Co, SABSCIC, Nevada IA), ground and analyzed using the combustion method (Campbell and Plank, 1992). Total grain N concentration was used to calculate the grain N removal (GNR), which is the product between grain N concentration and grain yield. We calculated N recovery (Varvel and Peterson, 1990) and AE (Duncan et al., 2018), according to Eq. (2) and (3):

$$NRecovery (\%) \left( \frac{Kg_{grain\ N}}{Kg\ N} \right) = \frac{GNR_{treat} - GNR_{control}}{fert\ N} \quad (2)$$

$$AE \left( \frac{Kg_{grain\ N}}{Kg\ N} \right) = \frac{Yield_{treat} - Yield_{control}}{fert\ N} \quad (3)$$

### 2.2.5 Environmental data for gas sampling campaigns and winter wheat experimental plots

Precipitation, wind speed and direction data for Ash1, Ash2, Ash3 and Sol were collected from the closest Kansas Mesonet Station. For locations Ash1, Ash2 and Ash3 the station (Kansas Mesonet - Ashland Bottoms) was located within less than 0.5 km from the gas sampling campaigns. Sol was located 20 km from the closest Mesonet station (Kansas Mesonet – Gypsum). For Kon, precipitation was obtained from the Long Term Ecological Research (LTER) (Nippert, 2019) meteorological station, located less than 0.5 from the sampling campaign. For this same location, wind speed and direction were obtained from Kansas Mesonet - Ashland Bottoms. For Ash 1 and Son, the soil temperature was obtained from the Mesonet station, which was measured at 5 cm using a soil temperature probe (BetaTherm 100K6A11A, Campbell Scientific, Logan UT). The wind speed and direction were measured at 2 m above the ground using an anemometer (Model 05103, Young Company, Traverse City, MI). Wind speed and direction were grouped in different classes to investigate their frequency distributions for each location during the NH<sub>3</sub> volatilization sampling campaigns. A tipping bucket rain gauge (TB525, Hydrological Services America, Lake Worth, FL) was used to measure precipitation. For Kon, a weighing rain gauge (OTT Pluvio<sup>2</sup>, OTT Hydromet, VA) was used to measure precipitation. For Ash2, Ash3 and Kon, soil temperature was measured at 2 cm using six dual-probe heat-pulse sensors (Campbell et al., 1991; Bristow et al., 1994) connected to a datalogger (CR 1000, Campbell Scientific, Logan UT).

For Ash1 and Sol, volumetric water content ( $\theta_v$ ) was obtained from seven soil samples (depth 5 cm) using a metal cylinder (height = 5 cm and radius = 2.5 cm). For Ash1, soil samples were collected on the fertilization date and on the following sampler exchange. For Sol, soil

samples were collected on the fertilization date and on all sampler exchange dates. For Ash2, Ash3 and Kon,  $\theta_v$  was measured at 2 cm using the same six dual-probe heat-pulse sensors (Campbell et al., 1991; Bristow et al., 1994).

### 2.2.6 Analytical methods and interpretation

The impacts of urea amendment with NBPT on winter wheat yield, N recovery and AE were assessed using single degree-of-freedom orthogonal contrasts. The contrast comparisons were made between urea and urea + NBPT for the four different rates of N application. The contrasts considered all location-years combined, and no interaction (*p-value 0.1004*) between rates and source (urea and urea + NBPT) was found. In addition, we also evaluated the influence of NBPT on winter wheat yield, N recovery and AE for each location using non-linear regression models.

## 2.3 Results and Discussion

### 2.3.1 Environmental conditions

Ash1 and Sol had predominantly southern wind direction, and most of these events, 74% and 80% for Ash1 and Sol, respectively, had the wind speed between 2 to 6 m s<sup>-1</sup>. Ash2 had predominant northwestern wind events, and 81% of wind speed data points varying between 2 to 6 m s<sup>-1</sup>. Ash3 and Kon also had predominant southern wind events, and 49% of wind speed events ranged from 2 to 4 m s<sup>-1</sup>, for both locations (Fig. 2.1).

For Ash1, Sol and Ash2, the largest precipitation event following urea broadcast occurred at Ash1 (11.4 mm) 18 d post fertilization (DPF) (Fig. 2.2 a, c, e), and the average volumetric soil water content ( $\overline{\theta v}$ ) during the first two sampler exchanges at this location was 0.32 m<sup>3</sup>m<sup>-3</sup>. All other precipitation events were light (< 6.5 mm). The occurrence of light precipitation events helps to explain the low variability on soil water content for Sol ( $\overline{\theta v} = 0.33 \text{ cm}^3\text{cm}^{-3}$ ) and Ash2 ( $\overline{\theta v} =$

0.20 cm<sup>3</sup>cm<sup>-3</sup>). Average daily soil temperatures were 6.2, 7.5 and 7.7 °C, for Ash1, Sol and Ash2, respectively (Fig. 2.2 a, c, e). For Ash3 and Kon,  $\overline{\theta v}$  were 0.36 and 0.33 cm<sup>3</sup>cm<sup>-3</sup>, respectively. The total precipitation was 35.6 and 41.4 mm, and the average daily soil temperature for both locations were 2.6 °C and 3.2 °C, respectively.

### 2.3.2 NH<sub>3</sub> fluxes measurements from sampling campaigns

Maximum urea ( $F_{N-Urea}$ ) and urea + NBPT ( $F_{N-NBPT}$ ) NH<sub>3</sub> fluxes occurred around 20 DPF for all sampling campaigns (Fig. 2.2). The highest  $F_{N-Urea}$  happened at Ash3 and Kon, and maximum values at both locations coincides a with a considerable precipitation event (28 and 34 mm, respectively). At Sol, there is a declining curve of  $F_{N-Urea}$  and  $F_{N-NBPT}$  toward the last day of sampling, however, the final fluxes values were not minimal, as observed on the others sampling campaigns.

$F_{N-Urea}$  and  $F_{N-NBPT}$  emission peak at the Ash1, Sol and Ash2 was preceded by rainfall events between 4.0 and 12 mm. According to Rochette et al. (2009), rainfall events smaller than 12-15 mm can increase the soil moisture and enhance the urease activity, nevertheless, these events are not enough to carry N into deeper layers of the soil profile. This could be an explanation to the emissions found at Ash1, Sol and Ash2.

Silva et al. (2017) reported  $F_{N-Urea}$  and  $F_{N-NBPT}$  from 35 studies under cold (temperate regions) and warm (tropical regions) weather conditions. They found that when urea was broadcast, it took 3.3, 4.8 and 6.3 days for 25, 50 and 75%, respectively, of the total NH<sub>3</sub> volatilization loss to occur. Meanwhile, when urea was amended with NBPT, 25, 50 and 75% the total NH<sub>3</sub> volatilization losses occurred at 6.0, 8.3 and 10.6 DPF, respectively. Other studies have shown that the peak of NH<sub>3</sub> volatilization occurs within the first 3 days after urea application on the surface with soils with high water content (Black et al., 1985, 1987; Turner et al., 2010, 2012).

On the other hand, Engel et al., (2011) observed a long duration of  $\text{NH}_3$  emissions from surface applied urea for 12 campaigns during winter months in the state of Montana, US. These authors reported that 90% of the  $\text{NH}_3$  volatilization occurred within 30 DPF in more than 60% of their trials. The reasons for these prolonged  $\text{NH}_3$  emission periods in cold months could be associated to the reduction of urea hydrolysis rate resulting from dry soil conditions and cold temperatures (Ernst and Massey, 1960; Kissel et al. 2008; Behera et al., 2013) common in the US Northern Great Plains (Montana, Wyoming and North Dakota) (Engel et al., 2011). In our study, we observed that 75% of the  $\text{NH}_3$  volatilization occurred around 25 DPF for campaigns Ash1, Ash2 and Sol. Meanwhile, 75% of the total  $\text{NH}_3$  volatilization occurred at 15 DPF for campaigns Ash3 and Kon. The results for Ash3 and Kon are in agreement to Ni et al. (2014), who found  $F_{\text{N-Urea}}$  lasting from 15 to 30 DPF under cold weather conditions for winter wheat plots in Germany. We observed reduction on  $\text{NH}_3$  fluxes (Fig. 2.2 h and j) 20 DPF at these locations, and this is in agreement with the findings of Ma et al. (2010), who reported that  $\text{NH}_3$  volatilization decreased after 20 to 28 DPF under in temperate conditions in Canada.

### 2.3.3 Cumulative N losses from sampling campaigns

Cumulative N losses through  $\text{NH}_3$  volatilization from surface applied urea ( $N_{\text{L-Urea}}$ ) and urea + NBPT ( $N_{\text{L-NBPT}}$ ) are shown in Fig. 2.3.  $N_{\text{L-Urea}}$  ranged from 3.2 to 29.6% of applied N. Highest values of  $N_{\text{L-Urea}}$  were found at Ash3 and Kon. Meanwhile,  $N_{\text{L-NBPT}}$  ranged from 0.3% to 17.0 % of applied N, and the highest value was found at Sol.

The NBPT urea amendment reduced nitrogen losses for Ash1 by 2.8% of applied N. However, it was not effective on reducing nitrogen losses at Sol ( $N_{\text{L-NBPT}}$  1.29% higher than  $N_{\text{L-Urea}}$ ) and Ash2 ( $N_{\text{L-NBPT}}$  0.92% higher than  $N_{\text{L-Urea}}$ ). For Ash3 and Kon, the NBPT reduced nitrogen losses by 26.8% and 21.8% of applied N, respectively.

Cantarella et al. (2018) reviewed the agronomic efficiency of NBPT as a urease inhibitor. They argued that one of the NBPT limitations is related to the short period of effective inhibition (10 to 15 days), and that  $\text{NH}_3$  volatilization is not completely eliminated when amending urea with NBPT. This helps to explain the NBPT inconsistency in reducing  $\text{NH}_3$  volatilization losses at Sol and Ash2. In addition, the  $\text{NH}_3$  fluxes at Ash2 are within the range of the methodology error (~ 5 to 10%). Although we have not measured the uncertainty of the IHF approach for each location, we carried out an inter-comparison trial with  $\text{NH}_3$  samplers by placing them at the same height above the ground (~ 1 m) and we found a coefficient of variation among samplers of approximately 10%. Other authors estimated uncertainty of the IHF approach in 10% (Ryden and McNeill, 1984) and up to 20% (Wilson and Shum, 1992). Engel et al. (2011) calculated an average coefficient of variation of 6.3% of the horizontal flux for the locations evaluated in their study.

The largest cumulative  $\text{NH}_3$  losses (23.2 to 29.6 % of applied N) occurred when urea was broadcast onto a moist soil ( $\overline{\theta v} = 0.41$  and  $0.34 \text{ cm}^3\text{cm}^{-3}$  for Ash3 and Kon, respectively) and followed by at least four consecutive days with no precipitation. Losses were moderate (maximum ~ 17%) for Sol and low (< 5%) for Ash1 and Ash2. Engel et al. (2011) found  $N_{\text{L-Urea}}$  ranging from 3.1 to 44.1% and  $N_{\text{L-NBPT}}$  between 1.4 and 18%. These authors reported that the largest nitrogen losses (30 - 44% of applied N) occurred when urea was broadcast onto a wet surface and followed by low soil evaporation conditions and light precipitation events ( $\leq 6$  mm). The authors observed that minimal losses (< 10% of applied N) occurred when the fertilizer was broadcast on a dry surface or followed by a large single-event precipitation (18 to 25 mm). Turner et al. (2012) used a simplified mass balance micrometeorological method (Denmead 1983; Freney et al. 1985) to estimate  $F_{\text{N-Urea}}$  and found  $N_{\text{L-Urea}}$  ranging from 13 to 23% of applied N during cold and dry weather conditions for cereal production season in Australia. Ni et al. (2014) found values of  $N_{\text{L}}$ .

Urea from urea broadcast application varying between 2.7 to 24 % of applied N during the cold season Germany.

Rochette et al. (2009) showed that the presence of crop residues on the soil surface contributes to enhance urease activity, leading to an increase of  $F_{N-Urea}$ . They also reported that the presence of crop residues potentially helps to trigger higher N losses through  $NH_3$  volatilization. The presence of crop residues on Sol could explain the higher N losses in this location when comparing it to Ash1 and Ash2, considering that all these locations had similar environmental conditions (Fig.2.2 and Table 2.2). Nonetheless, we observed larger  $NH_3$  losses for Ash3 (conventional tillage) than for Kon (no-tillage). As both locations were located within 3 km of each other, resulting in similar weather conditions, it is likely that the crop residue had a minimal contribution on  $NH_3$  volatilization under these environments.

#### 2.3.4 Effect of N rate application on winter wheat grain yield, N recovery and AE

Grain yield response to different rates of urea and urea + NBPT is shown in Fig. 2.4. Across all locations, the average grain yield increments for different N application rates when compared to control were 16.2%, 32.1%, 44.5% and 46.1% respectively to 30, 60, 90 and 120 kg N ha<sup>-1</sup> (Fig. 2.4). These increments were described using a non-linear regression model to investigate the relationship between grain yield and N fertilization rate. In addition, and a very similar regression model was found for urea and urea + NBPT for all locations. Fig. 2.5 shows the relationship between N recovery and N application rates. We found a significant negative relationship ( $p < 0.05$ , Fig. 2.5) between N recovery and application rates for urea treatments in Ash2 and Sol. Meanwhile, urea + NBPT treatments had a significant negative relationship ( $p < 0.05$ , Fig. 2.5) between N recovery and N application rates in all locations. AE decreased at a significant negative linear relationship ( $p < 0.05$ , Fig. 2.6) when increasing N application rates for

urea + NBPT at all locations. Nonetheless, this relationship for urea treatments was only significant at Ash1 ( $p = 0.017$ , Fig. 2.6). For grain yield, N recovery and AE, the main differences between treatments within each location are due to different rates of N application, especially when comparing 60 and 90 kg N ha<sup>-1</sup> to 30 kg N ha<sup>-1</sup>. The confidence interval of the regressions for urea and urea + NBPT, for grain yield, N recovery and AE, overlapped in all locations, indicating no statistical difference between the regressions for urea and urea + NBPT.

The grain yield quadratic response to N application rate (Fig. 2.4) was found in previous studies (Girma et al., 2007; Howard et al., 1994; Lollato et al., 2019; Nelson et al., 2014). The notable increase on grain yield at low rates of N application is attributed to increase on tiller formation and survival and increase in kernel number when available N is insufficient to achieve maximum yield (Borghini, 1999). A synthesis of long-term wheat experiments reported that the declining trend towards higher N rates can be driven by several factors (Lollato et al., 2019). Possible drivers decreasing grain yield at high N rates entails: increasing lodging potential (Lollato and Edwards, 2015), weakening of vegetative organs (Borghini, 1999) and parasite vulnerability (Howard et al., 1994). Our results showed that urea and urea + NBPT had a very similar quadratic response to grain yield. For Ash1, urea + NBPT resulted in lower N loss (-2.8% of applied N) when compared to urea only, and this loss equates only to 1.68 kg of N ha<sup>-1</sup> of 60 kg of N ha<sup>-1</sup> fertilization rate, which is a small fraction compared to total N pool (fertilization + soil available N) 156 kg of N ha<sup>-1</sup>. Previous studies showed that NBPT mitigation of cumulative NH<sub>3</sub> losses in more than 30% resulted in minimal or no improvements on rainfed barley and spring wheat grain yield (Thapas et al., 2015; Abalos et al., 2012).

Our results pointed that higher N application rates resulted in lower N recovery (Fig. 2.5) for urea and urea + NBPT. An assessment of N recovery by grain crops (Krupnik et al., 2004)



reported that N recovery will decrease with increase N application rates due to higher chances of N losses through run-off, leaching and gaseous emissions (Raun and Johnson, 1999; Baligar et al., 2001). Our results showed no statistical difference between urea and urea + NBPT. Meanwhile, Romero et al. (2017) found that amending urea with NBPT improved N recovery, in particular where NBPT reduced cumulative NH<sub>3</sub> loss by over 60%. The authors found a strong relationship between cumulative NH<sub>3</sub> losses and N recovery, which reinforced the importance of NH<sub>3</sub> volatilization as a N loss pathway. Additionally, the authors highlighted that largest NBPT benefits on N recovery was found under environmental conditions that promoted NH<sub>3</sub> losses. Our findings showed that AE was sensitive to N fertilization as it decreased with higher N application rates (Fig. 2.6). However, no improvements were found when amending urea with NBPT, and this is because NBPT had minimal effects on grain yield (Fig.2.4). Lastly, our low NH<sub>3</sub> losses findings (< 5% of applied N, Fig. 2.3) could be an explanation to minimal differences between urea and urea + NBPT on N recovery and AE.

Our study is one of a few efforts to measure NH<sub>3</sub> emissions continuously from broadcast urea, and to assess the agronomic impact of NH<sub>3</sub> volatilization on winter wheat production. Future studies should consider the use of the IHF approach, which is a robust method to measure NH<sub>3</sub> volatilization from agricultural sites (Denmead et al., 1983; Sha et al., 2006). One should have in mind this approach requires extensive sampling area (at least 0.5 ha) and it is time and labor demanding. Future studies should also investigate the effect of different N application rates – constant at 60 kg of N ha<sup>-1</sup> in this study – on NH<sub>3</sub> volatilization when using the IHF approach. Chen et al. (2015) reported that increasing the amount of broadcast N can significantly increase cumulative NH<sub>3</sub> volatilization losses. In addition, we only considered a one-time N application. Accounting for different application times, as performed by Engel et al. (2017) and Romero et al.

(2017), would bring a better understanding on the relationship between  $\text{NH}_3$  emissions and different weather conditions. Furthermore, considering that different biotic and abiotic variables govern  $\text{NH}_3$  production and transport between soil and atmosphere, the use of mechanistic biogeochemical models to interpret the  $\text{NH}_3$  fluxes could be bring new insights into the variables governing the  $\text{NH}_3$  volatilization process under cold weather environments (Dutta et al., 2016; Dubache et al., 2019; Li et al., 2019). From a practical perspective, these models could also be used by stakeholders as a decision support tools to improve N fertilization efficiency at the farm level.

Finally, our results (Ash3 and Kon, Fig. 2.3) indicates that broadcast urea to cold surface soils can lead to substantial  $\text{NH}_3$  volatilization losses (> 20% of applied N) and suggests that winter wheat growers should carefully evaluate the soil moisture conditions before broadcast urea to avoid potential  $\text{NH}_3$  volatilization losses. As pointed by Engel et al. (2011), in the absence of NBPT the best strategy to avoid  $\text{NH}_3$  losses is to delay the application of urea until the soil is dry.

#### 2.4 Conclusions

Total  $\text{NH}_3$  cumulative losses varied from <1% to 29%. Largest N losses happened when urea was broadcasted to soils with high water content followed by a dry period. These conditions likely reduced the transport of urea into deeper layers of the soil profile. Typically,  $\text{NH}_3$  emissions peaked after 20 DPF. Amending urea with NBPT helped to reduce  $\text{NH}_3$  volatilization losses by more than 20% at locations where the largest N losses occurred (locations Ash3 and Kon). However, the use of NBPT resulted in small (2.8%) or no cumulative N loss reductions at locations (Ash1, Ash3 and Sol) where  $\text{NH}_3$  volatilization were low to moderate. The impact of  $\text{NH}_3$  volatilization on winter wheat was only evaluated at these last three locations, which were fertilized during the spring. Our results show minimal agronomic benefits of amending urea with

NBPT on winter wheat grain yield, N recovery and AE. Future research is still necessary to understand the role of different environmental drivers on NH<sub>3</sub> volatilization.

### 2.5 Acknowledgments

We are grateful to the Kansas Fertilizer Research Fund and Koch Agronomic Services for supporting this research. We would also like to thank Prajaya Prajapati, Fernando Dubou Hansel, Hugo Abelardo Gonzalez Villalba and the undergraduate students involved in this project.

## Chapter 2 – Tables and Figures

**Table 2.1** Field experiments locations, fertilization date, sampler exchange dates and winter wheat plots planting and harvest date and seeding rate.

| Site | Location       |                 | Fertilization day | Sampler exchange dates | Winter wheat plots   |               |
|------|----------------|-----------------|-------------------|------------------------|----------------------|---------------|
|      | Latitude       | Longitude       |                   |                        | d post fertilization | Planting date |
| Ash1 | 39° 7' 16.46"  | -96° 38' 26.12" | 2/2/2017          | 7, 14, 22, 27, 35, 41  | 10/18/2016           | 6/22/2017     |
| Sol  | 38° 56' 27.21" | -97° 26' 26.18" | 2/8/2017          | 7, 15, 23, 29          | 10/14/2016           | 6/23/2017     |
| Ash2 | 39° 7' 26.40"  | -96° 38' 23.71" | 3/1/2018          | 7, 14, 22, 29, 34, 42  | 10/23/2017           | 6/20/2018     |
| Ash3 | 39° 7' 30.46"  | -96° 38' 31.39" | 11/13/2018        | 4, 7, 14, 24, 29       |                      |               |
| Kon  | 39° 6' 43.78"  | -96° 36' 42.50" | 11/12/2018        | 3, 6, 10, 17, 30       |                      |               |

**Table 2.2** Soil characteristics (particle size distribution, cation exchange capacity (CEC), pH and organic matter) for all five locations and tillage practice. Except for NO<sub>3</sub>-N, all other soils characteristics were measured at depth: 0 to 15 cm.

| Site | Soil series             | Soil texture (%) |      |      | CEC<br>cmol kg <sup>-1</sup> | pH  | Organic matter<br>g kg <sup>-1</sup> | NO <sub>3</sub> -N*<br>ppm | Tillage           |
|------|-------------------------|------------------|------|------|------------------------------|-----|--------------------------------------|----------------------------|-------------------|
|      |                         | Sand             | Clay | Silt |                              |     |                                      |                            |                   |
| Ash1 | Smolan silt loam        | 20               | 24   | 56   | 21.0                         | 5.5 | 2.6                                  | 11.0                       | Conventional till |
| Sol  | Detroit silty clay loam | 12               | 32   | 56   | 24.5                         | 6.2 | 3.4                                  | 1.7                        | No-till           |
| Ash2 | Smolan silt loam        | 38               | 30   | 32   | 22.7                         | 5.7 | 2.3                                  | 4.7                        | Conventional till |
| Ash3 | Smolan silt loam        | 12               | 54   | 34   | 18.2                         | 6.7 | 3.0                                  | -                          | Conventional till |
| Kon  | Sutphen silty clay      | 12               | 54   | 34   | 26.8                         | 6.2 | 3.2                                  | -                          | No-till           |

\*Soil property measured at depth: 0 to 60 cm.

**Table 2.3** Pairwise comparisons ( $p = 0.05$ ) between urea and urea + NBPT for different nitrogen application rates (30, 60, 90 and 120 kg N ha<sup>-1</sup>), considering yield, N recovery and AE.

| Contrast           | Yield    |                | N recovery |                | AE       |                |
|--------------------|----------|----------------|------------|----------------|----------|----------------|
|                    | Estimate | <i>p value</i> | Estimate   | <i>p value</i> | Estimate | <i>p value</i> |
| Urea x NBPT        | -0.585   | 0.076          | -0.349     | 0.007**        | -13.374  | 0.040*         |
| Control x Urea     | -3.837   | <.0001         | -1.533     | <.0001         | -51.519  | <.0001         |
| Control x NBPT     | -4.421   | <.0001         | -1.882     | <.0001         | -64.893  | <.0001         |
| Urea vs NBPT (30)  | -0.276   | 0.094          | -0.242     | 0.0003**       | -9.186   | 0.005*         |
| Urea vs NBPT (60)  | -0.213   | 0.195          | -0.086     | 0.183          | -3.546   | 0.273          |
| Urea vs NBPT (90)  | 0.057    | 0.726          | 0.028      | 0.668          | 0.638    | 0.843          |
| Urea vs NBPT (120) | -0.154   | 0.348          | -0.048     | 0.453          | -1.280   | 0.692          |

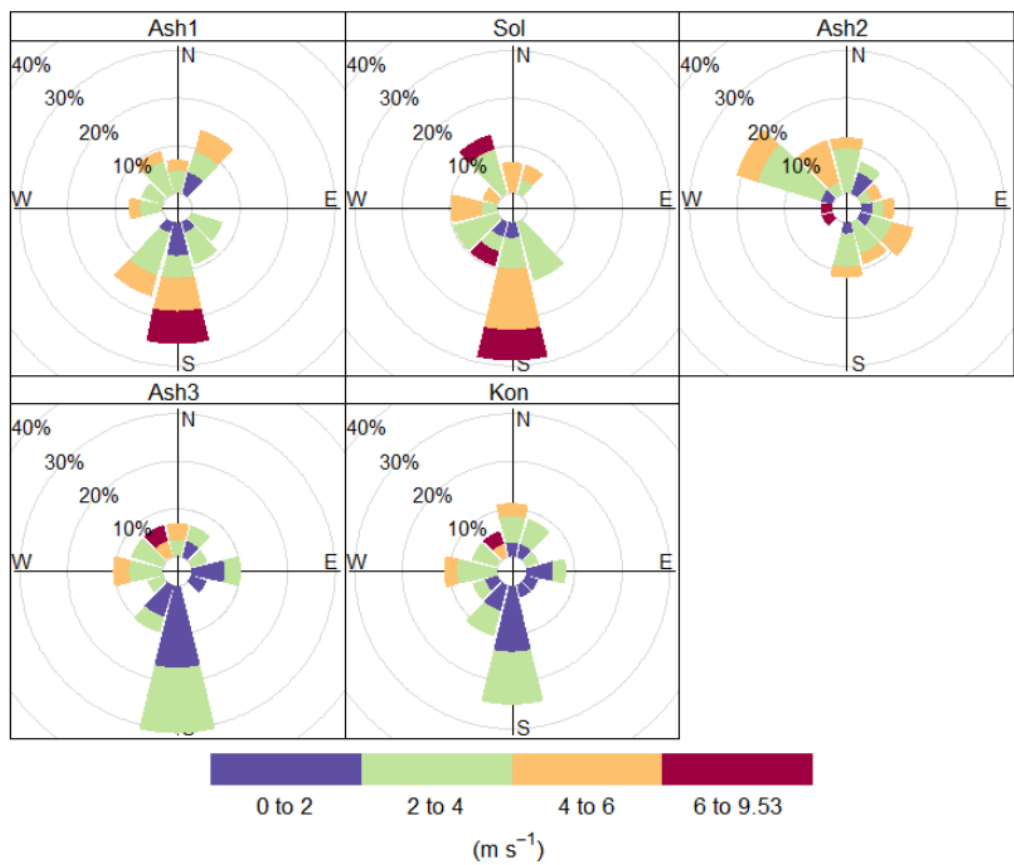


**Figure 2.1** - Frequency distribution of wind speed and direction during the  $\text{NH}_3$  volatilization measurements period (Table 2.1) for all five locations.

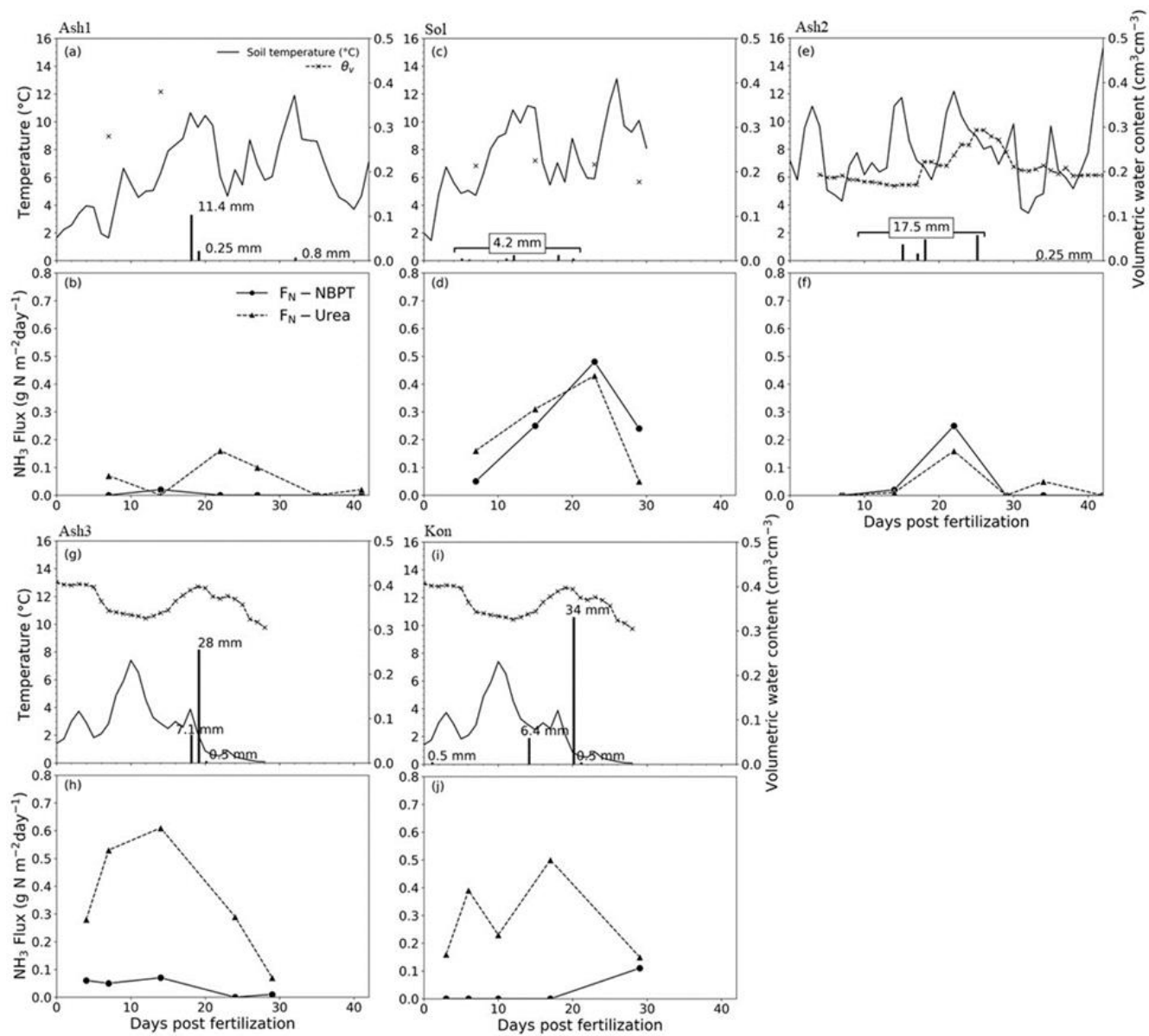


**Figure 2.2** Average daily soil temperature ( $^{\circ}\text{C}$ ) and volumetric soil water content ( $\theta_v$ )( $\text{cm}^3\text{cm}^{-3}$ ) (upper panels – a, c, e, g and i).  $\text{NH}_3$  flux for soil plots treated with urea and urea + NBPT (lower panels – b, d, f, h and j). Soil temperature was measured at 5 cm depth and obtained from the closest Kansas Mesonet weather station for Ash1 and Sol. For Ash2, Ash3 and Kon soil temperature was measured at 2 cm depth using dual-probe heat-pulse sensors (Campbell et al., 1991; Bristow et al., 1994). For Ash1 and Sol,  $\theta_v$  was measured from seven soil samples (depth 5 cm) using a metal cylinder (height = 5 cm and radius = 2.5 cm). For Ash1, Ash3 and Kon  $\theta_v$  was measured at 2 cm depth using dual-probe heat-pulse sensors (Campbell et al., 1991; Bristow et al., 1994).

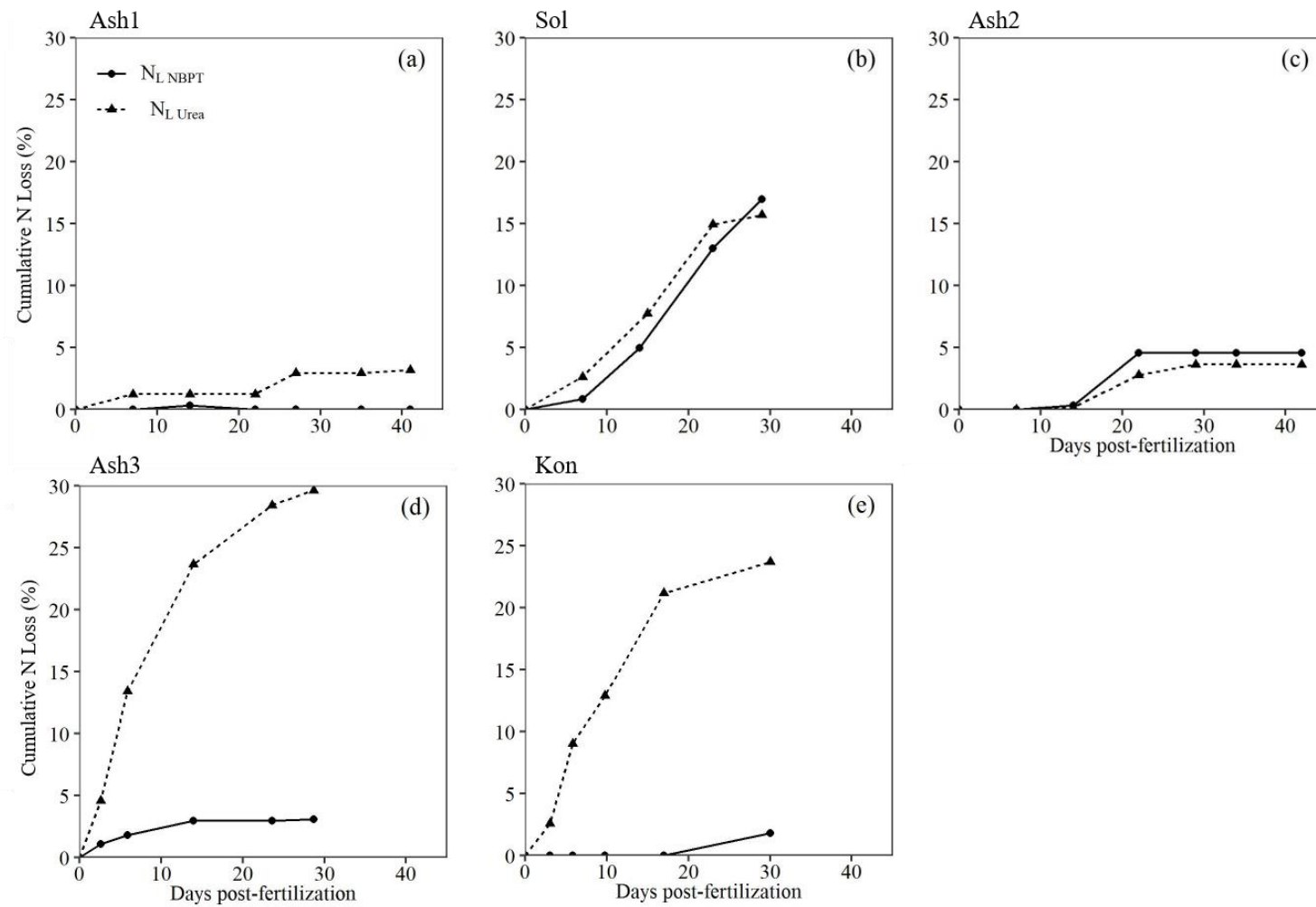


**Figure 2.3** Cumulative N losses (% of N applied) for all five sampling campaigns, for urea and urea + NBPT.



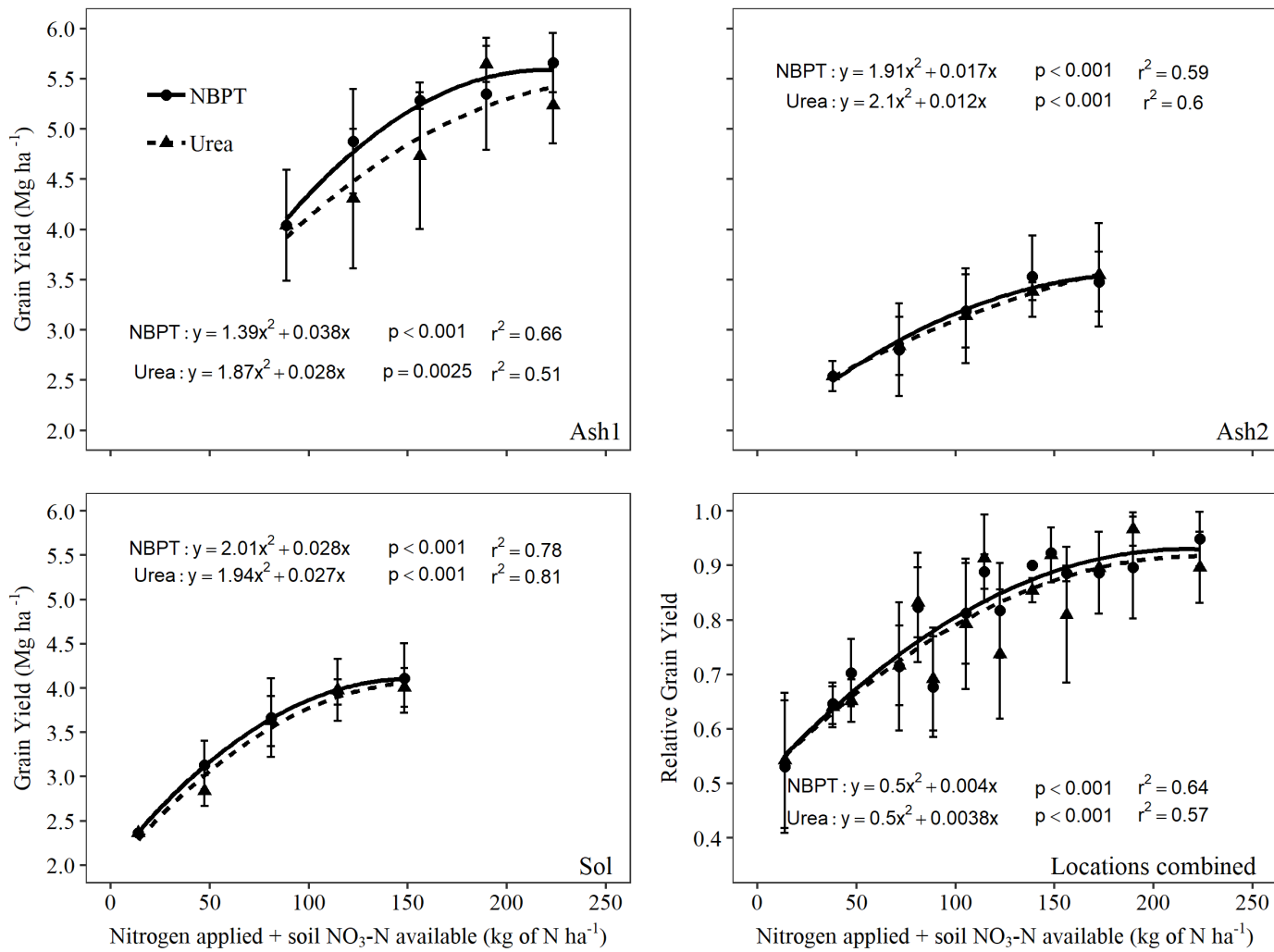


**Figure 2.4** Grain yield response to soil available N (0-60 cm) + N application rates (kg of N ha<sup>-1</sup>) for the three experimental locations (Ash1, Sol and Ash2) and for all locations combined. Bars represent standard errors.

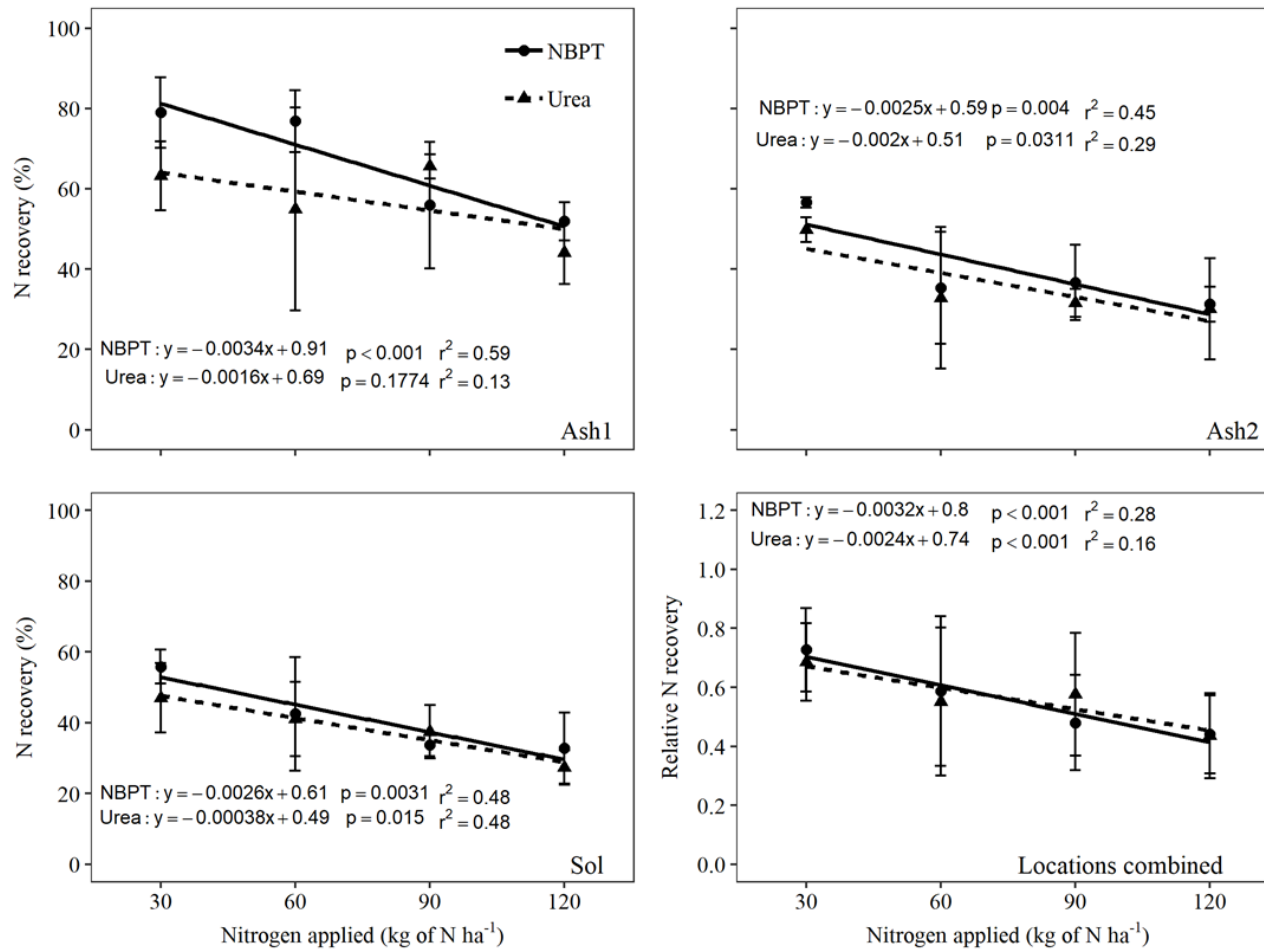


**Figure 2.5** N recovery as a function of soil available N (0-60 cm) + N application rates (kg of N ha<sup>-1</sup>) for the three experimental locations (Ash1, Sol and Ash2) and for all locations combined. Bars represent standard errors.

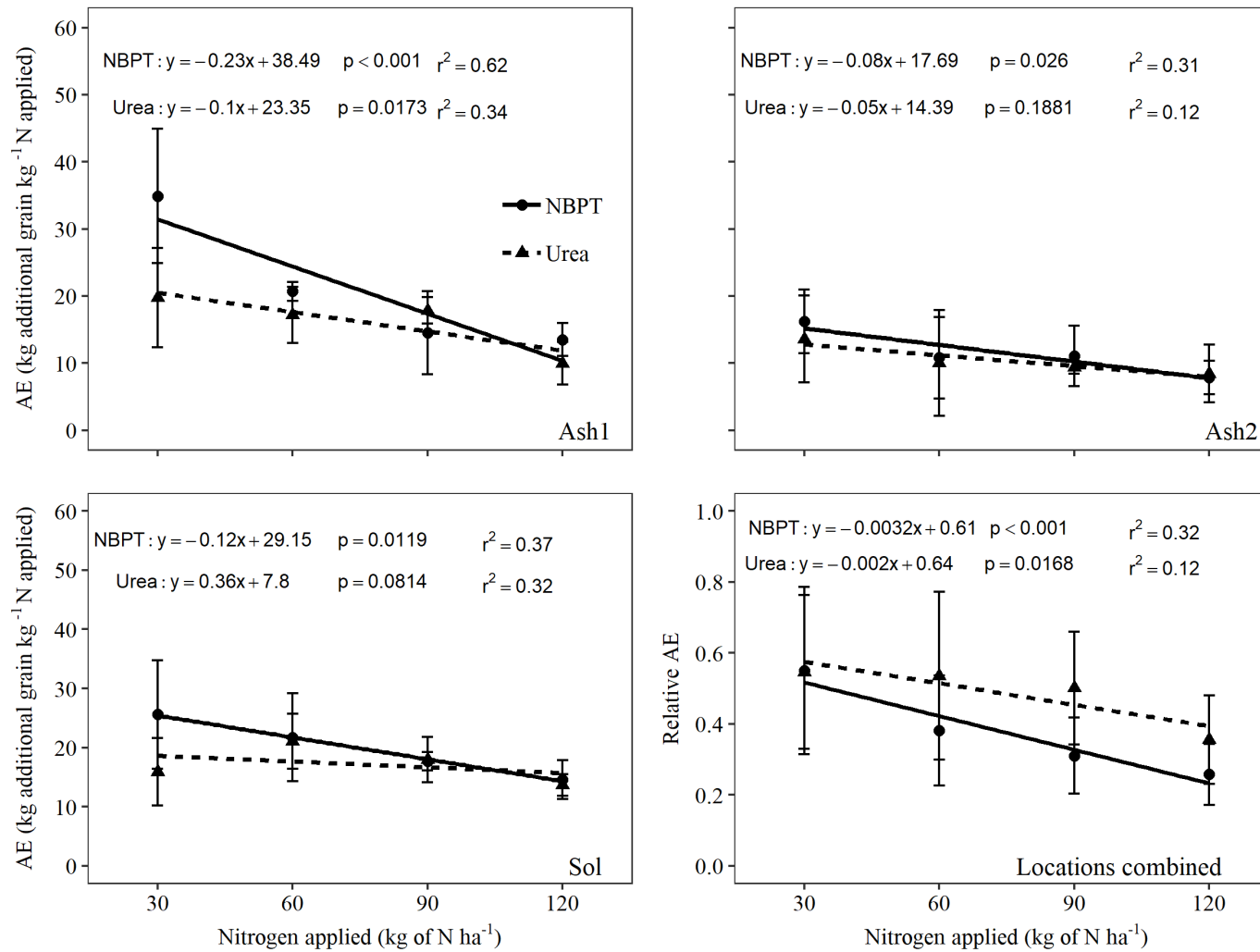


**Figure 2.6** Agronomic efficiency (AE) as a function of soil available N (0-60 cm) + N application rates (kg of N ha<sup>-1</sup>) for the three experimental locations (Ash1, Sol and Ash2) and for all locations combined. Bars represent standard errors.

## **Chapter 3 - Assessment of the Denitrification-Decomposition (DNDC) model simulations of ammonia volatilization from broadcast urea**

### **ABSTRACT**

The Denitrification-Decomposition (DNDC) process-based biogeochemical model can be a resourceful tool for understanding temporal variability in  $\text{NH}_3$  emissions from agricultural fields. We compared the performance of two versions of the DNDC (to simulate  $\text{NH}_3$  volatilization losses from broadcast urea in 29 sampling campaigns conducted in the US Great Plains (Montana and Kansas). All sampling campaigns were conducted employing the integrated horizontal flux approach to measure  $\text{NH}_3$  volatilization continuously and over circular plots with 20 m in diameter. For the majority of the sampling campaigns, the DNDC v.CAN simulated  $\text{NH}_3$  emissions with lower errors ( $\overline{\text{RMSE}} = 10.9 \text{ kg of N ha}^{-1}$ ) when compared to the DNDC 9.5 ( $\overline{\text{RMSE}} = 32.8 \text{ kg of N ha}^{-1}$ ). In addition, both models  $\text{NH}_3$  emissions simulations had strong correlation ( $r \geq 0.8$ ) but poor accuracy ( $d \leq 0.7$ ) when compared with measured  $\text{NH}_3$  emissions. Furthermore, both models were able to simulate soil temperature with a strong correlation and good to excellent accuracy ( $d \geq 0.85$ ). However, the soil volumetric water content ( $\theta_v$ ) was poorly simulated by both models ( $\overline{\text{RMSE}} \geq 0.13 \text{ cm}^3\text{cm}^{-3}$ ). Our sensitivity analysis showed that soil pH and rate of N application were the most sensitive parameters affecting  $\text{NH}_3$  volatilization from broadcast urea. Moreover, a Random Forest (RF) importance feature analysis showed that soil pH and soil temperature are the most important factors contributing to  $\text{NH}_3$  emissions on both models. Finally, our study indicates the main limitations of the DNDC for simulating  $\text{NH}_3$  volatilization from broadcast urea that could be addressed in future model versions. These are: *i*) limitations in the soil-hydrology water sub-model affected the accuracy of the simulations of the effects of soil water content on urea

hydrolysis, which has direct effect on NH<sub>3</sub> volatilization; *ii*) both models failed to simulate the effects of accumulated precipitation ( $\geq 20$  mm) on NH<sub>3</sub> volatilization during the first 5-15 d post fertilization; *iii*) future developments of the DNDC should consider adding a more robust routine to simulate the effects of urease inhibitor on NH<sub>3</sub> volatilization and *iv*) the timing of the NH<sub>3</sub> volatilization peak after fertilization was underestimated by the DNDC v.CAN and largely overestimated by the DNDC 9.5

### 3.1 Introduction

Ammonia volatilization from broadcast urea can significantly reduce crop nitrogen use efficiency (Freney, 1988; Sommer et al., 2004; Rochette et al., 2009; Cantarella et al., 2018) and lead to air pollution (Vitousek et al., 1997). Therefore, adapting the current agricultural N management practices to mitigate NH<sub>3</sub> volatilization from broadcast urea is necessary for achieving global food security during the next decades.

Soil NH<sub>3</sub> emissions from broadcast urea are variable in time and in the landscape (Ernst and Massey, 1960; Freney et al., 1983). Therefore, continuous measurement of NH<sub>3</sub> volatilization over large areas are needed to capture this spatial-temporal variability. Micrometeorological techniques can be employed to measure NH<sub>3</sub> emissions from larger areas than commonly used soil chambers. Among the micrometeorological techniques, the integrated horizontal flux (IHF) method has been shown to accurately estimate NH<sub>3</sub> fluxes between surface and the atmosphere (Denmead, 1983; Ryden and McNeill, 1984; Wilson and Shum, 1992; Misselbrook et al., 2005). The IHF technique is based on mass balance principles, which leads to the assumption that the NH<sub>3</sub> emissions from a known surface area is equal to the NH<sub>3</sub> flux transported by the wind through a vertical plane downwind from the source area (Denmead, 1983).

Process-based models, such as DNDC (Li et al., 1992), Volt' Air (Génermont and Cellier, 1997) and HERMES (Kersebaum and Richter, 1991; Kersebaum, 1995), can be powerful tools for understanding the temporal variability of NH<sub>3</sub> emissions at the field scale and evaluating different strategies to mitigate NH<sub>3</sub> emissions from N fertilization on agroecosystems (Michalczyk et al., 2014; Dutta et al., 2016; Pacholski et al., 2018). However, predicting NH<sub>3</sub> volatilization losses is a multifaceted challenge, as it can occur relatively fast (Giltrap et al., 2017) and is influenced by several environmental factors (e.g. soil pH, soil water content and temperature, crop residue, etc.) (Ernst and Massey, 1960; Freney, 1988; Zhenghu and Honglang, 2000; Behera et al., 2013). Thus, field measurements across different environmental conditions are necessary to improve current process-based models.

The DNDC model was first developed to simulate greenhouse gas emissions from agroecosystems (Li et al., 1992). Throughout the years, there has been improvements to the DNDC model to simulate N mobility in the soil-air continuum. For example, improvements have been made on DNDC representations of processes governing nitrous oxide emissions (Giltrap et al., 2010; Dutta et al., 2018), N leaching (Tonitto et al., 2007), and NH<sub>3</sub> volatilization from slurry application (Congreves et al., 2016) and from broadcast urea (Dutta et al., 2016; Dubache et al., 2019; Li et al., 2019). Detailed information regarding the current DNDC framework can be found on Global Research Alliance Modeling Platform (GRAMP) (Yeluripati et al., 2015). The DNDC 9.5, the US version of the DNDC model (Li et al., 1992), is the base model code for the Canadian DNDC version (DNDC v.CAN) (Congreves et al., 2016; Dutta et al., 2016, 2018). The latter has a modified urea hydrolysis mechanism based on a soil pH buffer capacity factor, which simulates changes on soil pH based on the rate of urea hydrolysis. The DNDC v.CAN has been widely used to simulate NH<sub>3</sub> volatilization under Canadian conditions, but it can also be applied to other

temperate regions (Dutta et al., 2016). Although the DNDC model has been tested and adapted for other parts of the world (Dutta et al., 2016; Giltrap et al., 2017; Dubache et al., 2019; Li et al., 2019), there is no study that assessed these current versions of the model to simulate NH<sub>3</sub> volatilization from broadcast urea in the US Great Plains. Furthermore, most of the studies carried out in other countries assessed the DNDC comparing simulated NH<sub>3</sub> emissions with field experiments with intermittent measurements of NH<sub>3</sub> emissions from small plots using chamber measurements. It is known that chamber measurements can affect the soil micro-environmental, thus, influencing the NH<sub>3</sub> volatilization process (Shah et al., 2006; Liu, 2018).

In this study, we assessed two different versions of the DNDC model: DNDC9.5 (Li et al., 1992) and DNDC v.CAN (Congreves et al., 2016; Dutta et al., 2016, 2018) to simulate NH<sub>3</sub> volatilization from broadcast urea at sites in Kansas and Montana. Simulations of NH<sub>3</sub> volatilization were compared to 29 IHF NH<sub>3</sub> sampling campaigns that were conducted under Montana (21 campaigns) and Kansas (8 campaigns) environmental conditions. The primary goals of this study were to (i) evaluate the performance of DNDC 9.5 and DNDC v.CAN to simulate NH<sub>3</sub> volatilization from broadcast urea and (ii) investigate possible modeled processes that could be improved in future versions of the DNDC model.

## 3.2 Material and Methods

### 3.2.1 NH<sub>3</sub> emission sampling campaigns

Ammonia flux measurements for 29 field sampling campaigns conducted in the states of Kansas and Montana were used to evaluate the DNDC model simulations. The NH<sub>3</sub> sampling campaigns in Montana consisted of 12 NH<sub>3</sub> sampling campaigns reported by Engel et al. (2011) and nine sampling campaigns by Engel et al. (2017). For Kansas a total of eight NH<sub>3</sub> sampling campaigns were used including five campaigns described in Chapter 2, and additional three

sampling campaigns that were conducted following the exact same sampling protocol described in Section 2.2.2. Detailed information regarding geographical location, soil series and soil characteristics, including particle size distribution, pH, CEC and SOC, for all NH<sub>3</sub> sampling campaigns are shown on Table 3.1.

In all sampling campaigns, the IHF approach (section 2.2.2) was used to measure NH<sub>3</sub> volatilization from broadcast urea from three circular plots with a 20-m radius. One circular plot was fertilized with urea and one with urea amended with a urease inhibitor (NBPT, N-(n-butyl) thiophosphoric triamide) (Agrotain Ultra, Koch Agronomic Services, Wichita, KS). Urea and urea + NBPT were broadcast over the circular plots at rates of 100 and 60 kg of N ha<sup>-1</sup> for the sampling campaigns in Montana and Kansas, respectively. The urease inhibitor NBPT was used in its liquid formulation (1 g kg<sup>-1</sup>) and at rate recommended by the manufacturer (2.1 ml kg<sup>-1</sup>). The background NH<sub>3</sub> concentration, required for IHF flux calculations (Eq. 2.1), was obtained above an unfertilized plot. Further details on the NH<sub>3</sub> sampling campaigns are reported by Engel et al. (2011) and Engel et al. (2017). Additional information on sampling campaigns agriculture management system and state county in which the field experiment was conducted is available on Table 3.2.

With the exception of campaigns 25-29, all other NH<sub>3</sub> sampling campaigns were conducted during cold weather conditions, which are typical periods of the year in which farmers top dressing urea on winter wheat in Montana (Engel et al., 2011) and Kansas (Shroyer et al., 1997). Although the warm-weather campaigns (25-29) do not represent the typical environmental fertilizer application conditions in these states, these campaigns are useful for understanding how the DNDC model performs under warm environmental conditions.



### 3.2.2 Meteorological data

In-situ meteorological data were collected for all NH<sub>3</sub> sampling campaigns. For campaigns 1-21, weather stations (Hobo U30 NRC, Onset Computer corp., Bourne, MA) were installed to record air-temperature at 1.2-m height and soil temperature at 1-cm depth at 10-min intervals. For campaigns 1-12, precipitation was recorded using a tipping bucket rain gauge (Hobo RG3-M, Onset Computer corp., Bourne, MA). For campaigns 6-12, a stationary 8-inch standard rain gauge was utilized as a back-up. Precipitation gaps were filled with the closest National Oceanic and Atmospheric Administration (NOAA) weather station, with distances ranging from 9.0 to 13 km from the measuring site (Table 1 A). For campaigns 13-21, the precipitation was recorded using the tipping bucket rain gauge (Hobo RG3-M, Onset Computer corp., Bourne, MA) and a stationary 203-mm rain gauge (NovaLynx corp. Grass Valley, CA) was used to provide back up measurements when precipitation occurred in the form of snowfall. More details on these datasets are provided by Engel et. al (2017) and Romero et. al (2017).

For campaigns 22-29, precipitation was obtained from the closest Kansas Mesonet Station (Kansas Mesonet - Ashland Bottoms), which was located within 0.5 km from the experimental fields for campaigns 22 and 24-29, and 20 km from the experimental site for campaign 23. For campaigns 22 and 23,  $\theta_v$  was estimated using a metal ring (height = 5 cm and radius = 2.5 cm). For campaigns 24-29, soil temperature and  $\theta_v$  at 2-cm depth were measured using six dual-probe heat-pulse sensors (Campbell et al., 1991; Bristow et al., 1994) connected to a data logger (CR1000, Campbell Scientific, Logan UT).

### 3.2.3 DNDC model description and NH<sub>3</sub> volatilization sub-model

The DNDC (Denitrification Decomposition) is a process-based biogeochemical model that was developed to simulate greenhouse gas emissions from cropland soils in the US (Li et al.,

1992). The model has four main sub-models: (1) soil-climate/thermal-hydraulic flux, (2) crop growth, (3) decomposition and (4) denitrification. Newer versions of the model include a more detailed soil C and N cycling algorithms for GHGs emission simulations (Li et al., 2012). The DNDC model has also been adapted to different country-specific conditions (e.g. climate, soil, agricultural practices), such as in Canada (Congreves et al., 2016; Dutta et al., 2016), United Kingdom (Dubache et al., 2019), New Zealand (Giltrap et al., 2010, 2017) and China (Li et al., 2019). Furthermore, routines to simulate NH<sub>3</sub> volatilization from N fertilizer have been implemented since the early versions of the DNDC (Li et al. 1992; Li et. al 2000, 2001).

Briefly, the DNDC routine to simulate NH<sub>3</sub> volatilization takes into account the process of urea hydrolysis, which is the chemical reaction in which a water molecule is split into hydrogen and hydroxide ions, and it promptly reacts with urea molecules [CO(NH<sub>2</sub>)<sub>2</sub>]. During the hydrolysis reaction, the molecules of urea are converted into two molecules of NH<sub>4</sub><sup>+</sup> with a hydroxyl group (OH<sup>-</sup>) being released:



The urea hydrolysis is catalyzed by the activity of the urease enzyme, which is controlled by the soil temperature, moisture content and dissolved organic carbon (Kissel et al., 2008). These variables are used in the DNDC base model (DNDC 9.5) to simulate the urease activity. The urea hydrolysis rate is calculated as the first order function of the urease activity and urea concentration. In addition, the urea hydrolysis results in an increase in soil pH due to hydroxide release, which affects the model estimations of NH<sub>3</sub> volatilization (Li et al., 2012). Once NH<sub>4</sub><sup>+</sup> is produced from urea hydrolysis, the dissolved NH<sub>4</sub><sup>+</sup> rapidly reaches an equilibrium with dissolved NH<sub>3</sub>:



Eq. 3.2 can occur in both directions, and will be governed by the concentrations of  $\text{NH}_4^+$ ,  $\text{NH}_3$  and  $\text{H}^+$  in the soil liquid phase (Kissel et al., 2008). The DNDC 9.5 determines the direction and the rate of the reaction based on the two dissociation constants,  $K_a$  and  $K_w$ , for  $\text{NH}_4^+/\text{NH}_3$  and  $\text{H}^+/\text{OH}^-$  equilibrium, respectively, which are used to calculate the chemical reaction kinetics. The DNDC 9.5 model calculates  $K_w$  and  $K_a$  as function of soil temperature (Li et al., 2012). Dutta et al. (2016) used the base code from the DNDC 9.5 to improve the DNDC v.CAN by incorporating a modified urea hydrolysis mechanism based on a soil pH buffer capacity factor, which simulates changes on soil pH based on the rate of urea hydrolysis. This new version of the model was calibrated and tested using data from four experimental studies in Quebec, Canada. The authors concluded that the modifications on the urea hydrolysis mechanism improved the model's ability to predict  $\text{NH}_3$  volatilization.

#### 3.2.4 Model input preparation

The DNDC model simulations require primary meteorological input parameters (e.g. air temperature, precipitation, etc.), soil properties (e.g. soil pH, SOC, clay content, soil bulk density, etc.) and agricultural management practices (e.g. fertilization, tillage, etc.). Table 3.1 shows campaign latitude and soil properties (i.e. soil clay content, soil pH and SOC) used as model input. In addition, the model can be run using basic meteorological datasets, considering only mean air temperature and precipitation, or with a more complete dataset, which can include maximum and minimum air temperature, precipitation, wind speed, solar radiation and air humidity. For campaigns 1-21, daily meteorological input variables included maximum air temperature ( $^{\circ}\text{C}$ ), minimum air temperature ( $^{\circ}\text{C}$ ) and precipitation (cm). These meteorological variables were obtained from the closest NOAA weather station (Table A 1). In-situ precipitation records were replaced in the annual daily input during the  $\text{NH}_3$  sampling campaigns periods. For campaigns 22-

29, daily meteorological input included maximum temperature ( $^{\circ}\text{C}$ ), minimum temperature ( $^{\circ}\text{C}$ ), precipitation (cm), windspeed ( $\text{m s}^{-1}$ ), solar radiation ( $\text{MJ m}^{-2} \text{ day}^{-1}$ ) and relative humidity (%). These variables were obtained from the closest Kansas Mesonet Station (Table A 1). For all sampling campaigns, the required annual average of atmospheric  $\text{NH}_3$  concentration and ammonium ( $\text{NH}_4^+$ ) + nitrate ( $\text{NO}_3^-$ ) concentration were obtained from the National Atmospheric Deposition Program (2018).

For campaigns 1-12, soil particle distribution, bulk density, soil pH and SOC were directly obtained from Engel et al. (2011). For campaigns 13-21, these same soil properties were obtained from Engel et. al (2017) and Romero et. al (2017). For campaigns 22-29, soil particle distribution, soil pH and SOC were obtained from composite soil samples consisting of six individual soil cores. Soil samples were collected at each location prior to fertilization at depths of 0-15 and 15-60 cm. Bulk density was estimated for each sampling field using the same stainless steel ring that was used to estimate  $\theta_v$  (section 2.2.5). For all campaigns, the Soil-Plant-Air-Water (SPAW) computer model (Saxton and Willey, 2005) was used to estimate soil field capacity (FC) and wilting point (WP). Field porosity was calculated assuming soil particle density of  $2.65 \text{ g cm}^{-3}$ .

For campaigns 1-21, the different model versions were programmed to run consecutively for 11 years. The model input parameters are shown on Table 3.3. For the model initialization, the initial nine years were spin-up to stabilize soil environmental conditions. During this spin-up period, we assumed that the winter wheat was sown on September 25<sup>th</sup> and harvested on July 25<sup>th</sup>, typical dates mentioned by Romero et al. (2017). In addition, we assumed that  $150 \text{ kg of N ha}^{-1}$  of ammonium nitrate was applied annually on July 7<sup>th</sup> to avoid crop N starvation and keep the soil N balance stable during the spin-up, which is a similar procedure as the ones adopted by Dubache et al. (2019) and Li et al. (2019). It was also assumed a fraction of 0.5 for the field straw retention

after harvest. The 10<sup>th</sup> consecutive year on the model input file represented the treatment and management practices described by Engel et al. (2011), Engel et al. (2017) and Romero et al. (2017). The 11<sup>th</sup> consecutive year was programmed to simulate sampling campaigns that happened during two different years, for instance, when the fertilization happened in December and the sampling period prolonged thorough January and/or February of the following year. For campaigns 22-29 (i.e., the sites located in Kansas), we performed a 10-year spin-up. Depending on the campaign management practices, we assumed that winter wheat was sown on October 1<sup>st</sup> and harvested on June 1<sup>st</sup>, and maize was sown on May 1<sup>st</sup> and harvest on September 27<sup>th</sup>. Ammonium nitrate at rate 150 kg of N ha<sup>-1</sup> was applied on July 1<sup>st</sup>. Crop residue fraction post-harvest was assumed to be 0.5 for winter wheat and maize. The 11<sup>th</sup> consecutive year represented the treatment and practices that happened during the NH<sub>3</sub> sampling campaign period. The climate file and soil input parameters were recycled for the 11-year simulation for all sampling campaigns in this study.

#### 3.2.4 Model evaluation and statistical analysis

In this study we performed a comparative analysis between the DNDC 9.5 and DNDC v. CAN. The assessments included model comparisons with observed data for all 29 sampling campaigns. We evaluated the ability of the model to simulate soil temperature,  $\theta_v$  and NH<sub>3</sub> emissions from broadcast urea and urea amended with NBPT. The statistical analysis was carried out using linear regression models and by assessing the results based on coefficient of determination ( $R^2$ ), Pearson coefficient of correlation ( $r$ ), mean absolute error (MAE), root mean square error (RMSE) and index of agreement ( $d$ ), proposed by Willmott et al., (2018). These indices are calculated as follows:

$$R^2 = \frac{SSR}{SST} \quad (3.3)$$

$$r = \frac{\sum_{i=1}^n (x_i - \bar{x}_i)(y_i - \bar{y}_i)}{\sqrt{\sum_{i=1}^n (y_i - \bar{y}_i)^2} \sqrt{\sum_{i=1}^n (x_i - \bar{x}_i)^2}} \quad (3.4)$$

$$MAE = \frac{1}{N} \sum_{i=1}^n |y_i - x_i| \quad (3.5)$$

$$RMSE = \sqrt{\frac{1}{N} \sum_{i=1}^n (y_i - x_i)^2} \quad (3.6)$$

$$d = 1 - \frac{\sum_{i=1}^n (y_i - x_i)}{\sum_{i=1}^n (|y_i - \bar{x}_i| + |x_i - \bar{x}_i|)^2} \quad (3.7)$$

where  $x_i$  is the observed value,  $\bar{x}_i$  is the average of the observed values,  $y_i$  is the modeled value,  $\bar{y}_i$  is the average of the modeled values,  $n$  represents a value in the total  $N$  number of observations, SSR is the sum squared regression error and SST sum squared total error. The index  $d$  is dimensionless and it is commonly applied to evaluate the accuracy of the model (Willmott et al., 2018). The examination of the  $d$  index is proposed as follows:  $d \geq 0.9$  indicates excellent agreement; when  $0.8 \leq d \leq 0.9$  a good agreement; a moderate agreement when  $0.7 \leq d \leq 0.8$  and when  $d \leq 0.7$  a poor agreement (Willmott et al., 2018).

### 3.2.5 Sensitivity analysis

A series of sensitivity tests were conducted to investigate the responses of DNDC simulations of  $\text{NH}_3$  volatilization to variations in N application rate, SOC, soil clay content, urease inhibitor efficiency and duration. We selected the sampling campaign 29 as a baseline scenario due to its significant  $\text{NH}_3$  volatilization losses from broadcast urea (53% of applied N) and urea amended with NBPT (23% of applied N). The sensitivity scenarios were created by varying the baseline values between -20% and 20% with steps of 5% increment. The sensitivity scenarios along with the baseline values for each parameter are shown on Table 3.4. The annual  $\text{NH}_3$  volatilization simulated for each scenario was compared to the annual baseline scenario. The

simulations were done with input parameters being changed one at a time using the DNDC v.CAN and DNDC 9.5 interface.

In addition, we investigated the impact of soil (e.g. pH, temperature, moisture, SOC) and environmental (e.g. precipitation, snowpack, wind speed) factors on NH<sub>3</sub> volatilization simulations using a decision tree algorithm (Random Forest - RF) (Breiman, 2001) through the Python Module Scikit-learn (Pedregosa et al., 2011). The factors were chosen based on prior knowledge of their effect on NH<sub>3</sub> volatilization from broadcast urea (Ernst et al., 1969; Jones et al., 2013; Silva et al., 2017; Engel et al., 2011; Engel et al., 2017). The RF consists of an ensemble of unpruned regression trees which are created by bootstrapping (i.e. create several subsets from the training sample chosen randomly with replacement). For each bootstrap a simple decision tree is created, and the process is repeated according to the number of decision trees (Breiman, 2001). We used 30% of the dataset as test sample. Each single tree was created based on a set of randomized inputs. We built 1000 trees with three randomly sampled candidate variables evaluated at each split. The RF algorithm is considered to be an efficient approach to detect the importance of explanatory variables (Tulbure et al., 2012; Krupnik et al., 2015). Each explanatory variable is analyzed individually while others are left unchanged during the algorithm iterations (Breiman, 2001). The relative variable importance ranges from 0 to 1, in which variables with higher values have higher impact on NH<sub>3</sub> volatilization.

### 3.3 Results

#### 3.3.1 NH<sub>3</sub> volatilization simulations from broadcast urea and urea amended with NBPT

Figure 3.1 shows the relationship between cumulative simulated N losses through NH<sub>3</sub> volatilization for urea (Fig. 3.1A) and urea + NBPT (Fig. 3.1B) for all sampling campaigns.

Overall, the DNDC v.CAN underestimated NH<sub>3</sub> emissions from broadcast urea and urea + NBPT, and the DNDC 9.5 overestimated on both scenarios, especially for urea + NBPT.

Table 3.5 shows the statistical indices for daily cumulative NH<sub>3</sub> volatilization from broadcast urea and urea + NBPT for all sampling campaigns. The DNDC v.CAN simulated daily NH<sub>3</sub> volatilization more accurately to observed values when compared to DNDC 9.5. However, when the DNDC 9.5 model simulated with smaller errors (e.g. Campaign 5 and 28), the difference between both models was less than 10%. The DNDC v.CAN simulated NH<sub>3</sub> emissions from broadcast urea with an average MAE ( $\overline{\text{MAE}}$ ) and average RMSE ( $\overline{\text{RMSE}}$ ) of 10.1 and 10.9 kg of N ha<sup>-1</sup>, respectively. Meanwhile, the DNDC 9.5 had 31.8 and 32.8 kg of N ha<sup>-1</sup> for  $\overline{\text{MAE}}$  and  $\overline{\text{RMSE}}$ , respectively. Although the DNDC 9.5 simulated NH<sub>3</sub> volatilization with larger errors, the simulations were strongly correlated ( $r \geq 0.8$ ) in 80% of the campaigns. The DNDC v.CAN simulations also showed strong correlation with observed NH<sub>3</sub> fluxes for the majority of the sampling campaigns. Overall, both models showed poor accuracy (index  $d \leq 0.7$ ). Fig. A.1, 2 and 3 show the plots for simulated and observed daily cumulative NH<sub>3</sub> volatilization from broadcast urea for all campaigns.

The same analysis was done to evaluate the simulation of NH<sub>3</sub> volatilization from broadcast urea + NBPT (Table 3.5, Fig. A.4, 5 and 6). The DNDC v.CAN simulations showed smaller errors than DNDC 9.5, but both models showed poor accuracy (index  $d \leq 0.7$ ). The DNDC v.CAN  $\overline{\text{MAE}}$  and  $\overline{\text{RMSE}}$  were 3.2 and 3.8 kg of N ha<sup>-1</sup>, respectively. The DNDC 9.5 failed to simulate the effects of urease inhibitor, and the  $\overline{\text{MAE}}$  and  $\overline{\text{RMSE}}$  were 38.4 and 39.6 kg of N ha<sup>-1</sup>, respectively. Additionally, the simulations of NH<sub>3</sub> volatilization for these scenarios were the same for broadcast urea. We hypothesized that a glitch in the DNDC 9.5 base code is probably causing the model to



fail to simulate the urease inhibitor effects, since this model functionality has been reported previously (Gilhespy et al., 2014).

### 3.3.2 Daily soil temperature and $\theta_v$ simulations

Table A.2 and Fig. A.7-9 show the statistical indices and the simulations of mean daily soil temperature for all sampling campaigns. Both models were capable of simulating soil temperature relatively well. The DNDC v.CAN had smaller simulation errors with respect to measured temperatures in 70% of the campaigns, with  $\overline{MAE}$  and  $\overline{RMSE}$  of 2.8 and 3.5 °C, respectively, when compared to 3.6 and 4.3 °C, obtained from the DNDC 9.5 simulations. A strong correlation ( $r \geq 0.8$ ) was found in 85% of the campaigns and good to excellent accuracy ( $d \geq 0.85$ ) in 60% of campaigns. The DNDC 9.5 had a strong correlation ( $r \geq 0.8$ ) and good to excellent accuracy ( $d \geq 0.85$ ) in 66% and 20% of the sampling campaigns, respectively. Nonetheless,  $\theta_v$  was poorly simulated by both model versions, with  $\overline{MAE}$  and  $\overline{RMSE}$  of 0.14 and 0.18 cm<sup>3</sup> cm<sup>-3</sup> for the DNDC v.CAN, and 0.12 and 0.13 cm<sup>3</sup> cm<sup>-3</sup> for the DNDC 9.5 both models performed poorly when simulating  $\theta_v$  (Fig. A.10).

### 3.3.3 Sensitivity analysis and factors influencing NH<sub>3</sub> volatilization simulations

Results from the model sensitivity tests performed by varying each parameter (one-at-time) for specific ranges of values are shown on Fig. 3.2. Soil pH was the most sensitive parameter affecting NH<sub>3</sub> volatilization in the both models. The soil pH is directly associated with the NH<sub>4</sub><sup>+</sup> and NH<sub>3</sub> balance in the soil (Eq. 3.1). Both models were sensitive to changes in urea rate of application. Higher rates of application resulted in higher NH<sub>3</sub> emissions. Efficiency of urease inhibitor was sensitive only in DNDC v.CAN. Increase in the urease inhibitor efficiency reduced NH<sub>3</sub> emissions. As mentioned above, the most updated version of the DNDC 9.5 might have a glitch in the base code that is impeding the simulations of the urease inhibitor effects. Changes in

the soil clay content affected  $\text{NH}_3$  emissions simulations with higher sensitivity in the DNDC v.CAN. Although Fig. 3.2 shows small changes on  $\text{NH}_3$  volatilization, both models showed reduction on annual  $\text{NH}_3$  emissions when increasing the SOC in 15% and 20%.

The RF variable importance analysis (Fig. 3.3) shows that  $\text{NH}_3$  volatilization emissions from both models are mostly driven by soil pH. Soil temperature was the second most important variable. In addition, the difference between soil pH and soil temperature was more attenuated in the DNDC v.CAN. The other explanatory variables (wind speed, snowpack, precipitation, air humidity, soil moisture and SOC) had minor or no importance on  $\text{NH}_3$  volatilization simulations.

### 3.4 Discussion

Both models simulated soil temperature relatively well, and the correlation of soil temperature simulations with observed data are in agreements to previous studies (Cui et al., 2014; Dutta et al., 2016; Dutta et al., 2018). Regarding the poor simulation of  $\theta_v$ , several other studies have shown that the DNDC v.CAN and DNDC 9.5 tend to underestimate predictions of  $\theta_v$  (Smith et al., 2008; Congreves et al., 2016; Dutta et al., 2018).

The sensitivity analysis (Fig. 3.2) was helpful to understand how the model simulations of  $\text{NH}_3$  volatilization respond to variations in the input parameters. In addition, the RF variable importance analysis (Fig. 3.3) quantifies the importance of each variable in the DNDC  $\text{NH}_3$  emission simulations. The sensitivity analysis showed that both models were sensitive to changes in soil pH, and the RF analysis revealed that the soil pH is the most significant variable affecting  $\text{NH}_3$  volatilization in both models. Generally, alkaline soils favor the presence of  $\text{NH}_3$  over  $\text{NH}_4^+$  which leads to higher  $\text{NH}_3$  volatilization losses (Freney, 1988; Kissel et al., 2008).

The rate of urea application was the second most sensitive parameter in both models. Our results agree to the results of an experiment conducted by Rochette et al. (2013), who demonstrated

that cumulative  $\text{NH}_3$  volatilization increased nonlinearly with urea application rates. In addition, the authors attributed the higher losses found in their study to the increase on the proportion of  $\text{NH}_3$  and  $\text{NH}_4^+$  available in the soil.

Our sensitivity tests showed a positive relationship between  $\text{NH}_3$  volatilization and soil clay content. Nonetheless,  $\text{NH}_3$  volatilization losses tend to decrease in soils that have high clay content ( $\geq 35\%$  clay) (Fenn and Kissel, 1976; Jones et al., 2013; Pelster et al., 2018), and this is directly related to the higher absorption rate of  $\text{NH}_4^+$  by clay minerals (Kissel et al., 2008; Mikkelsen, 2009). This positive relationship could be related to the fact that our max upper variation (31.1% clay) is lower than what is considered a soil with high clay content. Also, the rate of  $\text{NH}_4^+$  adsorption is simulated using a logistic regression between  $\text{NH}_4^+$  and  $\text{NH}_3$  which will reduce  $\text{NH}_3$  emissions only at soils high clay contents (Congreves et al., 2016).

Both models simulated small changes on  $\text{NH}_3$  volatilization when changing the SOC. The decrease on  $\text{NH}_3$  volatilization when increasing the SOC is directly related to fact that soils with high SOC tend to have higher CEC, and as consequence lower chances of  $\text{NH}_3$  losses (Davis and Singh, 2002; Jones et al., 2013).

The difference in soil pH sensitivity (Fig. 3.2) and importance (Fig.3.3) between the DNDC v.CAN and DNDC 9.5 could be related to the fact that the DNDC 9.5 employs a soil pH modifier in the urea hydrolysis reaction that is unchanged by  $\text{NH}_3$  volatilization, nitrification, ammonification and soil pH buffering capacity (Dutta et al., 2016). These are known factors to influence the soil pH contributing directly to  $\text{NH}_3$  losses (Kissel et al., 2008). The soil pH buffer algorithm added by Dutta et al. (2016) to DNDC v.CAN simulations of soil pH changes based on the production of  $\text{OH}^-$  from the process of urea hydrolysis. Furthermore, the increase of the pH of the soil surrounding the urea granules tend to be smaller in soils with high CEC, contributing to a

decrease in  $\text{NH}_3$  volatilization losses (Davis and Singh, 2002; Kissel et al., 2008). In the DNDC v.CAN the maximum pH change is calculated as if the soil had no pH buffering capacity (Dutta et al., 2016), which is directly dependent on CEC (Jones et al. 2013). Our results are in agreement to the findings reported by Dutta et al. (2016) who found smaller errors for daily  $\text{NH}_3$  volatilization simulations for the DNDC v.CAN in comparison to the DNDC 9.5. Furthermore, our results (Fig. A.1-6) show that DNDC 9.5 is largely overestimating  $\text{NH}_3$  fluxes. Similar results were observed for studies carried out in Canada (Dutta et al., 2016) and in New Zealand (Giltrap et al., 2017).

The  $\text{NH}_3$  volatilization from broadcast urea is a complex process controlled by various soil variables (e.g. pH, CEC, organic matter, etc.) and environmental factors (e.g. precipitation, wind, etc.) (Ernst and Massey, 1960; Kissel et al., 2008; Behera et al., 2013). Therefore, simulating  $\text{NH}_3$  volatilization is very challenging. The difficulties are even larger when simulating the effects of a urease inhibitor (e.g. NBPT), since the effectiveness of a urease inhibitor can vary depending on its period of effective inhibition (10-20 d post fertilization) and the product shelf life (Cantarella et al., 2018). These factors impose challenges for simulating  $\text{NH}_3$  volatilization from urea amended with NBPT (Table 3.5, Fig. A 4-6). We have not expanded our analysis on the simulations of urease inhibitor effects, however, this should be studied in future assessments and improvements of the DNDC, since the importance and use of urease inhibitors has been growing steadily during the last two decades (Silva et al., 2017; Cantarella et al., 2018).

The RF variable importance analysis showed that soil temperature was the second most important factor influencing  $\text{NH}_3$  volatilization (Fig. 3.3). Soil temperature has a pivotal role on  $\text{NH}_3$  volatilization from broadcast urea, as higher soil temperatures tend to favor the presence of  $\text{NH}_3$  over  $\text{NH}_4^+$  and increase the rate of  $\text{NH}_3$  emissions (Kissel et al., 2008). Moreover, higher soil temperatures increase the urease enzyme activity and the rate of urea hydrolysis (Ernst and

Massey, 1960; Mikkelsen, 2009). Recent studies have shown that while the DNDC can simulate average soil temperature with low errors and high accuracy, the model regularly fails to capture the effect of different management practices (e.g. presence of crop residues) on soil temperature variations (Li et al., 2010; Sagggar et al., 2004; Umoza et al., 2015). Dutta et al. (2018) improved the DNDC v.CAN by adding a soil temperature sub-model to simulate the effects of long periods of soil snow cover, crop biomass and the influence of soil texture in soil temperatures. The overall better performance of the DNDC v.CAN when compared to the DNDC 9.5 at simulating soil temperature showed by our results (Table A.2 and Fig. A.7-9) is probably related to these developments.

The RF analysis indicates that important soil and environmental factors (e.g. wind speed, snowpack, air humidity, etc.) contributing to NH<sub>3</sub> volatilization from broadcast urea are being given minimal relevance by both model versions. These results indicate that better simulations from the DNDC could be achieved by implementing a routine to account for the influence of these factors on NH<sub>3</sub> volatilization from broadcast urea.

In this study, most of the sampling campaigns employed to assess the performance of the DNDC were carried out under cold weather conditions. While the DNDC 9.5 largely overestimated NH<sub>3</sub> fluxes for almost all campaigns, the DNDC v.CAN considerably underestimated NH<sub>3</sub> fluxes in certain campaigns (e.g. 3, 4 and 5). For campaigns 3, 4 and 5, the large N losses were attributed to the application of urea to a visibly damp or high-water-content soil surface ( $\theta_v \geq 0.32 \text{ cm}^3\text{cm}^{-3}$ ), which caused the dissolution of urea granules and losses of over 30% of applied N. The soil in these campaigns remained moist during the following 30 d ( $\theta_v \geq 0.25 \text{ cm}^3\text{cm}^{-3}$ ) with scattered rainfall ( $\leq 5 \text{ mm}$ ) events. Also, trace amount of snow was present on campaign 5 ( $\theta_v = 0.50 \text{ cm}^3\text{cm}^{-3}$ ), leading soil water content to near saturation (Engel et al., 2011). The DNDC v.CAN also greatly

underestimated  $\text{NH}_3$  volatilization in campaigns 25 and 26 (Fig. A 5), which had urea broadcast to soils with high water content ( $\theta_v \geq 0.41 \text{ cm}^3\text{cm}^{-3}$ ) (Fig. A.10), leading to N losses higher than 20% of applied N. As showed in previous studies,  $\text{NH}_3$  volatilization following urea broadcast is directly related to the soil water content, since the dissolution of  $\text{NH}_4^+$  and transportation of N from the soil surface to plant roots is highly dependent on the amount of water present in the soil (Ernst and Massey, 1960; Freney et al., 1983, Rochette et al., 2009). The DNDC soil-hydrology sub model employs a limited cascade approach ('tipping bucket') to simulate soil water processes (Li et al. 1992, Congreves et al., 2016; Dutta et al., 2016; Dutta et al., 2018). This approach simplifies the soil-hydrology mechanisms by dividing the soil into several vertical layers, in which the water flows from one layer to next (Li et al., 1992). Also, it limits the simulation of important processes, such as unsaturated flow, hydraulic potential and lateral flow of ground water (Dutta et al., 2016; Dutta et al., 2018). Finally, improvements on future versions of the model should consider the implementation of an enhanced algorithm to better simulate  $\text{NH}_3$  losses under high-water-content soil in cold weather conditions.

Both models overestimated  $\text{NH}_3$  volatilization for campaign 28, which was conducted during mid-summer in Kansas.  $\text{NH}_3$  fluxes were low (< 4% of applied N) on this campaign due to a series of precipitation events that added up 22 mm during the first 15 d post fertilization. Previous studies showed that accumulated rainfall or irrigation events of 15 to 20 mm can significantly reduce (up to 90%)  $\text{NH}_3$  volatilization (Black et al., 1987; Terman et al., 1979). The limited capacity of the model to simulate precipitation effects on  $\text{NH}_3$  volatilization following urea broadcast was also illustrated on Fig. 3.3, since precipitation had no importance to  $\text{NH}_3$  volatilization. Also, this limitation was reported in a previous study (Dubache et al., 2019). Future developments of the model should add a routine to better reflect the effects of accumulated

precipitation during the first 5-15 d post fertilization on NH<sub>3</sub> volatilization following broadcast urea.

We also observed that both models showed limitations to simulate the correct timing of NH<sub>3</sub> volatilization. Most of NH<sub>3</sub> fluxes simulated by the DNDC v.CAN occurred during the first 5-10 d post fertilization and zero fluxes were simulated after this period. On the other hand, for several campaigns (e.g. 1, 4, 10, 21 and 25), the DNDC 9.5 continued to simulate small NH<sub>3</sub> fluxes ( $\leq 0.1\%$  of applied N) for a very long period of time after fertilization (~ 170 d). The field campaigns used in this study showed that small NH<sub>3</sub> fluxes from broadcast urea can extend for over 40 d up to 110 d post fertilization. Normally, extended periods of NH<sub>3</sub> volatilization are found when urea is broadcast to cold and dry soil surfaces (Black et al., 1987; Engel et al., 2011). However, it is very unlikely that these emissions would exceed a period longer than 170 d post fertilization, since most of the NH<sub>3</sub> volatilization losses happen during the first three to four weeks post fertilization (Jones et al., 2013; Silva et al., 2017). Our results imply that improvements on newer versions of the model can be done by changing the algorithms responsible to suppressing completely the NH<sub>3</sub> volatilization in the DNDC v.CAN and the procedures governing the prolonged NH<sub>3</sub> volatilization in the DNDC 9.5.

We assessed both DNDC versions NH<sub>3</sub> volatilization simulations solely based on IHF approach (Denmead, 1983), which is considered to be one of the most accurate forms of measuring NH<sub>3</sub> emissions from fertilized fields (Denmead, 1983; Shah et al. 2006; Liu et al. 2018). Our findings (Fig A.1-6) demonstrate that the improvements built in the DNDC v.CAN can be further explored to reduce uncertainties present in process-based models for simulating N gas emissions (Misselbrook et al., 2004; Giltrap et al., 2015; Dutta et al., 2016; Pacholski et al., 2018).

Several authors have used empirical approaches for estimating NH<sub>3</sub> volatilization from agricultural fields (Sherlock and Goh, 1983; Misselbrook et al., 2004; Pacholski et al., 2018). These models are based on field observation data and several different techniques can be employed to ensure the best fit (e.g. linear regression, logistic regression). Empirical models can be advantageous as they are likely to require fewer assumptions and less computational power when compared to process-based models, and at times, similar or better robustness (Bell and Fischer, 1994). However, empirical models are limited in the scope by the set of observations used for their development and are generally less accurate. Alternatively, a process-based model, such as DNDC, offers a mathematical representation of several bio-geochemical processes governing NH<sub>3</sub> volatilization, and it can capture the complex relationship of different factors (e.g. soil temperature, urease activity, etc.) affecting NH<sub>3</sub> volatilization (Li et al., 1992). Additionally, the simulation of these complex relationships controlling bio-geochemical processes relies on continuous validations of field measured variables. Under this scenario, our assessment has a great importance to delineate the current limitations of the DNDC and identify future directions to improve DNDC NH<sub>3</sub> simulations.

### 3.5 Conclusions

Overall, the DNDC v.CAN simulated in-season measurements of NH<sub>3</sub> volatilization from broadcast urea with smaller errors ( $\overline{\text{RMSE}} = 10.9 \text{ kg of N ha}^{-1}$ ) when compared to the DNDC 9.5 ( $\overline{\text{RMSE}} = 32.8 \text{ kg of N ha}^{-1}$ ). Both model versions had strong correlation ( $r \geq 0.8$ ) with field measurements but poor accuracy ( $d \leq 0.7$ ). In addition, both versions were capable of simulating soil temperature with high correlation and good to excellent accuracy performance ( $d \geq 0.85$ ). However, volumetric soil water content was poorly simulated by both model versions ( $r \leq 0.35$ ;  $d \leq 0.45$ ).



The RF variable importance analysis showed the soil pH and soil temperature are the most important factors affecting simulations of NH<sub>3</sub> volatilization by the DNDC v.CAN and DNDC 9.5. In addition, the main limitations of the model that could be addressed in future improvements of the model are summarized below:

*i)* Both models showed a limited capacity to simulate soil water content ( $\overline{\text{RMSE}} \geq 0.12 \text{ cm}^3 \text{ cm}^{-3}$ ). This limitation leads to poor simulations of NH<sub>3</sub> volatilization when urea was broadcast in moist cold soils. Future model enhancements should consider adding a more robust representation of soil-hydrology to simulate the effect of the soil water content in urea hydrolysis and NH<sub>3</sub> volatilization.

*ii)* The models also failed to reproduce the effects of precipitation events during the first 5-15 d post fertilization. Normally, a sequence of precipitation events adding up to 20 mm is sufficient to dissolve urea granules and transport the N into deeper layers of the soil, which will significantly reduce NH<sub>3</sub> volatilization from broadcast urea (Black et al., 1987; Terman et al., 1979).

*iii)* DNDC improvements can also be done by creating a more robust routine to simulate the effects of urease inhibitor on NH<sub>3</sub> volatilization. Especially for the DNDC 9.5, which may have a glitch on the model code that is impeding the simulations of a urease inhibitor.

*iv)* Based on our sampling campaigns, NH<sub>3</sub> emissions from broadcast urea can extend from 40 to 110 d post fertilization. Future improvements should consider a better approach to simulate the timing of the NH<sub>3</sub> emissions. While most of the NH<sub>3</sub> volatilization happened during the first 5 to 10 d post fertilization in the DNDC v.CAN, these emissions extended to over ~170 d in the DNDC 9.5, which is very unrealistic.

### **Chapter 3 – Tables and Figures**

**Table 3.1** Location, NH<sub>3</sub> sampling campaign year, soil series, soil particles distribution, cation exchange capacity (CEC), pH and SOC for all campaigns.

| Site     | State | Latitude  | Longitude   | Sampling year | Soil series             | Sand  | Clay | Silt | CEC                   | pH                 | Organic C | Reference           |
|----------|-------|-----------|-------------|---------------|-------------------------|-------|------|------|-----------------------|--------------------|-----------|---------------------|
| Campaign |       |           |             |               |                         | --%-- |      |      | cmol kg <sup>-1</sup> | g kg <sup>-1</sup> |           |                     |
| 1        | MT    | 48°32'30" | -109°54'16" | 2008          | Phillips–Elloam         | 44.7  | 26.8 | 28.5 | 10.4                  | 6.1                | 9.2       | Engel et al. (2011) |
| 2        | MT    | 48°32'00" | -109°53'56" | 2008          | Phillips–Elloam         | 45.5  | 31.1 | 23.4 | 11.7                  | 6.4                | 12.8      | Engel et al. (2011) |
| 3        | MT    | 48°50'07" | -110°03'17" | 2008/09       | Telstad–Joplin          | 61.6  | 22.6 | 15.9 | 7.6                   | 5.5                | 10.2      | Engel et al. (2011) |
| 4        | MT    | 48°50'07" | -110°03'17" | 2009          | Telstad–Joplin          | 61.6  | 22.6 | 15.9 | 7.6                   | 5.5                | 10.2      | Engel et al. (2011) |
| 5        | MT    | 48°32'00" | -109°53'56" | 2009          | Phillips–Elloam         | 45.5  | 31.1 | 23.4 | 11.7                  | 6.4                | 12.8      | Engel et al. (2011) |
| 6        | MT    | 48°31'45" | -110°04'38" | 2009          | Phillips–Elloam         | 41.8  | 26.2 | 32.0 | 10.0                  | 6.0                | 13.2      | Engel et al. (2011) |
| 7        | MT    | 48°31'43" | -109°54'47" | 2009          | Scobey–Kevin            | 38.3  | 31.7 | 30.0 | 10.9                  | 6.5                | 19.0      | Engel et al. (2011) |
| 8        | MT    | 48°50'05" | -110°03'35" | 2009          | Telstad–Joplin          | 58.4  | 24.1 | 17.5 | 9.0                   | 5.5                | 14.3      | Engel et al. (2011) |
| 9        | MT    | 45°47'40" | -111°35'23" | 2010          | Brocko                  | 33.8  | 28.6 | 37.5 | 10.6                  | 8.4                | 10.1      | Engel et al. (2011) |
| 10       | MT    | 45°47'40" | -111°35'23" | 2010          | Brocko                  | 33.8  | 28.6 | 37.5 | 10.6                  | 8.4                | 10.1      | Engel et al. (2011) |
| 11       | MT    | 48°31'43" | -109°54'47" | 2010          | Scobey–Kevin            | 38.3  | 31.7 | 30.0 | 10.9                  | 6.5                | 19.0      | Engel et al. (2011) |
| 12       | MT    | 48°32'50" | -110°07'47" | 2010          | Scobey–Kevin            | 39.6  | 27.7 | 32.7 | 10.1                  | 6.0                | 14.7      | Engel et al. (2011) |
| 13       | MT    | 47°22'29" | -110°04'29" | 2011/12       | Danvers clay loam       | 35.4  | 36.2 | 28.4 | n/a                   | 6.3                | 18.5      | Engel et al. (2017) |
| 14       | MT    | 47°22'29" | -110°04'29" | 2011/12       | Danvers clay loam       | 35.4  | 36.2 | 28.4 | n/a                   | 6.3                | 18.5      | Engel et al. (2017) |
| 15       | MT    | 47°22'29" | -110°04'29" | 2011/12       | Danvers clay loam       | 35.4  | 36.2 | 28.4 | n/a                   | 6.3                | 18.5      | Engel et al. (2017) |
| 16       | MT    | 47°22'28" | -110°06'05" | 2012/13       | Tamaneen clay loam      | 28.3  | 45.4 | 26.3 | n/a                   | 7.3                | 13.6      | Engel et al. (2017) |
| 17       | MT    | 47°22'28" | -110°06'05" | 2012/13       | Tamaneen clay loam      | 28.3  | 45.4 | 26.3 | n/a                   | 7.3                | 13.6      | Engel et al. (2017) |
| 18       | MT    | 47°22'28" | -110°06'05" | 2012/13       | Tamaneen clay loam      | 28.3  | 45.4 | 26.3 | n/a                   | 7.3                | 13.6      | Engel et al. (2017) |
| 19       | MT    | 47°22'29" | -110°04'29" | 2013/14       | Danvers clay loam       | 35.4  | 36.2 | 28.4 | n/a                   | 6.3                | 18.5      | Engel et al. (2017) |
| 20       | MT    | 47°22'29" | -110°04'29" | 2013/14       | Danvers clay loam       | 35.4  | 36.2 | 28.4 | n/a                   | 6.3                | 18.5      | Engel et al. (2017) |
| 21       | MT    | 47°22'29" | -110°04'29" | 2013/14       | Danvers clay loam       | 35.4  | 36.2 | 28.4 | n/a                   | 6.3                | 18.5      | Engel et al. (2017) |
| 22       | KS    | 39°07'16" | -96°38'26"  | 2017          | Smolan silt loam        | 20.0  | 24.0 | 56.0 | 21.0                  | 5.5                | 26.0      | Chapter 2           |
| 23       | KS    | 38°56'27" | -97°26'26"  | 2017          | Detroit silty clay loam | 12.0  | 32.0 | 56.0 | 24.5                  | 6.2                | 34.0      | Chapter 2           |
| 24       | KS    | 39°07'26" | -96°38'23"  | 2018          | Smolan silt loam        | 38.0  | 30.0 | 32.0 | 22.7                  | 5.7                | 23.0      | Chapter 2           |
| 25       | KS    | 39°07'30" | -96°38'31"  | 2018          | Smolan silt loam        | 12.0  | 54.0 | 34.0 | 18.2                  | 6.7                | 30.0      | Chapter 2           |
| 26       | KS    | 39°06'43" | -96°36'42"  | 2018          | Sutphen silty clay      | 12.0  | 54.0 | 34.0 | 26.8                  | 6.2                | 32.0      | Chapter 2           |
| 27       | KS    | 39°07'49" | -96°38'38"  | 2018          | Smolan silt loam        | 26.0  | 20.0 | 54.0 | 17.8                  | 6.2                | 22.0      | Chapter 2           |
| 28       | KS    | 39°07'32" | -96°38'46"  | 2018          | Smolan silt loam        | 16.0  | 26.0 | 58.0 | 22.3                  | 5.8                | 25.0      | Chapter 2           |
| 29       | KS    | 39°06'53" | -96°38'19"  | 2018          | Smolan silt loam        | 14.0  | 36.0 | 50.0 | 16.2                  | 6.4                | 23.0      | Chapter 2           |

**Table 3.2** -Sampling campaigns agricultural management system and state county in which the field experiment was conducted.

| Sampling campaigns | Agricultural management            | County               |
|--------------------|------------------------------------|----------------------|
| 1-8, 11 and 12     | no-till winter wheat-fallow system | Hill County - MT     |
| 9 and 10           | tilled wheat-fallow system         | Gallatin County - MT |
| 13-21              | no-till winter wheat-fallow system | Fergus County - MT   |
| 22, 24, 25 and 28  | tilled winter wheat-fallow system  | Riley County - KS    |
| 26 and 27          | no-till maize fallow system        | Riley County - KS    |
| 23* and 29         | no-till winter wheat-fallow system | Riley County - KS    |

\*Sampling campaign conducted at Dickson County.

**Table 3.3** - Model input parameters for simulations for both DNDC model versions (DNDC 9.5 and DNDC v.CAN).

| Site | Latitude | Fertilization |            | Soil texture    | Bulk density | Porosity | FC   | WP   | Crop Residue | Tillage practice |       |     |
|------|----------|---------------|------------|-----------------|--------------|----------|------|------|--------------|------------------|-------|-----|
|      |          | Doy of year   | Date       |                 |              |          |      |      |              | g cm-3           | month | day |
| 1    | 48.5     | 94            | 4/3/2008   | Loam            | 1.30         | 0.51     | 29.4 | 16.5 | winter wheat |                  |       |     |
| 2    | 48.5     | 283           | 10/9/2008  | Sandy Clay Loam | 1.30         | 0.51     | 30.9 | 19.8 | winter wheat |                  |       |     |
| 3    | 48.8     | 323           | 11/18/2008 | Sandy Clay Loam | 1.30         | 0.51     | 23.8 | 14.4 | winter wheat |                  |       |     |
| 4    | 48.8     | 84            | 3/25/2009  | Sandy Clay Loam | 1.30         | 0.51     | 23.8 | 14.4 | winter wheat |                  |       |     |
| 5    | 48.5     | 85            | 3/26/2009  | Sandy Clay Loam | 1.30         | 0.51     | 30.9 | 19.8 | winter wheat |                  |       |     |
| 6    | 48.5     | 279           | 10/6/2009  | Loam            | 1.30         | 0.51     | 29.1 | 16.4 | winter wheat |                  |       |     |
| 7    | 48.5     | 286           | 10/13/2009 | Clay Loam       | 1.30         | 0.51     | 33.2 | 20.1 | winter wheat |                  |       |     |
| 8    | 48.8     | 292           | 10/19/2009 | Sandy Clay Loam | 1.30         | 0.51     | 25.4 | 15.3 | winter wheat |                  |       |     |
| 9    | 48.8     | 27            | 1/27/2010  | Clay Loam       | 1.30         | 0.51     | 31.7 | 17.9 |              | 1                | 1     | 2   |
| 10   | 48.8     | 57            | 2/26/2010  | Clay Loam       | 1.30         | 0.51     | 31.7 | 17.9 |              | 1                | 1     | 2   |
| 11   | 48.5     | 88            | 3/29/2010  | Clay Loam       | 1.30         | 0.51     | 33.2 | 20.1 | winter wheat |                  |       |     |
| 12   | 48.5     | 110           | 4/20/2010  | Clay Loam       | 1.30         | 0.51     | 30.6 | 17.6 | winter wheat |                  |       |     |
| 13   | 47.4     | 333           | 11/29/2011 | Clay Loam       | 1.21         | 0.54     | 0.36 | 0.21 | winter wheat |                  |       |     |
| 14   | 47.4     | 59            | 2/28/2012  | Clay Loam       | 1.21         | 0.54     | 0.36 | 0.21 | winter wheat |                  |       |     |
| 15   | 47.4     | 115           | 4/24/2012  | Clay Loam       | 1.21         | 0.54     | 0.36 | 0.21 | winter wheat |                  |       |     |
| 16   | 47.4     | 347           | 12/12/2012 | Clay Loam       | 1.21         | 0.54     | 0.33 | 0.18 | winter wheat |                  |       |     |
| 17   | 47.4     | 39            | 2/8/2013   | Clay Loam       | 1.21         | 0.54     | 0.33 | 0.18 | winter wheat |                  |       |     |
| 18   | 47.4     | 102           | 4/12/2013  | Clay Loam       | 1.21         | 0.54     | 0.33 | 0.18 | winter wheat |                  |       |     |
| 19   | 47.4     | 335           | 12/1/2013  | Clay Loam       | 1.21         | 0.54     | 0.36 | 0.21 | winter wheat |                  |       |     |
| 20   | 47.4     | 52            | 2/21/2014  | Clay Loam       | 1.21         | 0.54     | 0.36 | 0.21 | winter wheat |                  |       |     |
| 21   | 47.4     | 102           | 4/12/2014  | Clay Loam       | 1.21         | 0.54     | 0.36 | 0.21 | winter wheat |                  |       |     |
| 22   | 39.1     | 32            | 2/2/2017   | Silt Loam       | 1.22         | 0.54     | 0.62 | 0.29 |              | 1                | 15    | 3   |
| 23   | 39.2     | 38            | 2/8/2017   | Silt Clay Loam  | 1.26         | 0.52     | 0.71 | 0.39 | winter wheat |                  |       |     |
| 24   | 39.1     | 59            | 3/1/2018   | Silt Clay Loam  | 1.21         | 0.54     | 0.66 | 0.35 |              | 2                | 15    | 3   |
| 25   | 39.0     | 115           | 4/26/2018  | Silt Loam       | 1.10         | 0.58     | 0.53 | 0.23 |              | 11               | 1     | 3   |
| 26   | 39.1     | 196           | 7/16/2018  | Silt Clay       | 1.13         | 0.57     | 0.68 | 0.42 | maize        |                  |       |     |
| 27   | 39.1     | 198           | 7/18/2018  | Silt Loam       | 1.20         | 0.55     | 0.63 | 0.31 | maize        |                  |       |     |
| 28   | 39.1     | 317           | 11/13/2018 | Silt Clay Loam  | 1.22         | 0.54     | 0.70 | 0.39 |              | 7                | 1     | 3   |
| 29   | 39.1     | 315           | 11/12/2018 | Silt Clay Loam  | 1.45         | 0.45     | 0.82 | 0.46 | winter wheat |                  |       |     |

\*Tillage practice method: (2) ploughing slightly (5-cm) and (3) ploughing with disk or chisel (10-cm).

**Table 3.4** – Baseline (Sampling campaign 29) and alternative scenarios for sensitivity tests.

| Parameters                                   | Baseline scenario    | Variation scenario  |
|--|----------------------|---|
|  | Sampling campaign 29 |   |
| Application rate (kg N ha <sup>-1</sup> )    | 60                   | 48, 51, 54, 57, 63, 66, 69 and 72                                 |
| Application depth (cm)                       | 0.2                  | 2.5, 5, 7.5 and 10  |
| Organic Carbon (kg C kg soil <sup>-1</sup> ) | 0.027                | 0.0216, 0.0229, 0.0243, 0.0256, 0.0283, 0.0297, 0.0310 and 0.0324 |
| Clay Content (%)                             | 26                   | 20.8, 22.1, 23.4, 24.7, 27.3, 28.6, 29.9 and 31.2                 |
| Urease Inhibitor                             |                      |   |
| Duration (days)                              | 21                   | 16.8, 17.85, 18.9, 19.95, 22.05, 23.1, 24.15 and 25.2             |
| Effectiveness (%)                            | 100                  | 80, 85, 90, 95 and 100  |



**Table 3.5** – Statistical indices of the DNDC v.CAN and DNDC 9.5 simulations of cumulative NH<sub>3</sub> volatilization (kg of N ha<sup>-1</sup>) after urea and urea +NBPT broadcast for all sampling campaigns.

| Campaign | Urea   |       |        |       |           |      |          |      |  | Urea + NBPT |      |        |      |           |      |          |      |  |
|----------|--------|-------|--------|-------|-----------|------|----------|------|--|-------------|------|--------|------|-----------|------|----------|------|--|
|          | MAE    |       | RMSE   |       | Pearson r |      | <i>d</i> |      |  | MAE         |      | RMSE   |      | Pearson r |      | <i>d</i> |      |  |
|          | v. CAN | 9.5   | v. CAN | 9.5   | v. CAN    | 9.5  | v. CAN   | 9.5  |  | v. CAN      | 9.5  | v. CAN | 9.5  | v. CAN    | 9.5  | v. CAN   | 9.5  |  |
| 1        | 4.26   | 61.20 | 5.47   | 62.18 | 0.0       | 0.74 | 0.47     | 0.10 |  | 2.2         | 63.3 | 2.9    | 64.4 | 0.0       | 0.71 | 0.47     | 0.06 |  |
| 2        | 1.71   | 58.86 | 2.07   | 59.04 | 0.0       | 0.85 | 0.45     | 0.04 |  | 0.7         | 59.8 | 0.9    | 60.1 | 0.0       | 0.85 | 0.45     | 0.02 |  |
| 3        | 25.98  | 16.43 | 27.17  | 17.82 | 0.0       | 0.98 | 0.33     | 0.60 |  | 2.7         | 39.7 | 3.0    | 42.0 | 0.0       | 0.98 | 0.40     | 0.06 |  |
| 4        | 28.92  | 41.84 | 29.94  | 43.25 | 0.0       | 0.98 | 0.29     | 0.27 |  | 11.5        | 59.3 | 13.0   | 60.7 | 0.0       | 0.91 | 0.43     | 0.17 |  |
| 5        | 35.29  | 29.00 | 35.77  | 30.30 | 0.0       | 0.97 | 0.21     | 0.30 |  | 12.1        | 52.2 | 13.6   | 53.1 | 0.0       | 0.86 | 0.43     | 0.20 |  |
| 6        | 9.33   | 46.89 | 9.86   | 47.39 | 0.0       | 0.99 | 0.32     | 0.10 |  | 3.1         | 53.1 | 3.4    | 53.8 | 0.0       | 0.87 | 0.37     | 0.04 |  |
| 7        | 5.12   | 47.03 | 5.52   | 47.05 | 0.0       | 0.97 | 0.35     | 0.07 |  | 3.4         | 52.1 | 3.8    | 52.2 | 0.0       | 0.92 | 0.39     | 0.05 |  |
| 8        | 12.17  | 55.18 | 12.90  | 55.21 | 0.0       | 0.97 | 0.32     | 0.11 |  | 2.1         | 65.2 | 2.4    | 65.4 | 0.0       | 0.92 | 0.41     | 0.03 |  |
| 9        | 12.69  | 2.85  | 15.35  | 3.43  | 0.0       | 0.98 | 0.46     | 0.96 |  | 4.3         | 11.2 | 5.5    | 12.0 | 0.0       | 0.95 | 0.48     | 0.46 |  |
| 10       | 17.23  | 14.63 | 18.73  | 15.21 | 0.81      | 0.97 | 0.63     | 0.70 |  | 3.9         | 10.5 | 5.8    | 11.6 | 0.88      | 0.97 | 0.79     | 0.54 |  |
| 11       | 1.79   | 54.14 | 2.32   | 54.17 | 0.0       | 0.98 | 0.42     | 0.04 |  | 1.3         | 58.2 | 1.4    | 58.2 | 0.0       | 0.98 | 0.36     | 0.01 |  |
| 12       | 5.59   | 46.83 | 5.89   | 46.83 | 0.0       | 0.99 | 0.30     | 0.06 |  | 1.7         | 58.6 | 1.9    | 58.7 | 0.0       | 0.99 | 0.36     | 0.02 |  |
| 13       | 8.02   | 33.21 | 8.82   | 34.39 | 0.0       | 0.96 | 0.38     | 0.18 |  | 2.2         | 39.0 | 2.7    | 40.6 | 0.0       | 0.79 | 0.42     | 0.07 |  |
| 14       | 7.95   | 42.20 | 9.25   | 46.07 | 0.0       | 0.87 | 0.44     | 0.19 |  | 2.0         | 48.1 | 2.6    | 52.6 | 0.0       | 0.74 | 0.48     | 0.07 |  |
| 15       | 12.50  | 58.77 | 12.50  | 58.79 | 0.0       | 0.98 | 0.03     | 0.01 |  | 0.0         | 59.9 | 0.0    | 59.9 | 0.0       | 0.00 | 0.00     | 0.00 |  |
| 16       | 11.89  | 29.65 | 13.26  | 33.32 | 0.0       | 0.93 | 0.41     | 0.32 |  | 2.7         | 38.5 | 3.4    | 43.2 | 0.0       | 0.80 | 0.46     | 0.09 |  |
| 17       | 6.87   | 35.72 | 7.68   | 37.82 | 0.0       | 0.98 | 0.41     | 0.17 |  | 1.8         | 40.8 | 2.3    | 43.3 | 0.0       | 0.88 | 0.48     | 0.07 |  |
| 18       | 4.56   | 36.65 | 5.09   | 37.07 | 0.94      | 0.89 | 0.87     | 0.32 |  | 3.6         | 49.8 | 4.0    | 50.6 | 0.93      | 0.87 | 0.67     | 0.12 |  |
| 19       | 5.77   | 40.94 | 6.67   | 41.06 | 0.0       | 0.75 | 0.48     | 0.18 |  | 1.5         | 46.0 | 2.0    | 46.0 | 0.0       | 0.76 | 0.45     | 0.05 |  |
| 20       | 7.37   | 35.08 | 8.84   | 39.77 | 0.0       | 0.94 | 0.45     | 0.23 |  | 1.9         | 40.6 | 2.4    | 46.2 | 0.0       | 0.75 | 0.46     | 0.07 |  |
| 21       | 8.66   | 59.67 | 8.66   | 59.73 | 0.0       | 0.96 | 0.01     | 0.00 |  | 8.8         | 59.8 | 8.8    | 59.9 | 0.0       | 0.00 | 0.00     | 0.00 |  |
| 22       | 1.10   | 11.58 | 1.28   | 12.39 | 0.0       | 0.70 | 0.45     | 0.10 |  | 0.1         | 12.5 | 0.2    | 13.4 | 0.0       | 0.68 | 0.45     | 0.01 |  |
| 23       | 2.43   | 6.17  | 2.93   | 7.04  | 0.65      | 0.69 | 0.74     | 0.59 |  | 4.3         | 6.8  | 5.9    | 7.9  | 0.0       | 0.58 | 0.48     | 0.56 |  |
| 24       | 10.07  | 19.49 | 10.68  | 19.74 | 0.48      | 0.51 | 0.16     | 0.09 |  | 1.6         | 19.0 | 2.1    | 19.3 | 0.0       | 0.53 | 0.49     | 0.13 |  |
| 25       | 8.79   | 5.31  | 10.73  | 6.78  | 0.88      | 0.81 | 0.52     | 0.80 |  | 1.2         | 14.1 | 1.4    | 15.5 | 0.0       | 0.90 | 0.43     | 0.09 |  |
| 26       | 5.95   | 5.64  | 8.07   | 8.49  | 0.00      | 0.57 | 0.47     | 0.69 |  | 0.2         | 9.8  | 0.4    | 13.2 | 0.0       | 0.46 | 0.33     | 0.06 |  |
| 27       | 3.61   | 2.84  | 3.93   | 3.74  | 0.99      | 0.98 | 0.91     | 0.91 |  | 1.9         | 12.2 | 2.2    | 12.6 | 0.0       | 0.98 | 0.42     | 0.15 |  |
| 28       | 21.67  | 20.45 | 21.76  | 20.56 | 0.69      | 0.78 | 0.04     | 0.04 |  | 5.5         | 20.2 | 6.2    | 20.3 | 0.44      | 0.56 | 0.30     | 0.10 |  |
| 29       | 5.06   | 3.01  | 5.73   | 3.32  | 0.99      | 0.98 | 0.93     | 0.98 |  | 4.7         | 11.9 | 5.2    | 13.1 | 0.94      | 0.96 | 0.76     | 0.56 |  |

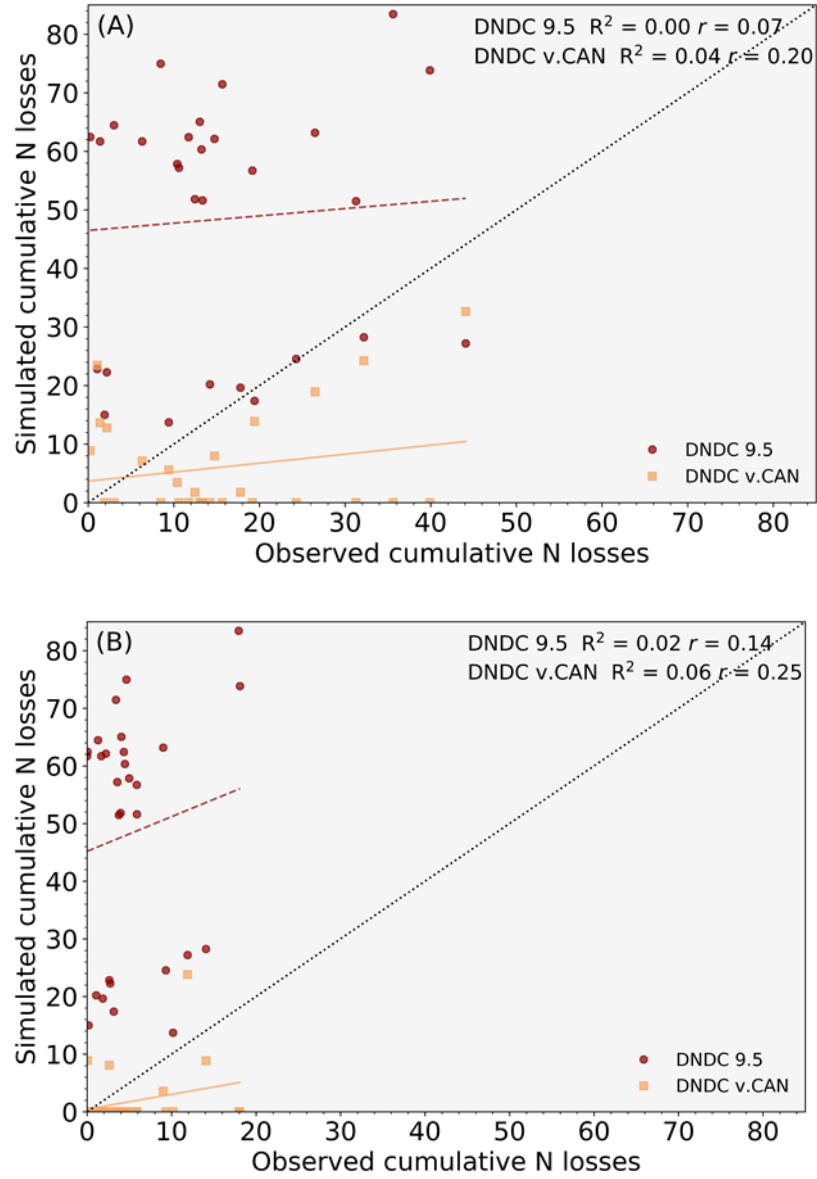


**Figure 3.1** Simulated and observed cumulative N losses for all sampling campaigns, for urea (A) and urea + NBPT (B)

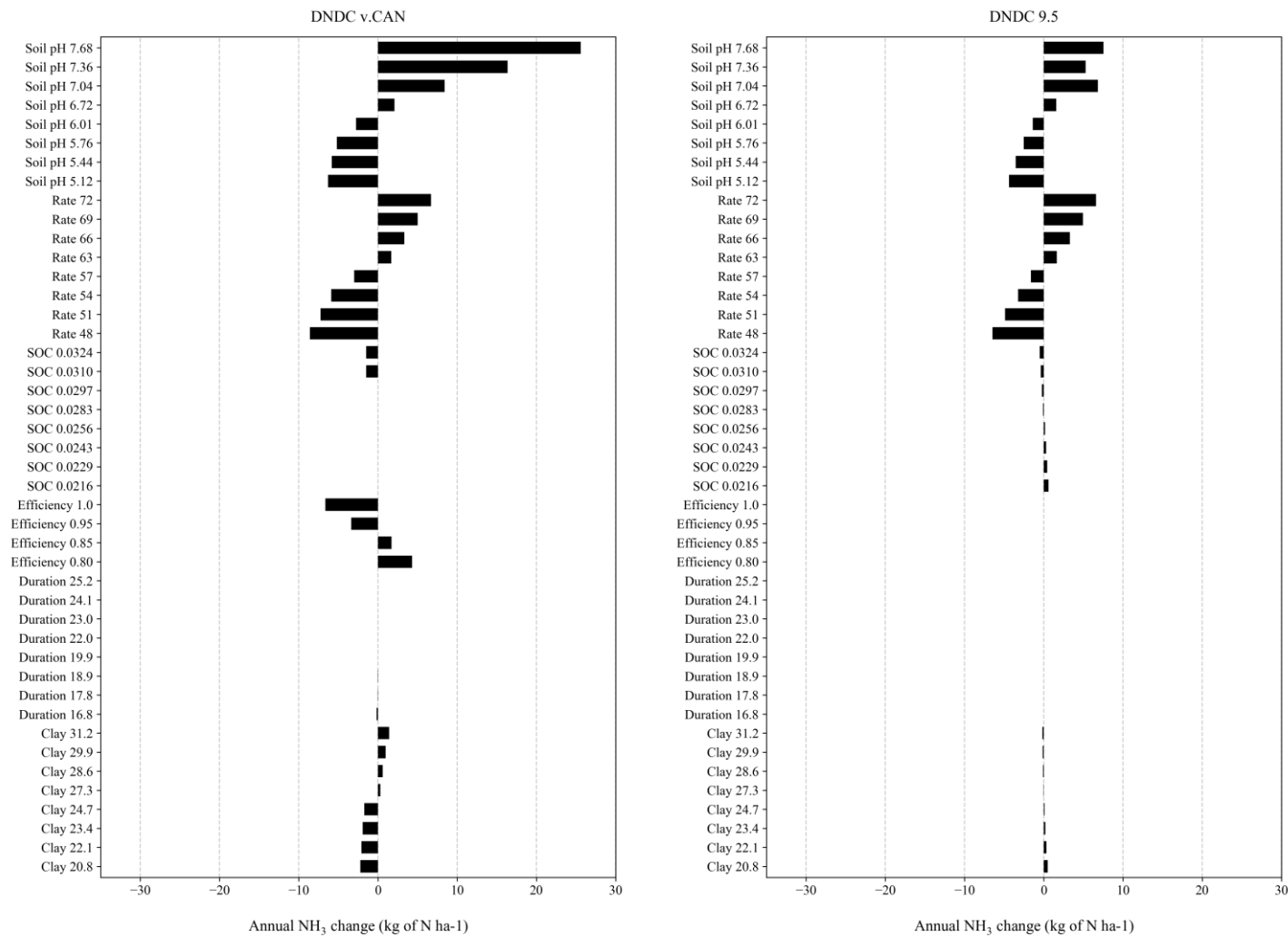


**Figure 3.2** Results of the sensitivity tests performed by varying each environmental or management input parameter in  $\pm 20\%$  with steps of 5%. Horizontal bars represent the variation from the sampling campaign 29 baseline scenario (Table 3). Soil pH, ‘Rate’ (urea rate of application in kg of N ha<sup>-1</sup>), ‘SOC’ (soil organic carbon in kg of C kg<sup>-1</sup> soil), ‘Efficiency’ (urease inhibitor efficiency in %), ‘Duration’ (urease inhibitor duration in d) and ‘Clay’ (soil clay content in %)



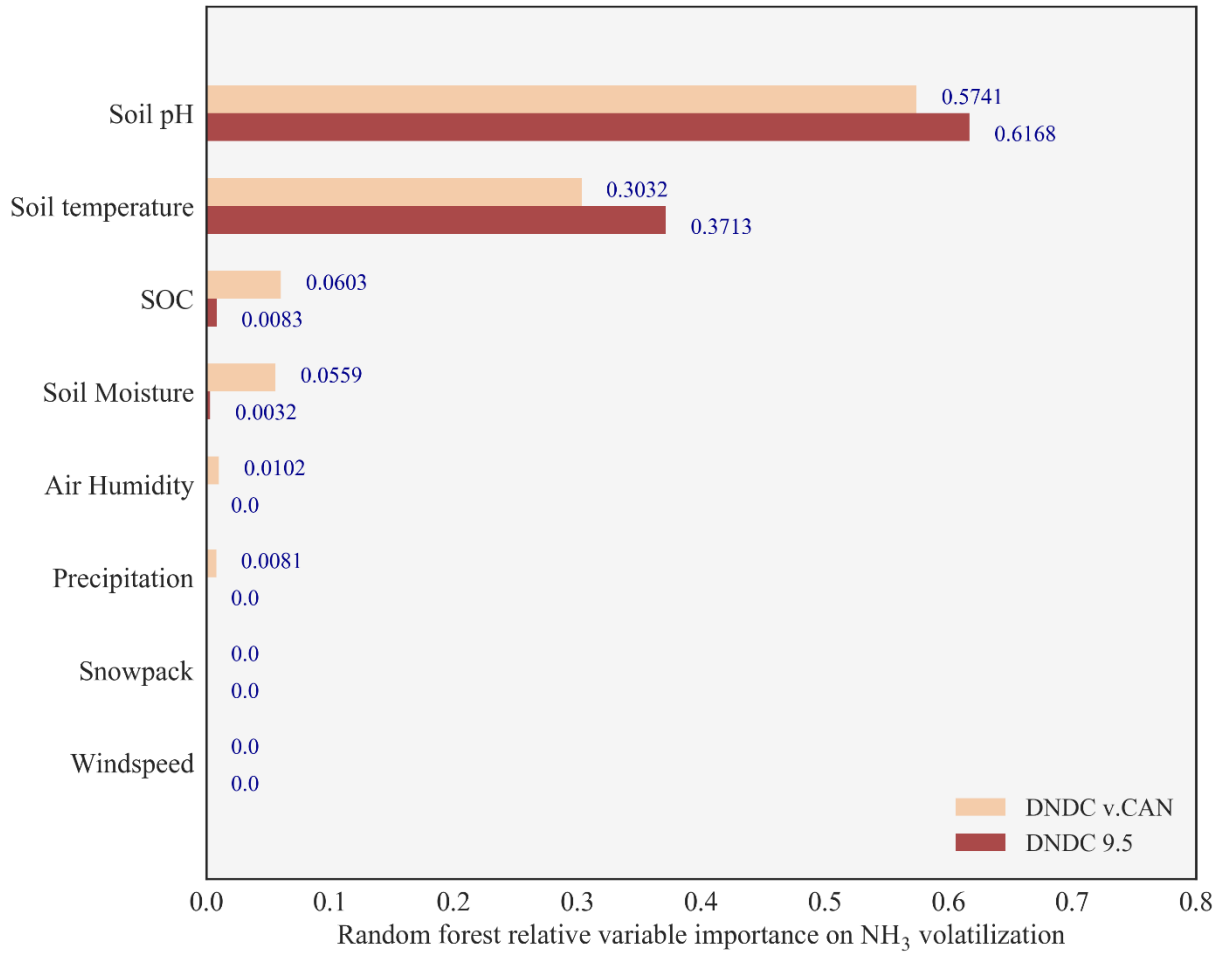


**Figure 3.3** Relative variable importance (0 – 1; from least to most important) in Random forest models of input variables for the NH<sub>3</sub> volatilization simulations using DNDC v.CAN and DNDC 9.5. Variable importance was based on model output values of soil pH, soil temperature, SOC, soil moisture, air humidity, precipitation, snowpack and wind speed.

## References

- Abalos, D., A. Sanz-Cobena, T. Misselbrook, and A. Vallejo. 2012. Effectiveness of urease inhibition on the abatement of ammonia, nitrous oxide and nitric oxide emissions in a non-irrigated Mediterranean barley field. *Chemosphere* 89(3): 310–318. doi: <https://doi.org/10.1016/j.chemosphere.2012.04.043>.
- Al-Kanani, T., A.F. MacKenzie, and N.N. Barthakur. 1991. Soil water and ammonia volatilization relationships with surface-applied nitrogen fertilizer solutions. *Soil Sci. Soc. Am. J.* 55(6): 1761–1766.
- Baligar, V.C., N.K. Fageria, and Z.L. He. 2001. Nutrient use efficiency in plants. *Commun. Soil Sci. Plant Anal.* 32(7–8): 921–950.
- Beauchamp, E.G., G.E. Kidd, and G. Thurtell. 1978. Ammonia Volatilization from Sewage Sludge Applied in the Field1. *J. Environ. Qual.* 7: 141–146. doi: 10.2134/jeq1978.00472425000700010030x.
- Behera, S.N., M. Sharma, V.P. Aneja, and R. Balasubramanian. 2013. Ammonia in the atmosphere: a review on emission sources, atmospheric chemistry and deposition on terrestrial bodies. *Environ. Sci. Pollut. Res.* 20(11): 8092–8131.
- Bell, M. A., and R. A. Fischer. "Using yield prediction models to assess yield gains: A case study for wheat." *Field Crops Research* 36.2 (1994): 161-166.
- Black, A.S., R.R. Sherlock, and N.P. Smith. 1987. Effect of timing of simulated rainfall on ammonia volatilization from urea, applied to soil of varying moisture content. *J. soil Sci.* 38(4): 679–687.
- Black, A.S., R.R. Sherlock, N.P. Smith, K.C. Cameron, and K.M. Goh. 1985. Effects of form of nitrogen, season, and urea application rate on ammonia volatilisation from pastures. *New*

- Zeal. J. Agric. Res. 28(4): 469–474.
- Borghini, B. 1999. Nitrogen as determinant of wheat growth and yield. *Wheat Ecol. Physiol. yield Determ.* Food Prod. Press. New York p: 67–84.
- Breiman, L. 2001. Random forests. *Mach. Learn.* 45(1): 5–32.
- Bristow, K.L., G.J. Kluitenberg, and R. Horton. 1994. Measurement of Soil Thermal Properties with a Dual-Probe Heat-Pulse Technique. *Soil Sci. Soc. Am. J.* 58: 1288–1294. doi: 10.2136/sssaj1994.03615995005800050002x.
- Campbell, G.S., C. Calissendorff, and J.H. Williams. 1991. Probe for measuring soil specific heat using a heat-pulse method. *Soil Sci. Soc. Am. J.* 55(1): 291–293.
- Campbell, C.R., and C.O. Plank. 1992. Determination of total nitrogen in plant tissue by combustion. *Plant Anal. Ref. Proced. South. US South. Coop. Ser. Bull* 368: 20–22.
- Cantarella, H., R. Otto, J.R. Soares, and A.G. de Brito Silva. 2018. Agronomic Efficiency of NBPT as a Urease Inhibitor: A review. *J. Adv. Res.*
- Chen, A., B. Lei, W. Hu, Y. Lu, Y. Mao, Z. Duan, and Z. Shi. 2015. Characteristics of ammonia volatilization on rice grown under different nitrogen application rates and its quantitative predictions in Erhai Lake Watershed, China. *Nutr. Cycl. agroecosystems* 101(1): 139–152.
- Congreves, K.A., B.B. Grant, B. Dutta, W.N. Smith, M.H. Chantigny, P. Rochette, and R.L. Desjardins. 2016. Predicting ammonia volatilization after field application of swine slurry: DNDC model development. *Agric. Ecosyst. Environ.* 219: 179–189.
- Davis, B.H., and K.S.W. Singh. 2002. Handbook of Porous Solids. *Handb. Porous Solids*: 1–23.
- Denmead, O.T. 1983. Micrometeorological methods for measuring gaseous losses of nitrogen in the field. p. 133–157. *In* Gaseous loss of nitrogen from plant-soil systems. Springer.
- Van Doren Jr, D.M., G.B. Triplett Jr, and J.E. Henry. 1977. Influence of long-term tillage and

crop rotation combinations on crop yields and selected soil parameters for an Aeric Ochraqualf soil.

Dubache, G., S. Li, X. Zheng, W. Zhang, and J. Deng. 2019. Modeling ammonia volatilization following urea application to winter cereal fields in the United Kingdom by a revised biogeochemical model. *Sci. Total Environ.* 660: 1403–1418. doi: <https://doi.org/10.1016/j.scitotenv.2018.12.407>.

Duncan, E.G., C.A. O’Sullivan, M.M. Roper, J.S. Biggs, and M.B. Peoples. 2018. Influence of co-application of nitrogen with phosphorus, potassium and sulphur on the apparent efficiency of nitrogen fertiliser use, grain yield and protein content of wheat. *F. Crop. Res.* 226: 56–65.

Dutta, B., K.A. Congreves, W.N. Smith, B.B. Grant, P. Rochette, M.H. Chantigny, and R.L. Desjardins. 2016. Improving DNDC model to estimate ammonia loss from urea fertilizer application in temperate agroecosystems. *Nutr. Cycl. agroecosystems* 106(3): 275–292.

Dutta, B., B.B. Grant, K.A. Congreves, W.N. Smith, C. Wagner-Riddle, A.C. VanderZaag, M. Tenuta, and R.L. Desjardins. 2018. Characterising effects of management practices, snow cover, and soil texture on soil temperature: Model development in DNDC. *Biosyst. Eng.* 168: 54–72.

Engel, R., C. Jones, C. Romero, and R. Wallander. 2017. Late-fall, winter and spring broadcast applications of urea to no-till winter wheat I. Ammonia loss and mitigation by NBPT. *Soil Sci. Soc. Am. J.* 81(2): 322–330.

Engel, R., C. Jones, and R. Wallander. 2011. Ammonia volatilization from urea and mitigation by NBPT following surface application to cold soils. *Soil Sci. Soc. Am. J.* 75(6): 2348–2357.

- Ernst, J.W., and H.F. Massey. 1960. The Effects of Several Factors on Volatilization of Ammonia Formed from Urea in the Soil 1. *Soil Sci. Soc. Am. J.* 24(2): 87–90.
- Fenn, L.B., and D.E. Kissel. 1976. The Influence of Cation Exchange Capacity and Depth of Incorporation on Ammonia Volatilization from Ammonium Compounds Applied to Calcareous Soils 1. *Soil Sci. Soc. Am. J.* 40(3): 394–398.
- Freney, J.R. 1988. Importance of ammonia volatilization as a loss process. *Adv. nitrogen Cycl. Agric. Ecosyst.:* 156–173.
- Freney, J.R., J.R. Simpson, and O.T. Denmead. 1983. Volatilization of ammonia. p. 1–32. *In* Gaseous loss of nitrogen from plant-soil systems. Springer.
- Galloway, J.N., F.J. Dentener, D.G. Capone, E.W. Boyer, R.W. Howarth, S.P. Seitzinger, G.P. Asner, C.C. Cleveland, P.A. Green, E.A. Holland, D.M. Karl, A.F. Michaels, J.H. Porter, A.R. Townsend, and C.J. Vöösmary. 2004. Nitrogen Cycles: Past, Present, and Future. *Biogeochemistry* 70(2): 153–226. doi: 10.1007/s10533-004-0370-0.
- Génermont, S., and P. Cellier. 1997. A mechanistic model for estimating ammonia volatilization from slurry applied to bare soil. *Agric. For. Meteorol.* 88(1–4): 145–167.
- Gilhespy, S.L., S. Anthony, L. Cardenas, D. Chadwick, A. del Prado, C. Li, T. Misselbrook, R.M. Rees, W. Salas, and A. Sanz-Cobena. 2014. First 20 years of DNDC (DeNitrification DeComposition): model evolution. *Ecol. Modell.* 292: 51–62.
- Giltrap, D.L., C. Li, and S. Saggar. 2010. DNDC: A process-based model of greenhouse gas fluxes from agricultural soils. *Agric. Ecosyst. Environ.* 136(3–4): 292–300.
- Giltrap, D., J. Rodriguez, P. Berben, T. Palmada, and S. Saggar. 2015. Modelling NH<sub>3</sub> volatilisation from a urine patch and urea application using NZ-DNDC. p. 10–12. *In* 28th annual FLRC workshop.

- Giltrap, D., S. Saggarr, J. Rodriguez, and P. Bishop. 2017. Modelling NH<sub>3</sub> volatilisation within a urine patch using NZ-DNDC. *Nutr. Cycl. Agroecosystems* 108(3): 267–277.
- Glibert, P.M., J. Harrison, C. Heil, and S. Seitzinger. 2006. Escalating Worldwide use of Urea – A Global Change Contributing to Coastal Eutrophication. *Biogeochemistry* 77(3): 441–463. doi: 10.1007/s10533-005-3070-5.
- Harper, L.A. 2005. Ammonia: measurement issues.
- Howard, D.D., A.Y. Chambers, and J. Logan. 1994. Nitrogen and Fungicide Effects on Yield Components and Disease Severity in Wheat. *J. Prod. Agric.* 7: 448–454. doi: 10.2134/jpa1994.0448.
- IFA. 2018. Fertilizer Outlook 2018-2022. Berlin, Germany.
- IPNI. 2008. Ammonia volatilization.
- Jones, C., B.D. Brown, R. Engel, D. Horneck, and K. Olson-Rutz. 2013. Nitrogen fertilizer volatilization. Mont. State Univ. Extension, EBO208.
- Jones, C.A., R.T. Koenig, J.W. Ellsworth, B.D. Brown, and G.D. Jackson. 2007. Management of urea fertilizer to minimize volatilization. *MSU Ext.*: 1–12.
- Kersebaum, K.C. 1995. Application of a simple management model to simulate water and nitrogen dynamics. *Ecol. Modell.* 81(1–3): 145–156.
- Kersebaum, K.C., and J. Richter. 1991. Modelling nitrogen dynamics in a plant-soil system with a simple model for advisory purposes. *Fertil. Res.* 27(2–3): 273–281.
- Kissel, D.E., M.L. Cabrera, S. Paramasivam, J.S. Schepers, and W.R. Raun. 2008. Ammonium, ammonia, and urea reactions in soils. *AGRONOMY* 49: 101.
- Krupnik, T.J., Z.U. Ahmed, J. Timsina, S. Yasmin, F. Hossain, A. Al Mamun, A.I. Mridha, and A.J. McDonald. 2015. Untangling crop management and environmental influences on wheat

- yield variability in Bangladesh: An application of non-parametric approaches. *Agric. Syst.* 139: 166–179. doi: <https://doi.org/10.1016/j.agsy.2015.05.007>.
- Krupnik, T.J., J. Six, J.K. Ladha, M.J. Paine, and C. Van Kessel. 2004. An assessment of fertilizer nitrogen recovery efficiency by grain crops. *Agric. nitrogen cycle Assess. impacts Fertil. use food Prod. Environ.*
- Leuning, R., J.R. Freney, O.T. Denmead, and J.R. Simpson. 1985. A sampler for measuring atmospheric ammonia flux. *Atmos. Environ.* 19(7): 1117–1124.
- Li, C., S. Frolking, and T.A. Frolking. 1992. A model of nitrous oxide evolution from soil driven by rainfall events: 1. Model structure and sensitivity. *J. Geophys. Res. Atmos.* 97(D9): 9759–9776.
- Li, C., W. Salas, R. Zhang, C. Krauter, A. Rotz, and F. Mitloehner. 2012. Manure-DNDC: a biogeochemical process model for quantifying greenhouse gas and ammonia emissions from livestock manure systems. *Nutr. Cycl. Agroecosystems* 93(2): 163–200.
- Li, S., X. Zheng, W. Zhang, S. Han, J. Deng, K. Wang, R. Wang, Z. Yao, and C. Liu. 2019. Modeling ammonia volatilization following the application of synthetic fertilizers to cultivated uplands with calcareous soils using an improved DNDC biogeochemistry model. *Sci. Total Environ.* 660: 931–946. doi: <https://doi.org/10.1016/j.scitotenv.2018.12.379>.
- Liu, J.Y. and Y.J. and W.Z.Y. and P.G. and S.G.B. and L.J. 2018. Review of methods for determination of ammonia volatilization in farmland. *IOP Conf. Ser. Earth Environ. Sci.* 113(1): 12022. <http://stacks.iop.org/1755-1315/113/i=1/a=012022>.
- Lollato, R.P., and J.T. Edwards. 2015. Maximum Attainable Wheat Yield and Resource-Use Efficiency in the Southern Great Plains. *Crop Sci.* 55: 2863–2876. doi: [10.2135/cropsci2015.04.0215](https://doi.org/10.2135/cropsci2015.04.0215).

- Lollato, R.P., B.M. Figueiredo, J.S. Dhillon, D.B. Arnall, and W.R. Raun. 2019. Wheat grain yield and grain-nitrogen relationships as affected by N, P, and K fertilization: A synthesis of long-term experiments. *F. Crop. Res.* 236: 42–57. doi: <https://doi.org/10.1016/j.fcr.2019.03.005>.
- Ma, B.L., T.Y. Wu, N. Tremblay, W. Deen, N.B. McLaughlin, M.J. Morrison, and G. Stewart. 2010. On-Farm Assessment of the Amount and Timing of Nitrogen Fertilizer on Ammonia Volatilization. *Agron. J.* 102: 134–144. doi: 10.2134/agronj2009.0021.
- McInnes, K.J., R.B. Ferguson, D.E. Kissel, and E.T. Kanemasu. 1986. Ammonia Loss from Applications of Urea-Ammonium Nitrate Solution to Straw Residue 1. *Soil Sci. Soc. Am. J.* 50(4): 969–974.
- Michalczyk, A., K.C. Kersebaum, M. Roelcke, T. Hartmann, S.-C. Yue, X.-P. Chen, and F.-S. Zhang. 2014. Model-based optimisation of nitrogen and water management for wheat–maize systems in the North China Plain. *Nutr. Cycl. agroecosystems* 98(2): 203–222.
- Mikkelsen, R. 2009. Ammonia emissions from agricultural operations: fertilizer. *Better Crop.* 93(4): 9–11.
- Misselbrook, T.H., F.A. Nicholson, B.J. Chambers, and R.A. Johnson. 2005. Measuring ammonia emissions from land applied manure: an intercomparison of commonly used samplers and techniques. *Environ. Pollut.* 135(3): 389–397. doi: <https://doi.org/10.1016/j.envpol.2004.11.012>.
- Misselbrook, T.H., M.A. Sutton, and D. Scholefield. 2004. A simple process-based model for estimating ammonia emissions from agricultural land after fertilizer applications. *Soil Use Manag.* 20(4): 365–372.
- Mosier, A., J.K. Syers, and J.R. Freney. 2013. Agriculture and the nitrogen cycle: assessing the



- impacts of fertilizer use on food production and the environment. Island Press.
- Nelson, A.K., P.P. Motavalli, and M. Nathan. 2014. Nitrogen Fertilizer Sources and Application Timing Affects Wheat and Inter-Seeded Red Clover Yields on Claypan Soils. *Agron.* 4(4). doi: 10.3390/agronomy4040497.
- Nippert J. 2019. AWE01 Meteorological data from the konza prairie headquarters weather station. Environmental Data Initiative. <https://doi.org/10.6073/pasta/fc379596bd014737c142bbcf0ace3179>. Dataset accessed 7/11/2019.
- Ni, K., A. Pacholski, and H. Kage. 2014. Ammonia volatilization after application of urea to winter wheat over 3 years affected by novel urease and nitrification inhibitors. *Agric. Ecosyst. Environ.* 197: 184–194. doi: <https://doi.org/10.1016/j.agee.2014.08.007>.
- Otto, R., E. Zavaschi, S. Netto, B. de A. Machado, and A.B. de Mira. 2017. Ammonia volatilization from nitrogen fertilizers applied to sugarcane straw. *Rev. Ciência Agronômica* 48(3): 413–418.
- Pacholski, A., G. Cai, R. Nieder, J. Richter, X. Fan, Z. Zhu, and M. Roelcke. 2006. Calibration of a simple method for determining ammonia volatilization in the field—comparative measurements in Henan Province, China. *Nutr. Cycl. Agroecosystems* 74(3): 259–273.
- Pacholski, A., J. Doehler, U. Schmidhalter, and T. Kreuter. 2018. Scenario modeling of ammonia emissions from surface applied urea under temperate conditions: application effects and model comparison. *Nutr. Cycl. agroecosystems* 110(1): 177–193.
- Pedregosa, F., G. Varoquaux, A. Gramfort, V. Michel, B. Thirion, O. Grisel, M. Blondel, P. Prettenhofer, R. Weiss, and V. Dubourg. 2011. Scikit-learn: Machine learning in Python. *J. Mach. Learn. Res.* 12(Oct): 2825–2830.

- Pelster, D.E., M.H. Chantigny, D.A. Angers, N. Bertrand, J.D. MacDonald, and P. Rochette. 2018. Can soil clay content predict ammonia volatilization losses from subsurface-banded urea in eastern Canadian soils? *Can. J. Soil Sci.* 98(3): 556–565. <https://doi.org/10.1139/cjss-2018-0036>.
- Raun, W.R., and G. V Johnson. 1999. Improving nitrogen use efficiency for cereal production. *Agron. J.* 91(3): 357–363.
- Rochette, P., D.A. Angers, M.H. Chantigny, M.-O. Gasser, J.D. MacDonald, D.E. Pelster, and N. Bertrand. 2013. NH<sub>3</sub> volatilization, soil concentration and soil pH following subsurface banding of urea at increasing rates. *Can. J. Soil Sci.* 93(2): 261–268. doi: 10.4141/cjss2012-095.
- Rochette, P., D.A. Angers, M.H. Chantigny, J.D. MacDonald, N. Bissonnette, and N. Bertrand. 2009. Ammonia volatilization following surface application of urea to tilled and no-till soils: A laboratory comparison. *Soil Tillage Res.* 103(2): 310–315. doi: <https://doi.org/10.1016/j.still.2008.10.028>.
- Romero, C.M., R.E. Engel, C. Chen, R. Wallander, and C.A. Jones. 2017. Late-fall, winter, and spring broadcast applications of urea to no-till winter wheat II. Fertilizer N recovery, yield, and protein as affected by NBPT. *Soil Sci. Soc. Am. J.* 81(2): 331–340.
- Ryden, J.C., and J.E. McNeill. 1984. Application of the micrometeorological mass balance method to the determination of ammonia loss from a grazed sward. *J. Sci. Food Agric.* 35(12): 1297–1310. doi: 10.1002/jsfa.2740351206.
- Sanz-Cobena, A., T.H. Misselbrook, A. Arce, J.I. Mingot, J.A. Diez, and A. Vallejo. 2008. An inhibitor of urease activity effectively reduces ammonia emissions from soil treated with urea under Mediterranean conditions. *Agric. Ecosyst. Environ.* 126(3): 243–249. doi:

<https://doi.org/10.1016/j.agee.2008.02.001>.

- Saxton, K.E., and P.H. Willey. 2005. The SPAW model for agricultural field and pond hydrologic simulation. *Watershed Model.*: 400–435.
- Shah, S.B., P.W. Westerman, and J. Arogo. 2006. Measuring ammonia concentrations and emissions from agricultural land and liquid surfaces: a review. *J. Air Waste Manage. Assoc.* 56(7): 945–960.
- Sherlock, R.R., and K.M. Goh. 1983. simple mathematical model simulating ammonia volatilization losses in the field. *In Proceedings... annual conference-Agronomy Society of New Zealand.*
- Shroyer, J.P., D. Whitney, and D. Peterson. 1997. *Wheat Production Handbook*. Manhattan, Kansas.
- Silva, A.G.B., C.H. Sequeira, R.A. Sermarini, and R. Otto. 2017. Urease inhibitor NBPT on ammonia volatilization and crop productivity: A meta-analysis. *Agron. J.* 109(1): 1–13.
- Sommer, S.G., J.K. Schjoerring, and O.T. Denmead. 2004. Ammonia emission from mineral fertilizers and fertilized crops. *Adv. Agron.* 82(5577622): 82004–82008.
- Tonitto, C., M.B. David, L.E. Drinkwater, and C. Li. 2007. Application of the DNDC model to tile-drained Illinois agroecosystems: model calibration, validation, and uncertainty analysis. *Nutr. Cycl. Agroecosystems* 78(1): 51–63.
- Torello, W.A., and D.J. Wehner. 1983. Urease Activity in a Kentucky Bluegrass Turf 1. *Agron. J.* 75(4): 654–656.
- Tulbure, M.G., M.C. Wimberly, A. Boe, and V.N. Owens. 2012. Climatic and genetic controls of yields of switchgrass, a model bioenergy species. *Agric. Ecosyst. Environ.* 146(1): 121–129. doi: <https://doi.org/10.1016/j.agee.2011.10.017>.

- Turner, D.A., R.E. Edis, D. Chen, J.R. Freney, and O.T. Denmead. 2012. Ammonia volatilization from nitrogen fertilizers applied to cereals in two cropping areas of southern Australia. *Nutr. Cycl. Agroecosystems* 93(2): 113–126. doi: 10.1007/s10705-012-9504-2.
- Turner, D.A., R.B. Edis, D. Chen, J.R. Freney, O.T. Denmead, and R. Christie. 2010. Determination and mitigation of ammonia loss from urea applied to winter wheat with N-(n-butyl) thiophosphorictriamide. *Agric. Ecosyst. Environ.* 137(3): 261–266. doi: <https://doi.org/10.1016/j.agee.2010.02.011>.
- USDA-ERS. 2017. United States Department of Agriculture Economic Research Service. <https://www.ers.usda.gov/data-products/>. Dataset accessed 03/04/2018.
- USDA-ERS. 2018. Fertilizer Use and Price. Fertil. Use Price. <https://www.ers.usda.gov/data-products/fertilizer-use-and-price.aspx>. Dataset accessed 03/04/2018.
- Varvel, G.E., and T.A. Peterson. 1990. Nitrogen fertilizer recovery by corn in monoculture and rotation systems. *Agron. J.* 82(5): 935–938.
- Vitousek, P.M., J.D. Aber, R.W. Howarth, G.E. Likens, P.A. Matson, D.W. Schindler, W.H. Schlesinger, and D.G. Tilman. 1997. Human alteration of the global nitrogen cycle: sources and consequences. *Ecol. Appl.* 7(3): 737–750.
- Willmott, C.J., S.G. Ackleson, R.E. Davis, J.J. Feddema, K.M. Klink, D.R. Legates, J. O'Donnell, and C.M. Rowe. 2018. Statistics for the evaluation and comparison of models. *J. Geophys. Res. Ocean.* 90(C5): 8995–9005. doi: 10.1029/JC090iC05p08995.
- Wilson, J.D., and W.K.N. Shum. 1992. A re-examination of the integrated horizontal flux method for estimating volatilisation from circular plots. *Agric. For. Meteorol.* 57(4): 281–295. doi: [https://doi.org/10.1016/0168-1923\(92\)90124-M](https://doi.org/10.1016/0168-1923(92)90124-M).
- Yan, L., Z. Zhang, Y. Chen, Q. Gao, W. Lu, and A.M. Abdelrahman. 2016. Effect of water and

temperature on ammonia volatilization of maize straw returning. *Toxicol. Environ. Chem.* 98(5–6): 638–647.

Yeluripati, J.B., A. del Prado, A. Sanz-Cobeña, R.M. Rees, C. Li, D. Chadwick, E. Tilston, C.F.E. Topp, L.M. Cardenas, and P. Ingraham. 2015. Global Research Alliance Modelling Platform (GRAMP): An open web platform for modelling greenhouse gas emissions from agro-ecosystems. *Comput. Electron. Agric.* 111: 112–120.

Zhenghu, D., and X. Honglang. 2000. Effects of soil properties on ammonia volatilization. *Soil Sci. Plant Nutr.* 46(4): 845–852. doi: 10.1080/00380768.2000.10409150.

## Appendix A - Figures and Tables Chapter 3

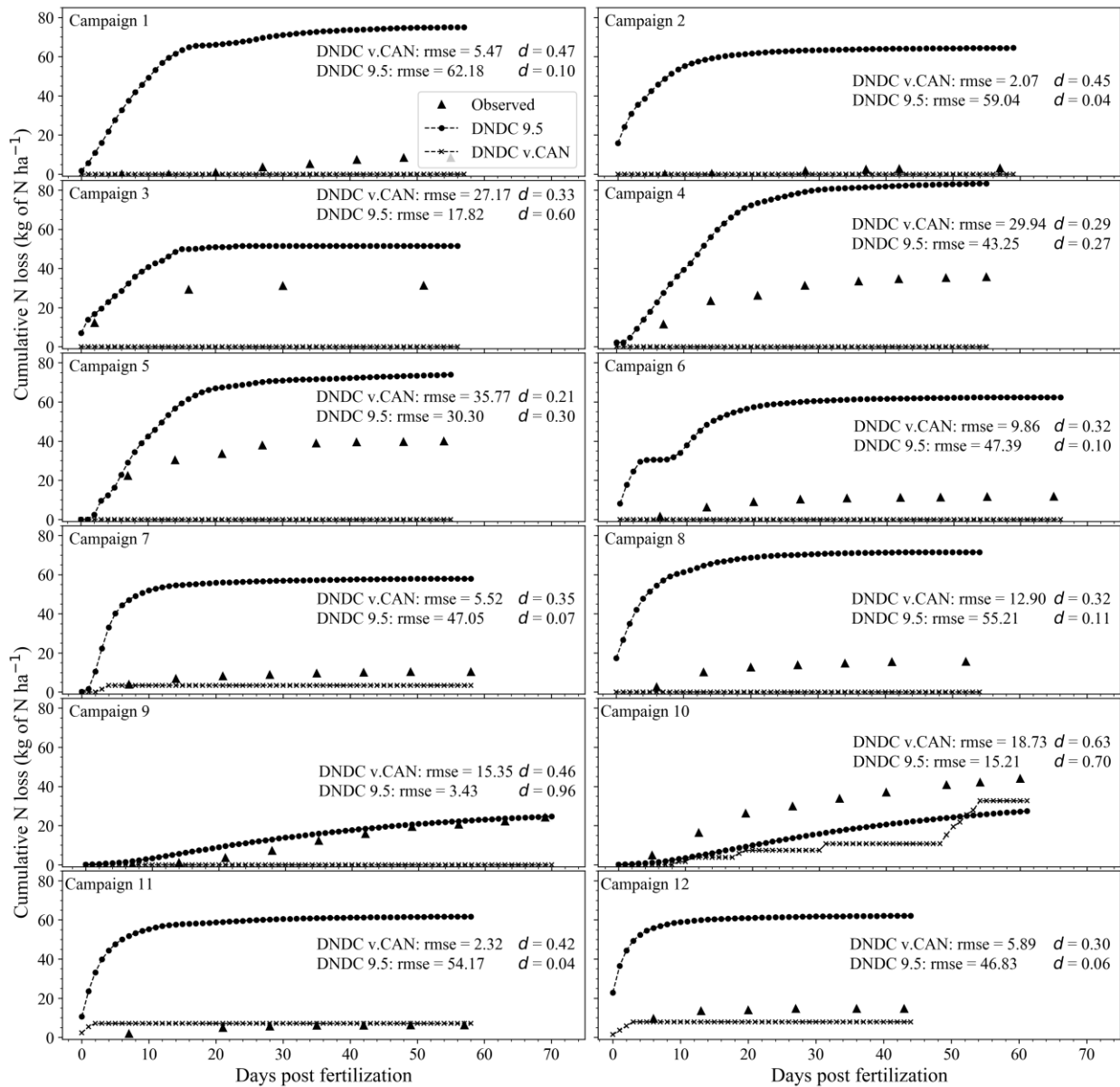


**Figure A.1** Cumulative N losses (kg of N ha<sup>-1</sup>) from broadcast urea for campaigns 1-12. Field sampling campaigns were obtained from Engel et al. (2011). Wilmot index of agreement (Willmott et al., 2018) is represented as '*d*' and root mean square error by 'rmse'.

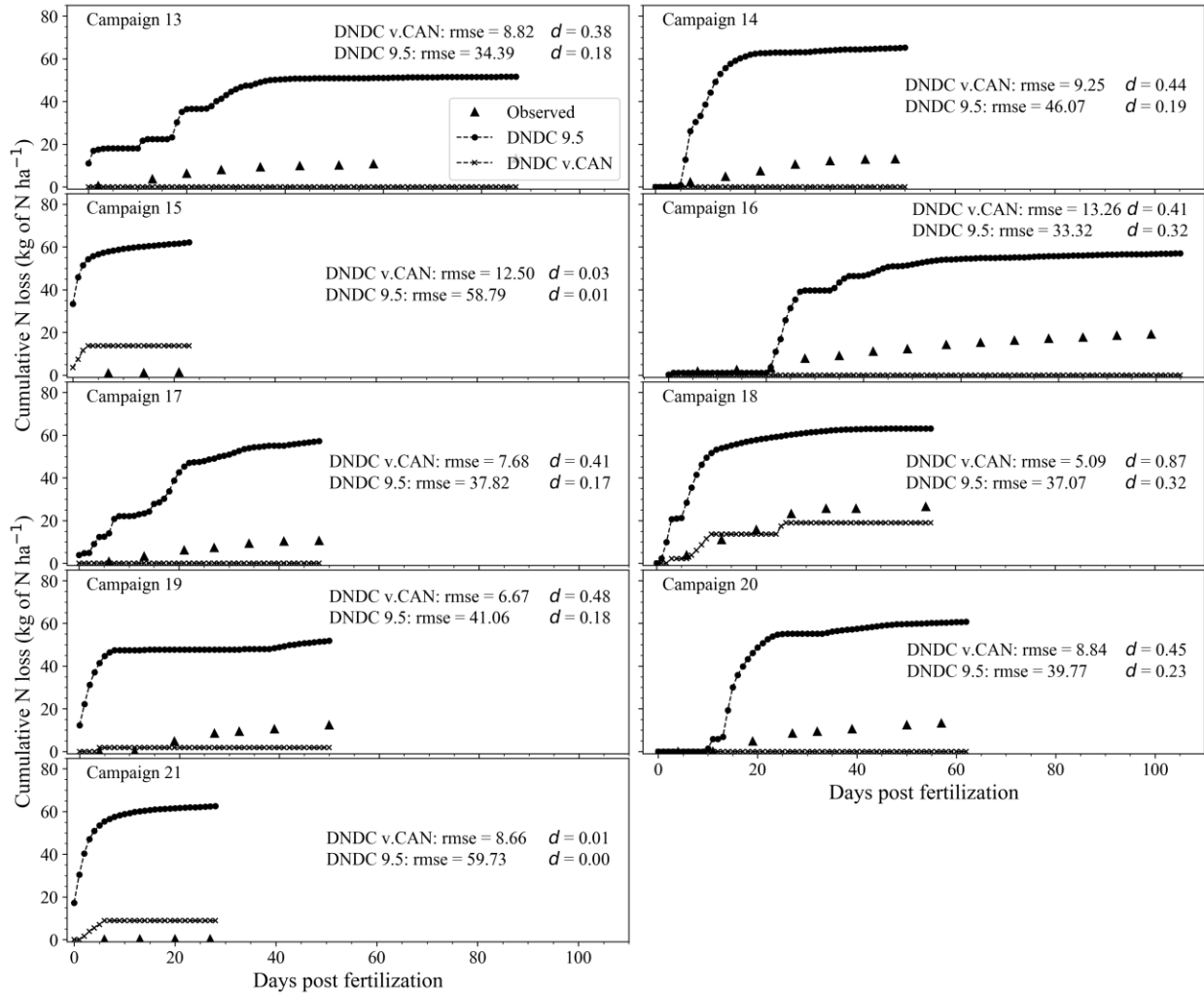


**Figure A.2** - Cumulative N loss ( $\text{kg of N ha}^{-1}$ ) from broadcast urea for campaigns 13-21. Field sampling campaigns were obtained from Engel et al. (2017) and Romero et al. (2017). Wilmot index of agreement (Willmott et al., 2018) is represented as ‘ $d$ ’ and root mean square error by ‘rmse’.

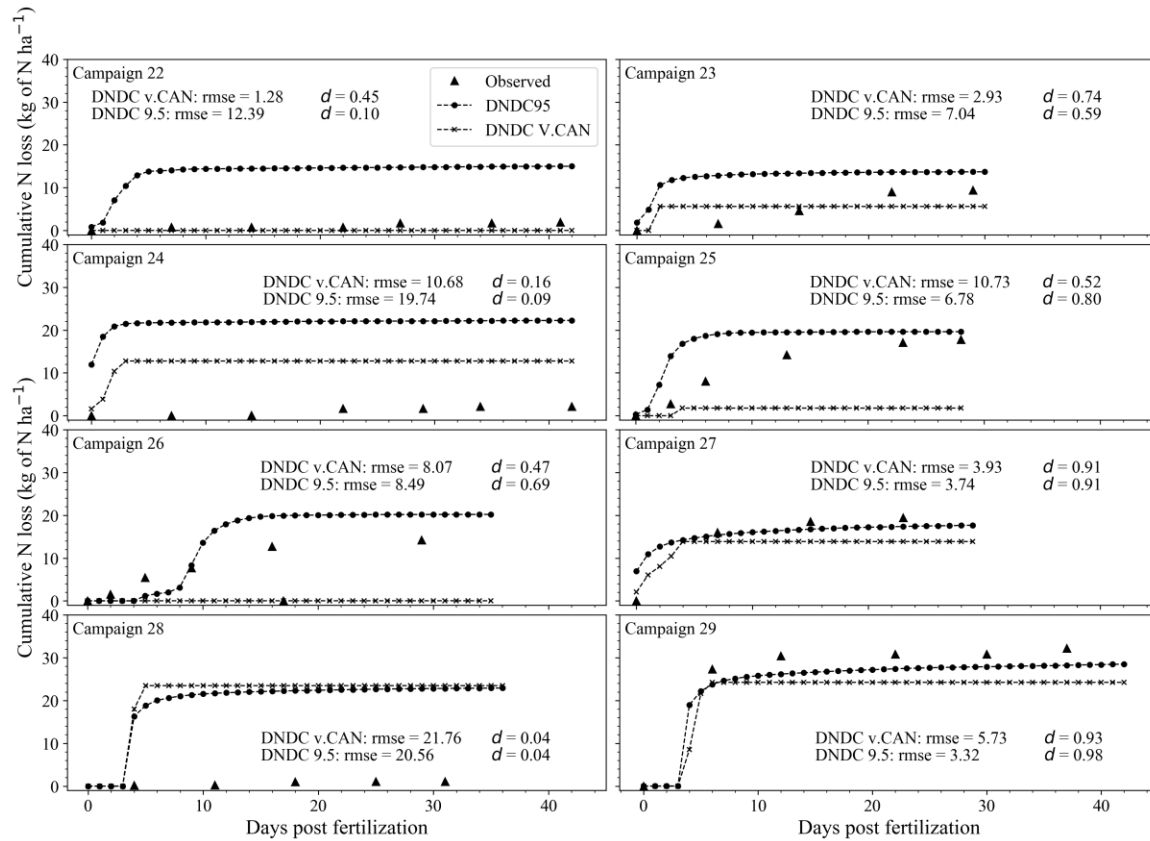


**Figure A.3** - Cumulative N loss (kg of N ha<sup>-1</sup>) from broadcast urea for campaigns 22-29. Field sampling campaigns are described on Chapter 2. Willmott index of agreement (Willmott et al., 2018) is represented as '*d*' and root mean square error by 'rmse'.



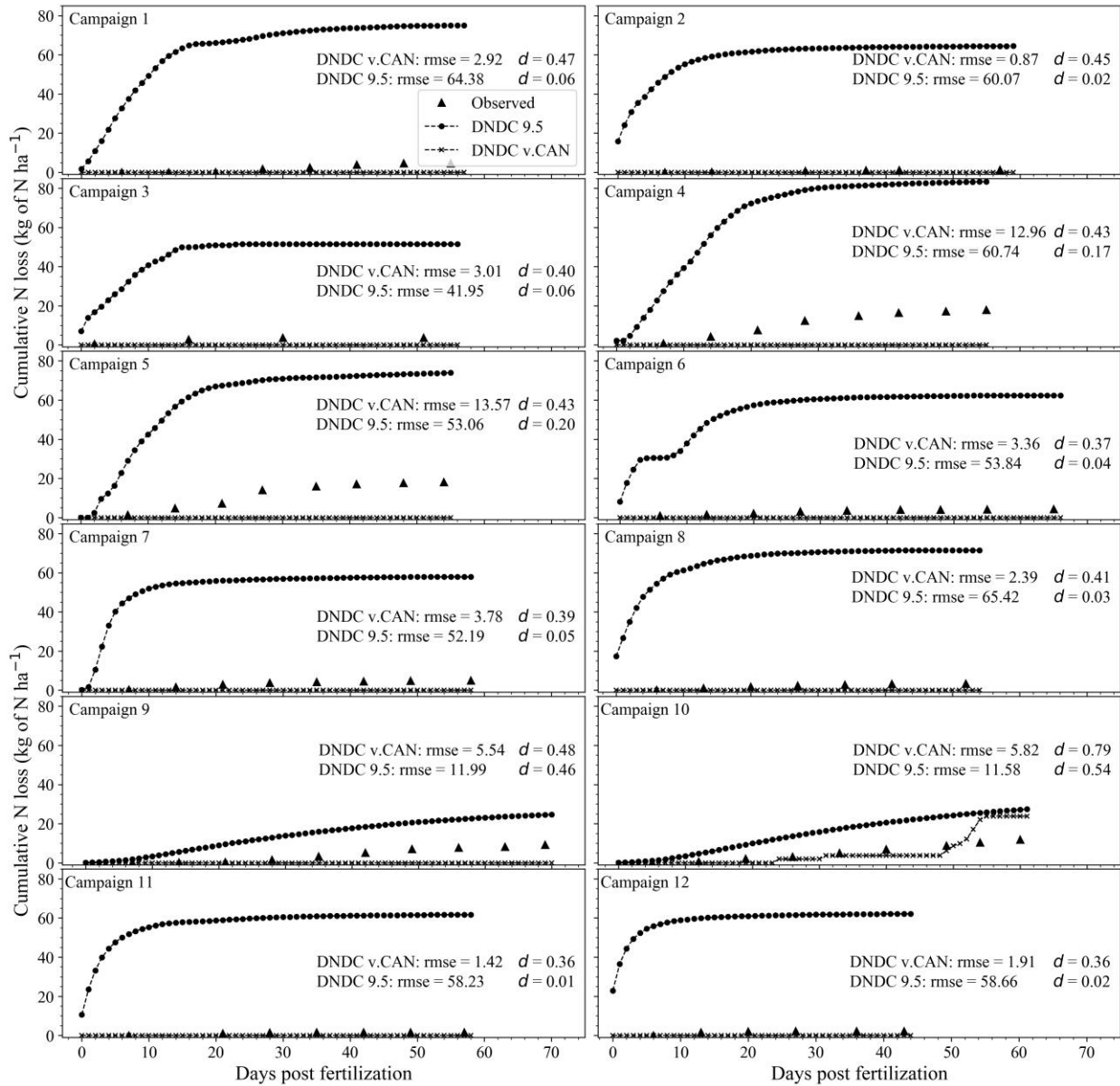


**Figure A.4** - Cumulative N loss (kg of N ha<sup>-1</sup>) from broadcast urea amended with urease inhibitor NBPT for campaigns 1-12. Field sampling campaigns were obtained from Engel et al. (2011). Wilmot index of agreement (Willmott et al., 2018) is represented as '*d*' and root mean square error by 'rmse'.

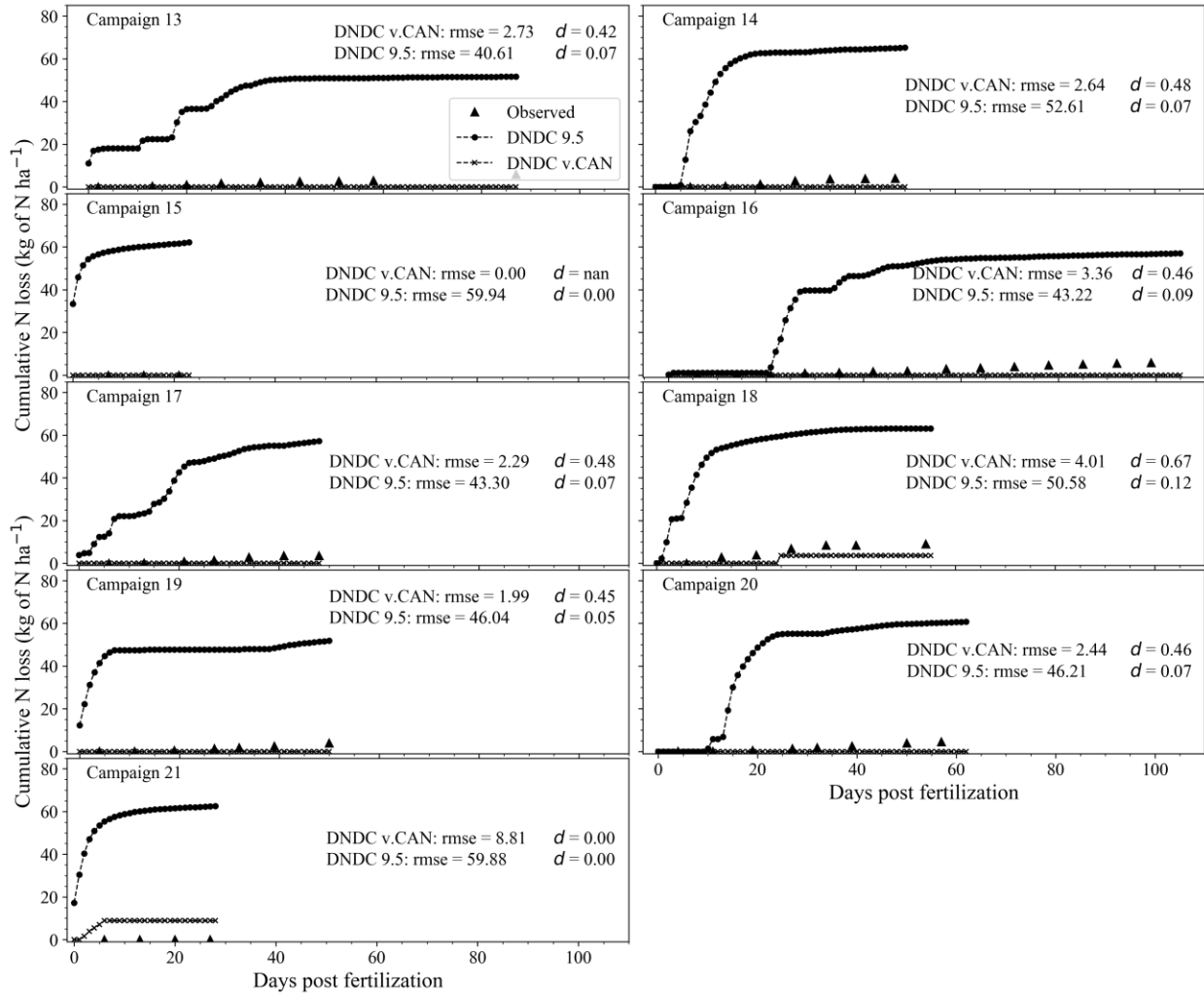


**Figure A.5** - Cumulative N loss ( $\text{kg of N ha}^{-1}$ ) from broadcast urea amended with urease inhibitor NBPT for campaigns 13-21. Field sampling campaigns were obtained from Engel et al. (2017) and Romero et al. (2017). Wilmot index of agreement (Willmott et al., 2018) is represented as ' $d$ ' and root mean square error by ' $\text{rmse}$ '.

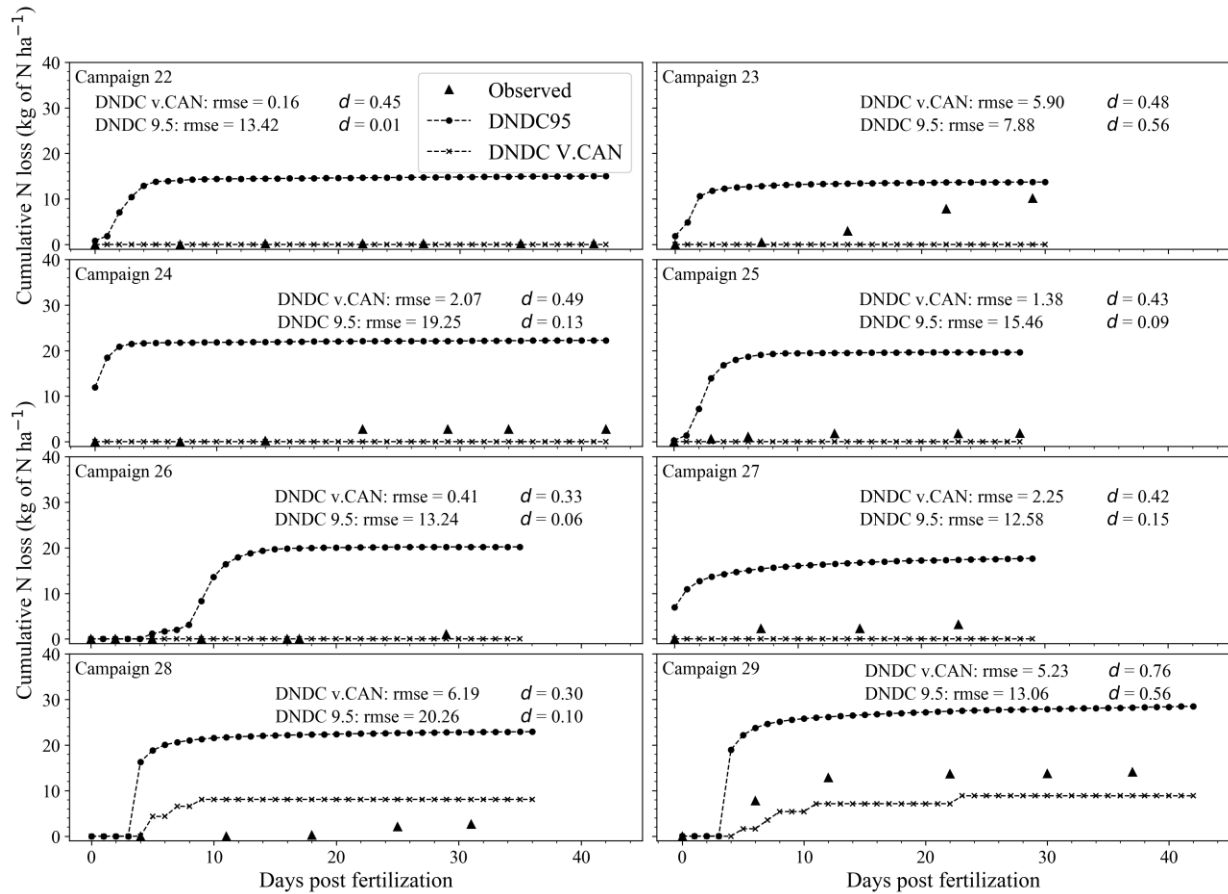


**Figure A.6** - Cumulative N loss (kg of N ha<sup>-1</sup>) from broadcast urea amended with urease inhibitor NBPT for campaigns 22-29. Field sampling campaigns are described on Chapter 2. Wilmot index of agreement (Willmott et al., 2018) is represented as ‘*d*’ and root mean square error by ‘rmse’.

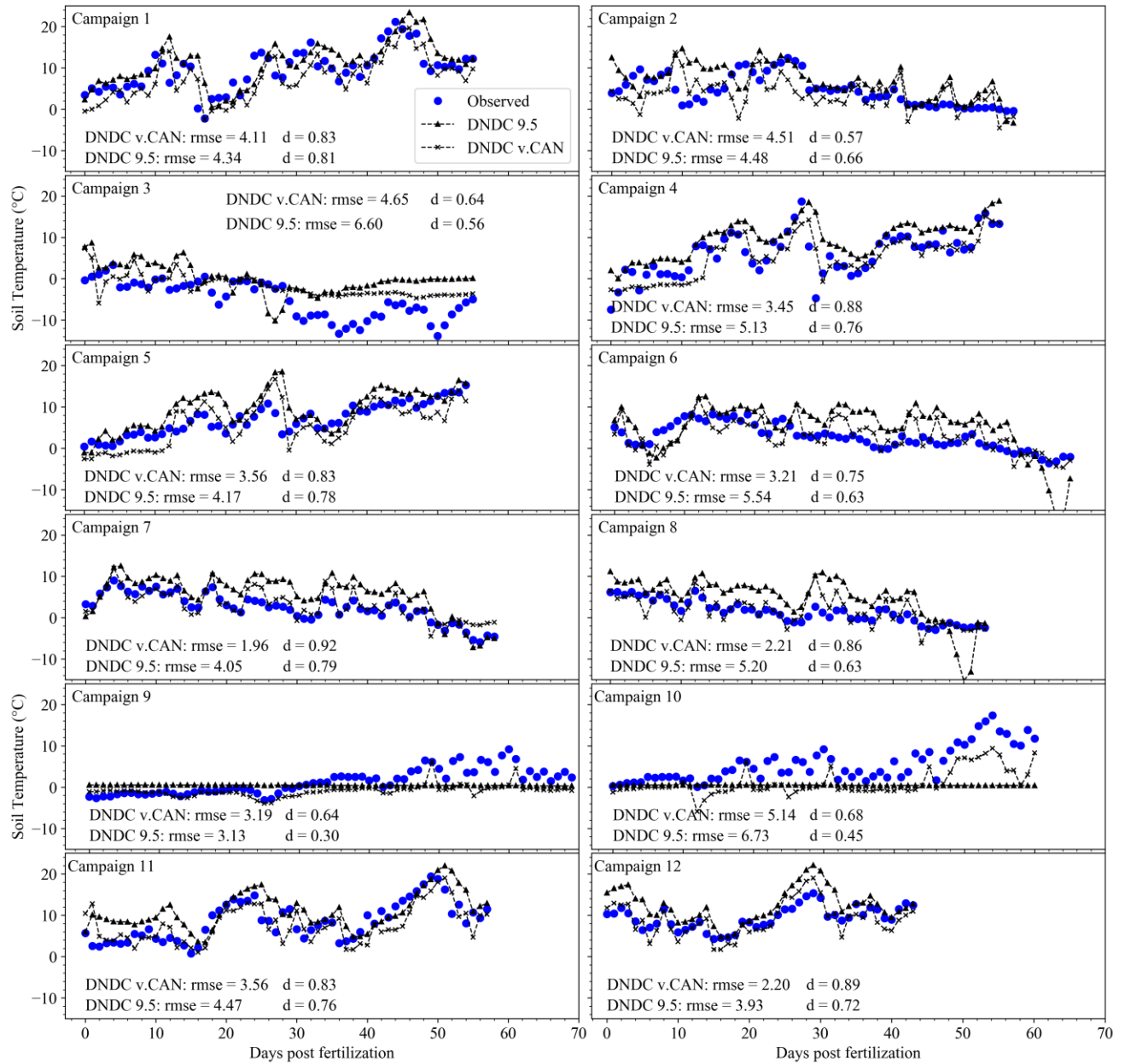


**Figure A.7** - Soil temperature (1-cm depth) for campaigns 1-12. Field observations were obtained from Engel et al., (2011). Wilmot index of agreement (Willmott et al., 2018) is represented as ‘*d*’ and root mean square error by ‘rmse’.

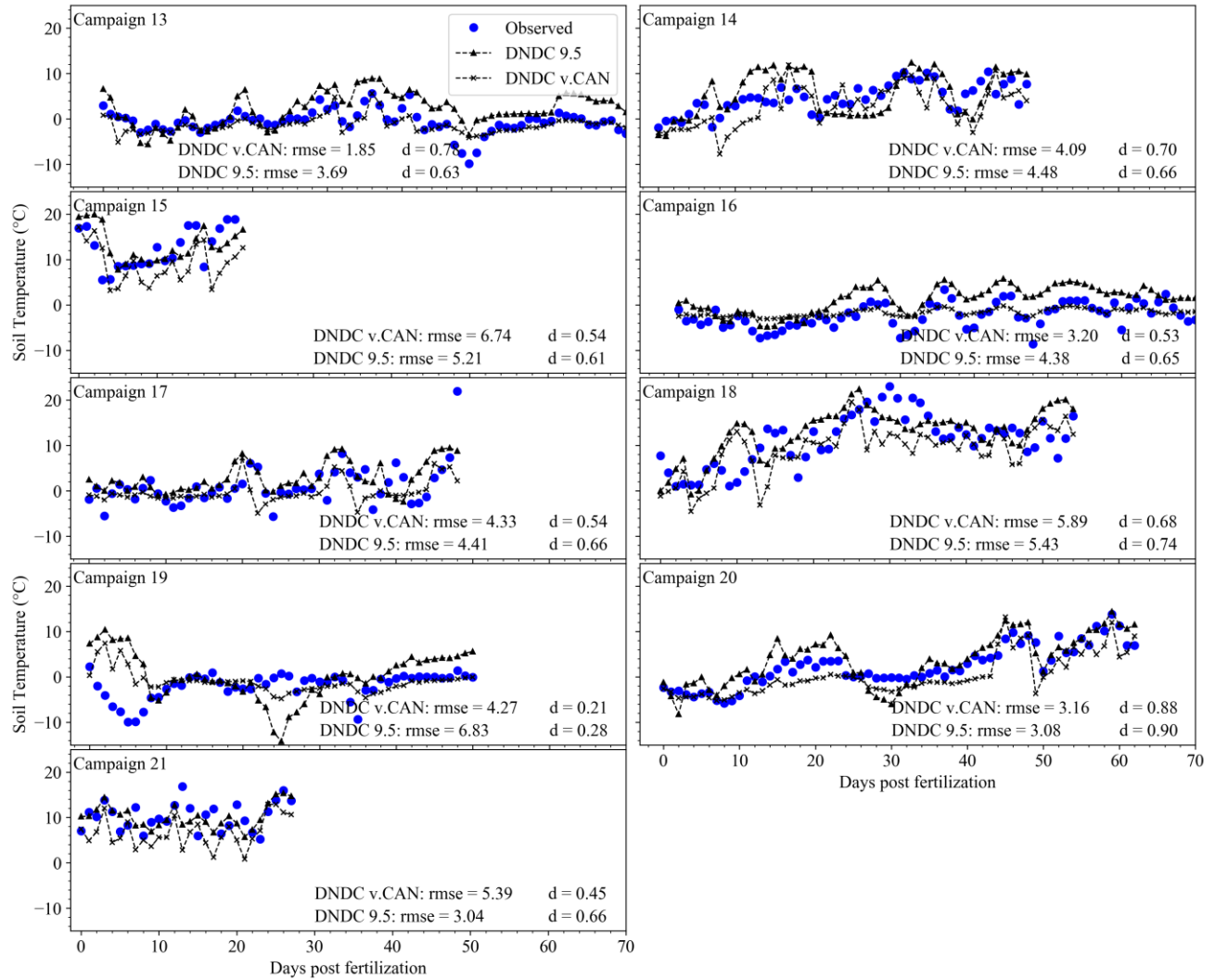


**Figure A.8** - Soil temperature (1-cm depth) for campaigns 13-21. Field observations were obtained from Engel et al., (2017) and Romero et al., (2017). Wilmot index of agreement (Willmott et al., 2018) is represented as ‘*d*’ and root mean square error by ‘rmse’.

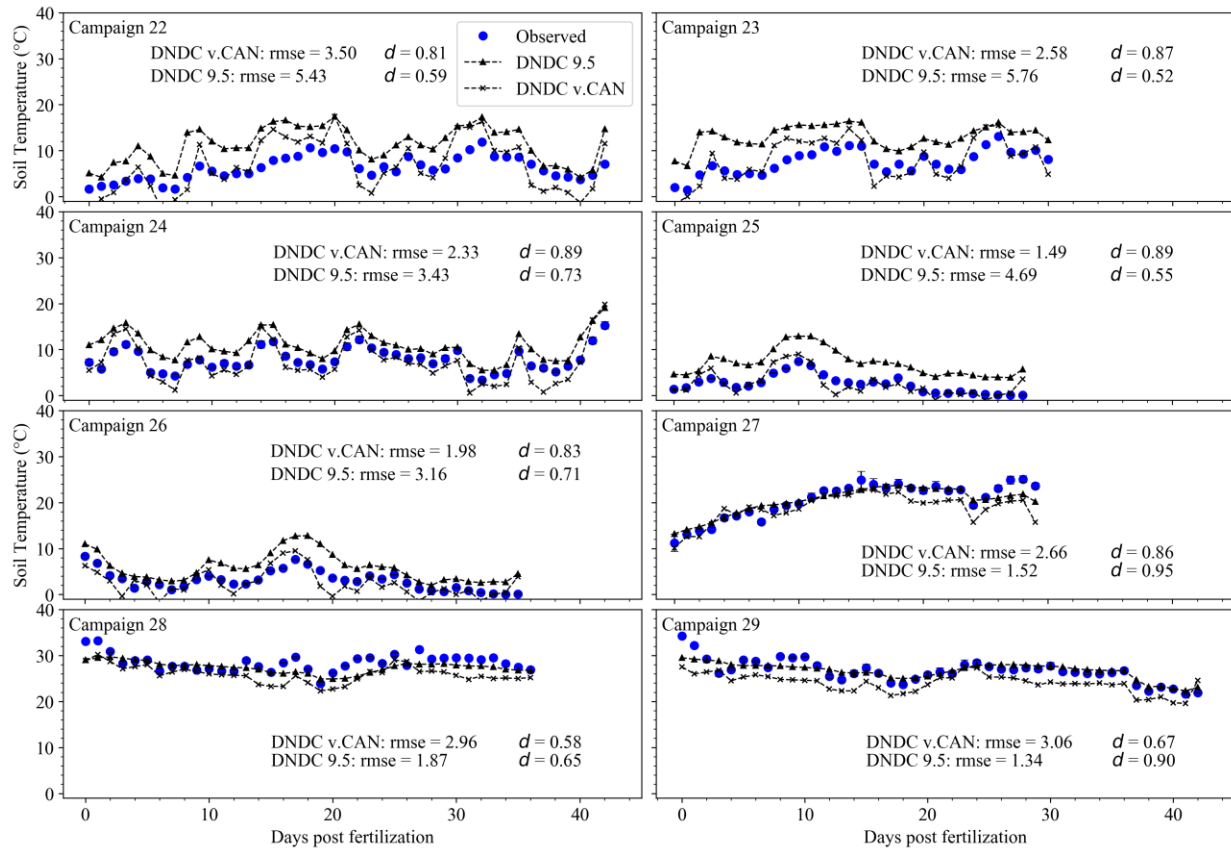


**Figure A.9** - Soil temperature (5-cm depth) for campaigns 22-29. Field observations collection are described on Chapter 2. Wilmot index of agreement (Willmott et al., 2018) is represented as ‘*d*’ and root mean square error by ‘rmse’.

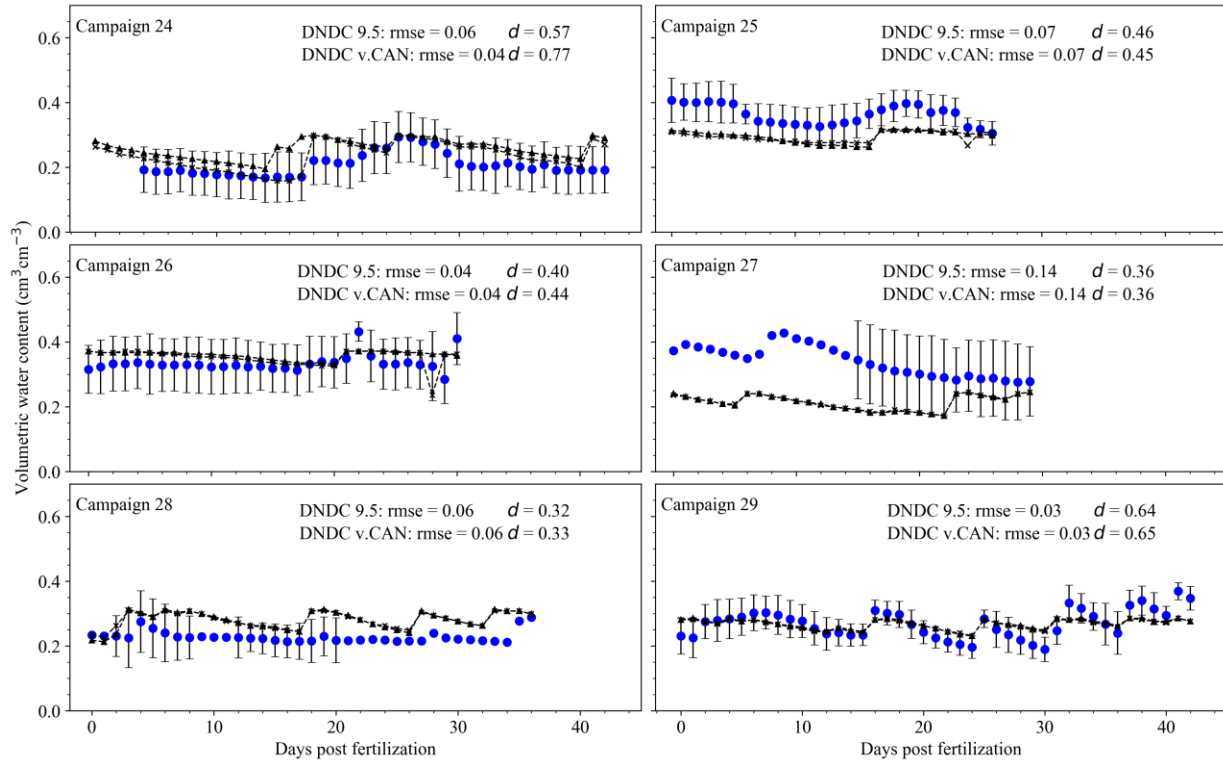


**Figure A.10** – Volumetric soil water content (cm<sup>3</sup> cm<sup>-3</sup>) (5-cm depth) for campaigns 22-29. Field observations collection are described on Chapter 2. Wilmot index of agreement (Willmott et al., 2018) is represented as ‘*d*’ and root mean square error by ‘rmse’.

**Table A.1** Meteorological stations used to extract climatic information for DNDC model simulations.

| Site                          | Weather station                  | Latitude  | Longitude     | distance (km) |
|-------------------------------|----------------------------------|-----------|---------------|---------------|
| Campaigns 1,2, 5-7, 10 and 11 | NOAA - Havre airport             | 48°32'34" | - 109°56'13"  | 9.6           |
| Campaign 3, 4 and 8           | NOAA - Simpson 6 N Wildhorse     | 48°29'53" | - 110°12' 56" | 8.2           |
| Campaign 9 and 10             | NOAA - Logan Landfill            | 45°52'32" | - 111°24'39"  | 13            |
| Campaign 13-21                | NOAA - Denton                    | 47°19'05" | - 109°56'13"  | 9.0           |
| Campaigns 22 and 24,25,26-29  | Kansas Mesonet - Ashland Bottoms | 39°07'33" | - 96°40'37"   | 0.5           |
| Campaign 26                   | Kansas Mesonet - Ashland Bottoms | 39°07'33" | - 96°40'37"   | 2.5           |
| Campaign 23                   | Kansas Mesonet - Gypsum          | 38°43'30" | - 97°26'38"   | 20            |

**Table A.2** Performance parameters of DNDC v.CAN and DNDC 9.5 of simulations of mean daily soil temperature (°C, campaigns 1-21: 2-cm depth and campaigns 22-29: 5-cm depth) after urea application during NH<sub>3</sub> volatilization measurement periods for all sampling campaigns. MAE (Mean Absolute Error) and RMSE (Root Mean Square Error).

| Site        | MAE    |     | RMSE   |     | Pearson r |       | <i>d</i> |      |
|-------------|--------|-----|--------|-----|-----------|-------|----------|------|
|             | v. CAN | 9.5 | v. CAN | 9.5 | v. CAN    | 9.5   | v. CAN   | 9.5  |
| Campaign 1  | 3.4    | 3.3 | 4.1    | 4.3 | 0.75      | 0.69  | 0.83     | 0.81 |
| Campaign 2  | 3.5    | 3.3 | 4.5    | 4.5 | 0.28      | 0.49  | 0.57     | 0.66 |
| Campaign 3  | 3.8    | 5.9 | 4.6    | 6.6 | 0.62      | 0.43  | 0.64     | 0.56 |
| Campaign 4  | 2.5    | 3.9 | 3.5    | 5.1 | 0.79      | 0.75  | 0.88     | 0.76 |
| Campaign 5  | 3.1    | 3.1 | 3.6    | 4.2 | 0.76      | 0.73  | 0.83     | 0.78 |
| Campaign 6  | 2.5    | 4.7 | 3.2    | 5.5 | 0.58      | 0.57  | 0.75     | 0.63 |
| Campaign 7  | 1.5    | 3.6 | 2.0    | 4.1 | 0.86      | 0.87  | 0.92     | 0.79 |
| Campaign 8  | 1.6    | 4.6 | 2.2    | 5.2 | 0.77      | 0.72  | 0.86     | 0.63 |
| Campaign 9  | 2.5    | 2.5 | 3.2    | 3.1 | 0.66      | -0.63 | 0.64     | 0.30 |
| Campaign 10 | 4.5    | 5.2 | 5.1    | 6.7 | 0.83      | -0.55 | 0.68     | 0.45 |
| Campaign 11 | 2.9    | 3.5 | 3.6    | 4.5 | 0.70      | 0.67  | 0.83     | 0.76 |
| Campaign 12 | 1.9    | 3.2 | 2.2    | 3.9 | 0.88      | 0.81  | 0.89     | 0.72 |
| Campaign 13 | 1.4    | 3.1 | 1.8    | 3.7 | 0.72      | 0.65  | 0.78     | 0.63 |
| Campaign 14 | 3.4    | 3.8 | 4.1    | 4.5 | 0.58      | 0.48  | 0.70     | 0.66 |
| Campaign 15 | 5.7    | 3.9 | 6.7    | 5.2 | 0.37      | 0.36  | 0.54     | 0.61 |
| Campaign 16 | 2.4    | 3.8 | 3.2    | 4.4 | 0.34      | 0.66  | 0.53     | 0.65 |
| Campaign 17 | 2.9    | 3.4 | 4.3    | 4.4 | 0.37      | 0.49  | 0.54     | 0.66 |
| Campaign 18 | 4.7    | 4.5 | 5.9    | 5.4 | 0.50      | 0.57  | 0.68     | 0.74 |
| Campaign 19 | 2.8    | 4.8 | 4.3    | 6.8 | -0.28     | -0.22 | 0.21     | 0.28 |
| Campaign 20 | 2.5    | 2.6 | 3.2    | 3.1 | 0.86      | 0.86  | 0.88     | 0.90 |
| Campaign 21 | 4.2    | 2.4 | 5.4    | 3.0 | 0.21      | 0.43  | 0.45     | 0.66 |
| Campaign 22 | 3.0    | 5.0 | 3.5    | 5.4 | 0.89      | 0.86  | 0.81     | 0.59 |
| Campaign 23 | 2.2    | 5.6 | 2.6    | 5.8 | 0.88      | 0.85  | 0.87     | 0.52 |
| Campaign 24 | 2.0    | 3.2 | 2.3    | 3.4 | 0.94      | 0.91  | 0.89     | 0.73 |
| Campaign 25 | 1.2    | 4.6 | 1.5    | 4.7 | 0.84      | 0.94  | 0.89     | 0.55 |
| Campaign 26 | 1.6    | 2.8 | 2.0    | 3.2 | 0.74      | 0.92  | 0.83     | 0.71 |
| Campaign 27 | 2.2    | 1.1 | 2.7    | 1.5 | 0.85      | 0.93  | 0.86     | 0.95 |
| Campaign 28 | 2.6    | 1.5 | 3.0    | 1.9 | 0.67      | 0.55  | 0.58     | 0.65 |
| Campaign 29 | 2.8    | 1.0 | 3.1    | 1.3 | 0.78      | 0.87  | 0.67     | 0.90 |